CMQM 2022

Condensed Matter and Quantum Materials

20–22 June 2022

University of Bath, Bath, UK

iop.org

IOP Institute of Physics

Monday 20 June

8:50	**Opening: Prof Ian White University of Bath Vice Chancellor (Room 1.10)**					
9:00	**Plenary: Amalia Patane (room 1.10)** **Chair:** Enrico Da Como					
	2D Materials (room 1.10) **Chair:** **John Lupton**		**Correlated Electron Systems (room 1.12)** **Chair: C Renner**		**Quantum phenomena (room 2.6)** **Chair:** **Kaveh Delfanazari**	
10:10	Theory Twist	Garcia-Ruiz, Aitor	CDW	Watson, Matthew	Quantum Information	McCaul, Gerard
10:25		Greenaway, Mark		Sven Friedemann		Romito, Alessandro
10:40		McEllistrim, Andrew		Flicker, Felix		Szyniszewski, Marcin
10:55		Patra, Sumanti				Hooley, Chris
11:10	Coffee break					
11:30	**Invited: Craciun (room 1.10)** **Chair: Sara Dale**		**Invited: Moll (room 1.12)** **Chair: Andreas Rost**		**Invited: McIver (room 2.6)** **Chair: Ettore Carpene**	
12:00	Synthesis	Felton, James	Super-conductivity	Sundar, Shyam	Out of equilibrium	Braunecker, Bernd
12:15		Balakrishnan, Nilanthy		Le Signe, Jamie		Verma, Sachin
12:30	Lunch break					
14:00	**Plenary: Matteo Mitrano (room 1.10)** **Chair:** Enrico Da Como					
15:10	Novel 2D **Chair: (room 1.10)**	Turnpenny, Liam	Lifshitz transition **Chair: A Rost (room 1.12)**	Broad, William	Out of equilibrium **Chair E Da Como (room 2.6)**	Mendoza Arenas, Juan Jose
15:25		Papadopoulou, Konstantina		de Almeida Marques, Carolina		Desaules, Jean-Yves
15:40	Coffee break					
16:00	**Invited: Renner** **Chair:** **(room 1.10)**		**Invited: Armitage** **Chair: Sven Friedemann** **(room 1.12)**		**Invited: Pashkin** **Chair:** **Kaveh Delfanazari** **(room 2.6)**	

16:30	CDW	Marini, Giovanni	Spin Liquids	Louat, Alex	Quantum Information	Kalsi, Tara
16:45		Antonelli, Tommaso		Brito, Francisco		
17:00	**POSTER SESSION/DRINKS RECEPTION** **Chancellors Building Foyer**					

Tuesday 21 June

9:00	**Plenary: Nigel Cooper (room 1.10)** **Chair:** Anton Souslov					
	2D Materials **Chair: MMK (room 1.10)**		**Correlated Electron Systems** **Chair: Chris Bell (room 1.12)**		**Quantum phenomena** **Chair: Anton Souslov (room 2.6)**	
10:10	Twist	Slizovskiy, Sergey	TaS/Se CDW	Aimee Nevill	Optics	Song, Bo
10:25		Nunn, James		Carpene, Ettore		Orfanakis, Konstantinos
10:40		Lupton, John		Feng, Xuanbo		Rouse, Dom
10:55		Majumder, Shantanu		Luckin, Will		
11:10	Coffee break					
11:30	**Invited: Rontani** **Chair: Chris Hooley (room 1.10)**		**Invited: King** **Chair: Phil Moll (room 1.12)**		**Invited: Shevyrin** **Chair:** **(room 2.6)**	
12:00	Optics	Thompson, Joshua	Ferro-magnetism	Farrar, Liam	Quantum Hall Effect	Hofmann, Johannes
12:15		Shiffa, Mustaqeem		Calahorra, Yonatan		Papic, Zlatko
12:30	Lunch break					
14:00	**Plenary: Peter Abbamonte** **Chair: Massimo Rontani (room 1.10)**					
15:10	Graphene Transport **Chair: MMK (room 1.10)**	Mehew, Jake	1D **Chair: M Rontani (room 1.12)**	Sesti, Giacomo	Junctions **Chair: P Moll (room 2.6)**	Ó Peatáin, Searbhán
15:25		Jones, Dylan		Askey, Joseph		Senapati, Tapas

15:40	Coffee break					
16:00	**Invited: Daniel Burrow** **Chair MMK (room 1.10)**		**Invited: Ciccareli** **Chair Enrico Da Como (room 1.12)**		**Invited: Downing** **Chair S Dale (room 2.6)**	
16:30	2D Transport	Chenattukuzhiyil, Safeer	Spin	Edwards, Brendan	Meta-materials	Roberts, Nathan
16:45		Berdyugin, Alexey				Baardink, Guido
17.00	**Plenary: Vladimir Fal'ko** **Chair: MMK (room 1.10)**					
19:00	**CONFERENCE DINNER** **Claverton Rooms (Pre-registered)**					

Wednesday 22 June

9:00	**Plenary: Eva Benckiser** **Chair: Chris Bell (room 1.10)**					
	2D Materials **Chair: D Wolverson (room 1.10)**		**Correlated Electron Systems** **Chair: Chris Bell (room 1.12)**		**Quantum phenomena** **Chair: Anton Souslov (room 2.6)**	
10:10	Optics	Morabito, Floriana	Pressure/strain		Skyrmions	Smith, Harry
10:25		Rostami, Habib				Bollard, Jack
10:40		Krishna Prasad, Madhava		Boyal, Prasun		Livesey, Karen
10:55		Lin, Kaiqiang		Abarca Morales, Edgar		
11:10	Coffee break					
11:30	Transport **Chair: Sara Dale (room 1.10)**	Gonzalez-Munoz, Sergio	Ruthenates **Chair: Enrico Da Como (room 1.12)**	Gibbs, Alex	Other Quantum effects **Chair: (room 2.6)**	Rhodes, Luke
11:45		Dey, Anubhab		Benedičič, Izidor		Nicolau, Eulàlia
12:00	**End of Conference**					

Zoom Links

Please refer to the program **here** to see what time the presentations will take place and in what room.

Room

1.10 https://us06web.zoom.us/j/82922883109?pwd=bEFwdlVFbkpBNkNwM0pWbEw2RXRxZz09

Passcode: 871692

Meeting ID: 829 2288 3109

Room 1.12

https://us06web.zoom.us/j/86228040953?pwd=cmh2MTh0aHBFa3F6NkROTTJ4WndxUT09

Passcode: 753048

Meeting ID: 862 2804 0953

Room 2.6

https://us06web.zoom.us/j/82918316984?pwd=QVNOaDl4bUIwclZUa0hMU29SdmpVQT09

Passcode: 290266

Meeting ID: 829 1831 6984

Dial by your location
+1 929 436 2866 US (New York)
+1 253 215 8782 US (Tacoma)
+1 301 715 8592 US (Washington DC)
+1 312 626 6799 US (Chicago)
+1 346 248 7799 US (Houston)
+1 669 900 6833 US (San Jose)
Find your local number: https://us06web.zoom.us/u/kn7WaGtfp

European Magnetic Field Laboratory: Science and Technologies

Amalia Patanè
School of Physics and Astronomy
University of Nottingham, Nottingham NG7 2RD, United Kingdom
email: amalia.patane@nottingham.ac.uk

This lecture will review recent advances at the European Magnetic Field Laboratory (EMFL) with focus on high magnetic fields as a powerful means of understanding and manipulating matter and procedures for researchers from all over the world to access the EMFL for research in high magnetic fields.

The EMFL unites, coordinates and reinforces all existing European large-scale high magnetic field research infrastructures in a single body. It includes the Laboratoire National des Champs Magnétiques Intenses (LNCMI) with sites in Grenoble and Toulouse, the High Field Magnet Laboratory (HFML - Nijmegen) and the Hochfeld-Magnetlabor (HLD - Dresden) providing access to the highest continuous and pulsed magnetic fields in Europe. The HFML-Nijmegen and the LNCMI-Grenoble are committed to generate the highest continuous magnetic fields, currently up to 38 T. The HLD-Dresden and the LNCMI-Toulouse focus on non-destructive pulsed fields, currently up to 100 T, and semi-destructive fields up to 200 T.

Besides the continuous improvement of the magnetic field strength, the realization and accessibility of top-class experimental infrastructure is of critical importance. Magnetic fields can be used in conjunction with a free electron laser (FEL) at the HLD-Dresden (FEL-ELBE) and at the HFML-Nijmegen (FELIX). Existing experimental setups are continuously improved, for instance, by using up-to-date instrumentation, reducing noise levels, and by the replacement of analogue with digital signal processing. Also, other experimental techniques, so far not often used in high fields, are under development at the EMFL, such as scanning-probe microscopy, high pressure and micro-calorimetry measurements.

Biography

Professor Amalia Patanè studied at the University of Rome “La Sapienza” where she graduated with first class honours in Physics in 1994 and obtained a PhD in 1997. She worked as an EPSRC Research Associate (1998/2002) at the University of Nottingham, appointed Lecturer at Nottingham in 2002, and later promoted to Associate Professor (2006), Professor of Physics (2011) and Director of Research (2019-present) in the School of Physics and Astronomy at Nottingham. Her research focuses on the quantum behavior of electrons in semiconductor materials and devices, most recently on two-dimensional systems. Her research achievements were recognized by the Sir Charles Vernon Boys Medal and Prize of the Institute of Physics (2007), an EPSRC Advanced Research Fellowship (2004/2009), a Leverhulme Trust Research Fellowship (2017/19), the Chinese Academy of Sciences (CAS) President’s International Fellowship (2018/19) and an Honorary Professorship at the Institute of Semiconductors (2018-present, CAS, Beijing). Prof. Patanè coordinates the UK Membership of the European Magnetic Field Laboratory, EMFL (2015-22). She has initiated the process by which the EMFL is now available as an EPSRC National Research Facility (NRF) to UK-based scientists working in different fields (magnetism, correlated systems, semiconductors, *etc*.). As a member of the EMFL Council and NRF Director, she has contributed to the development of the EMFL facilities and their access by a large community.

1-q backfolding but 2-q nesting in Ta_2NiSe_7

Matthew D Watson[1], Alex Louat[1], Timur K Kim[1], Cephise Cacho[1], Sungkyun Choi[2], Gideok Kim[2]

[1]Diamond Light Source, Harwell Science and Innovation Campus, Didcot, OX11 0DE, UK.
[2]Sungkyunkwan University (SKKU), Suwon 16419, Republic of Korea.

A structural cousin of the well-known Ta_2NiSe_5 [1], Ta_2NiSe_7 has a chain-like crystal structure, and exhibits metallic transport properties [2]. An anomaly in resistivity heralds the onset of a charge density wave (CDW) with a transition temperature of 63 K [3]. The structural properties of the material in CDW phase are already well characterised, with several reports agreeing on an incommensurate CDW with wavevector **q** = (0,0.483,0), where the b^* axis is along the chain direction. Further refinement observed that in addition to the transverse modulation at **q**, there is a significant longitudinal **2q** modulation [4].

Here we reveal the 3D Fermi surface of Ta_2NiSe_7 using high-resolution ARPES. We confirm the scenario of small, compensated Fermi surfaces, located around the Γ point of the Brillouin zone. Importantly, there is a lack of any plausible nesting at **q**. However, we observe a backfolding of valence bands in the CDW phase by a wavevector of **q**, with the backfolded bands appearing in a projected band gap. Thus Ta_2NiSe_7 exhibits the peculiar phenomenology of prominent backfolding of spectral weight that onsets below the CDW temperature, but with a wavevector that does not seem to connect any low energy states. However, we further show that there is a possible nesting at 2**q**, and associate the characters of these bands with the known atomic modulations at **2q**. We suggest that the CDW may be best understood as a unique coupled **q** & **2q** instability.

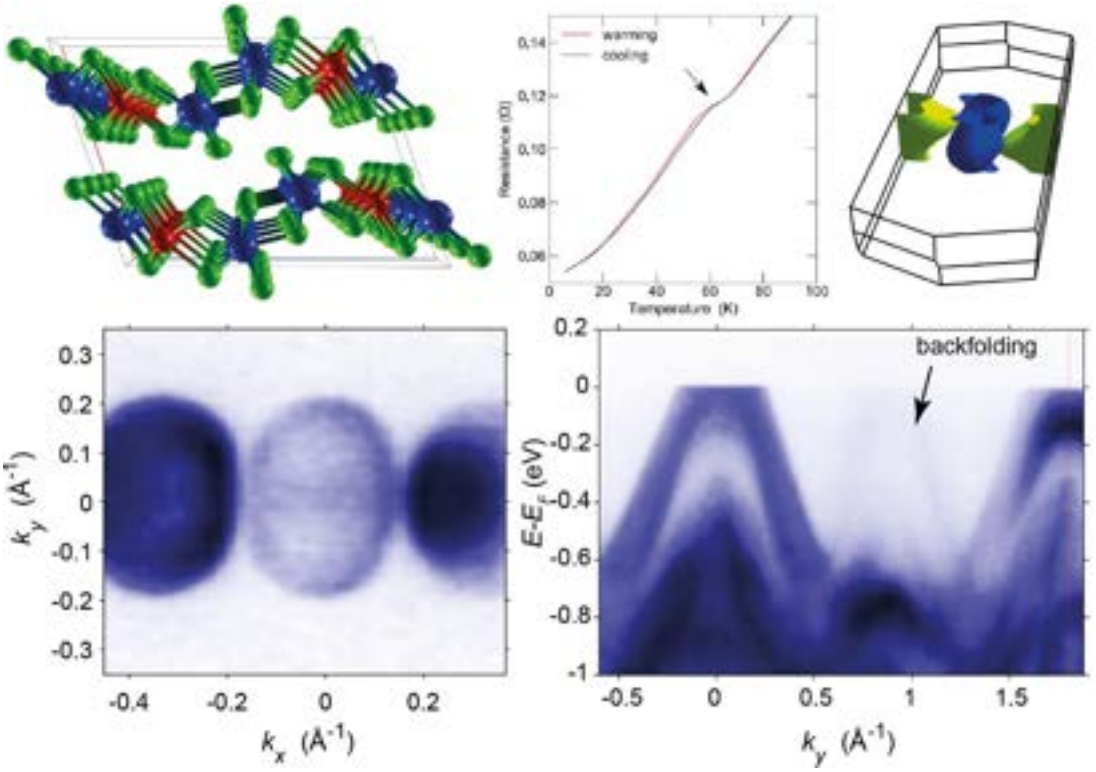

Fig. 1. Chain-like crystal structure of Ta_2NiSe_7, Resistivity showing CDW anomaly, Fermi surface calculated by DFT, measured Fermi surface, and signatures of backfolding that appear below T_c.

[1] Lu et al, Nat. Comms. 8, 14408 (2017)
[2] Sunshine and Ibers, Inorg. Chem. 25, 4355 (1986)
[3] Chen et al, J. Mater. Chem. C 9, 5162 (2021)
[4] Ludecke et al, J. Sol. Stat. Chem. 153, 152 (2000)

Ferroelectricity in twisted double bilayer graphene

A. Garcia-Ruiz[1,2], V. V. Enaldiev[1,2], and V. I. Fal'ko[1,2,3]

[1] National Graphene Institute, University of Manchester, Booth Street East, Manchester M13 9PL, UK
[2] Department of Physics and Astronomy, University of Manchester, Oxford Road, Manchester, M13 9PL, UK
[3] Henry Royce Institute for Advanced Materials, University of Manchester, Oxford Road, Manchester, M13 9PL, UK

Ferroelectric van der Waals heterostructures have attracted a lot of research attention, as they could be used on a wide range of device applications, such as non-volatile memory devices or pyroelectric sensors [1]. Experimentalists have constructed such structures using hexagonal boron nitride [2] or transition-metal dichalcogenides [3]. However, there has been no theoretical or experimental reports on single-element ferroelectric materials yet.

In this presentation, I will discuss the possibility of constructing a purely carbon-based ferroelectric structure. In particular, we propose that marginally twisted double bilayer graphene (AB/BA) can host ferroelectricity. In this material, the two domains within a moiré unit cell are related by space inversion, as shown in Fig. 1, and charge distribution inherits this symmetry. Following previous works [4], we develop a method to compute the ferroelectric polarisation map across the moiré unit cell, including the effects of lattice relaxation. We find that the ferroelectric polarisation has a definite orientation in each domain of the unit cell and propose an experimental setup that enable us to observe ferroelectricity.

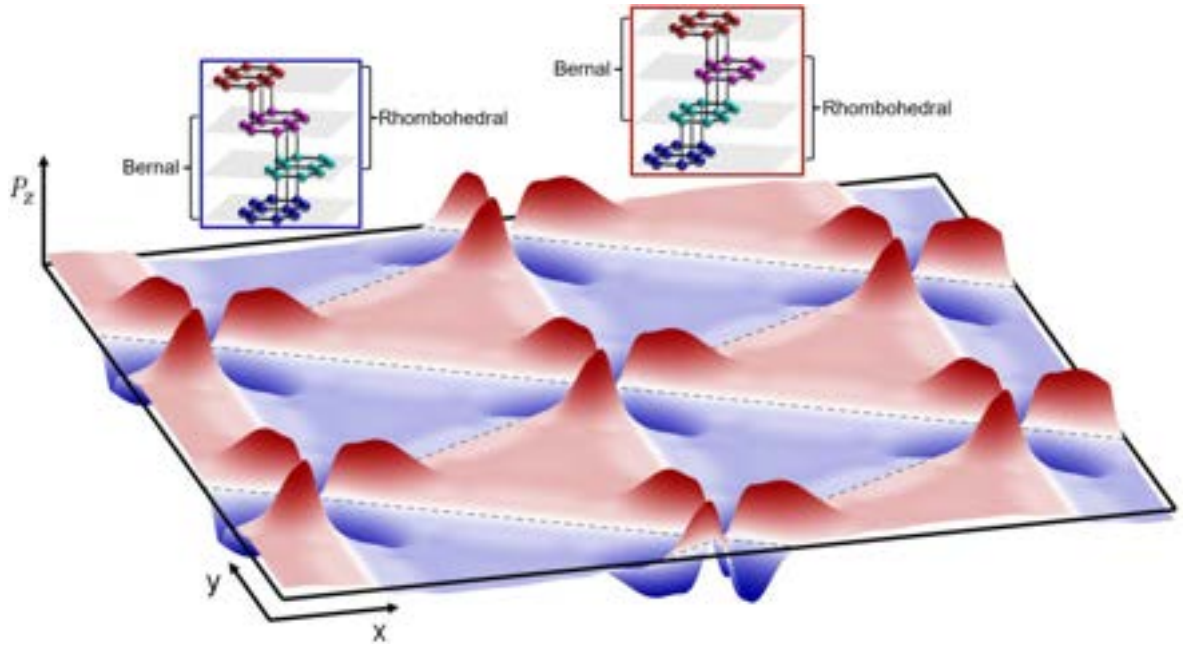

Fig. 1. Ferroelectric polarization across several moiré unit cells of AB/BA-twisted double bilayer graphene, with a twist angle of 0.5°. Inside the red (blue) colored domains, where the system has a stacking configuration ABCB (ABAC), we observe a definite positive (negative) value for the ferroelectric polarization.

[1] K. Uchino, Ferroelectric Devices (CRC Press, 2009).
[2] K. Yashuda et al., Science **372**, 1458 (2021).
[3] A. Weston et al., arXiv:2108.06489 (2021).
[4] A. Garcia-Ruiz et al., Phys. Rev. B, **104**, 085402 (2021).

Optical Indistinguishability Via Twinning Fields

Gerard McCaul[1], Alexander King[1] and Denys Bondar[1]

[1]Tulane University, New Orleans, USA

As our understanding of the physical world has progressed to mastery over it, it has become apparent that the qualities which define a material at equilibrium may be modified under driving. Exploiting the essential malleability of driven materials in one of the principal goals of quantum control theory, via the specification of the driving fields necessary either to steer a system to some desired state or fulfill a prespecified condition on its expectations. Recently developed quantum control techniques have shown that almost arbitrary control over the optical response of a large class of solid-state systems can be achieved [1]. While this has potential applications in nonlinear optics, materials science, and quantum technologies [2-4], a surprising consequence of this result is that two specially tailored driving fields will induce an identical response from two distinct systems [4].

Here we extend these results and introduce concept of a *twinning field* – a driving electromagnetic pulse which will induce an identical optical response in two distinct materials [5]. We show that for a large class of pairs of generic many-body systems, a twinning field which renders the systems optically indistinguishable exists. The conditions under which this field exists are derived, and this analysis is supplemented by numerical calculations of twinning fields for both the 1D Fermi-Hubbard model, and tight-binding models of graphene and hexagonal boron nitride. Finally, some potential applications of twinning fields are discussed.

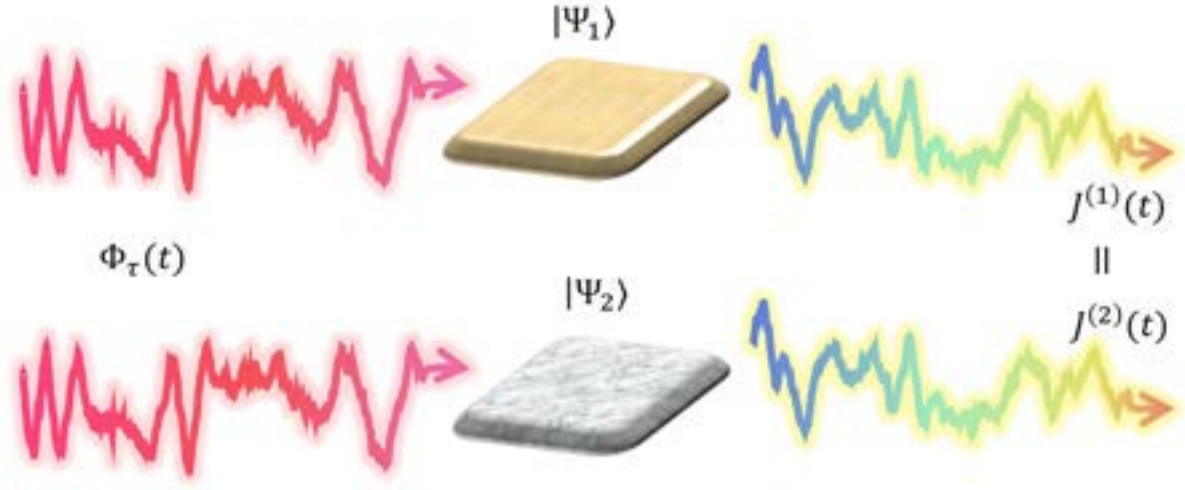

Fig. 1. Ordinarily, distinct systems will have different responses to the same driving field. A twinning field relates a pair of systems as the field under which the optical response of each system is identical.

[1] G. McCaul, C. Orthodoxou, K. Jacobs, G. H. Booth, and D. I. Bondar, Phys. Rev. A **101**, 053408 (2020).
[2] A . B. Magann, G. McCaul, H. A. Rabitz, and D. I. Bondar, Quantum **6**, 626 (2022)
[3] P. Ball, Nature Materials **19**, 710 (2020).
[4] A. Gorlach, N. Rivera, and I. Kaminer, Physics **13**, 75 (2020)
[5] G. McCaul, C. Orthodoxou, K. Jacobs, G. H. Booth, and D. I. Bondar, Phys. Rev. Lett. **124**, 183201 (2020)
[6] G. McCaul, A. F. King, and D. I. Bondar, Phys. Rev. Lett. **127**, 113201 (2021)

Graphene's non-equilibrium fermions reveal Doppler-shifted magnetophonon resonances accompanied by Mach supersonic and Landau velocity effects

M. T. Greenaway[1,2], P. Kumaravadivel[3,4], J. Wengraf[3,5], L. A. Ponomarenko[3,5], A. I. Berdyugin[3], J. Li[6], J. H. Edgar[6], R. Krishna Kumar[3], A. K. Geim[3,4], and L. Eaves[2,3]

[1]Department of Physics, Loughborough University, [2]School of Physics and Astronomy, University of Nottingham, [3]School of Physics and Astronomy, University of Manchester, [4]National Graphene Institute, University of Manchester, [5]Department of Physics, University of Lancaster, [6]Tim Taylor Department of Chemical Engineering, Kansas State University.

Resonant magnetoresistance measurements on graphene FETs under "ohmic" low current conditions have been used to study a wealth of novel physics. At high currents (up to 100 Am^{-1}), electrons are driven far from equilibrium with the atomic lattice vibrations so that their kinetic energy can exceed the thermal energy of the phonons. Here, we report three non-equilibrium phenomena in monolayer graphene at high currents [1]: (i) a "Doppler-like" shift and splitting of the frequencies of the transverse acoustic (TA) phonons, emitted resonantly when the electrons undergo inter-Landau level (LL) transitions and revealed by shifts of peaks in the differential resistance, r_y (see Fig. 1a); (ii) an intra-LL Mach effect with the emission of TA phonons when the electrons approach supersonic speed ($\sim$1.4 x 10^4 ms^{-1}), revealed by a strong and broad magnetic field-independent peak in r_y at $I \sim 1$ mA and (iii) the onset of elastic inter-LL transitions and an associated resonance maximum in r_y at a critical carrier drift velocity (see Fig 1b). The third phenomena is analogous to a "superfluid" Landau velocity and the formation of magneto-excitons involving a quantum jump, h/m, in the electron LL circulation. All three quantum phenomena can be unified in a single resonance equation. They offer avenues for research on out-of-equilibrium phenomena in other two-dimensional fermion systems.

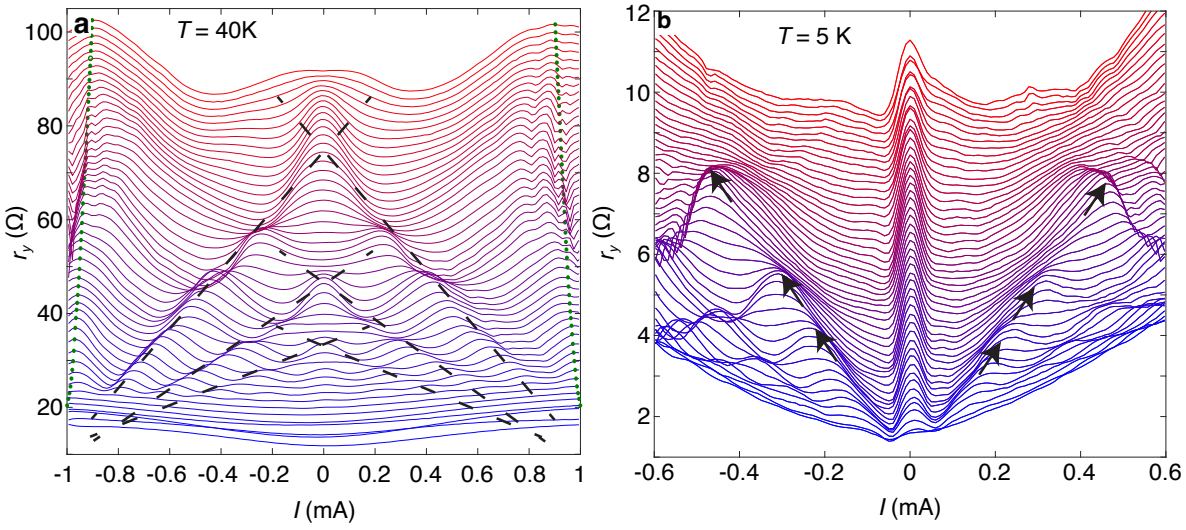

Fig. 1. (a) Non-equilibrium magnetoresistance oscillations at a temperature T = 40 K: magnetophonon resonance splitting and the Mach effect. Plot of the dependence of differential resistance $r_y(I)$, on current for magnetic fields, B, between 0 and 2 T in 0.04 T intervals, measured at a carrier density $n = 3.16 \times 10^{12}$ cm^{-2}. The curves are offset by 1.5 Ω and the dashed lines highlight the shift of the positions of the magnetophonon resonance peaks. The green markers show the position of the B-independent peak in $r_y(I)$ when the electrons approach supersonic speed. (b) Non-equilibrium magnetoresistance oscillations at T = 5 K: elastic inter-LL transitions. Plot of $r_y(I)$ for values of B between 0 to 1.2 T in 0.04 T intervals when $n = 3.16 \times 10^{12}$ cm^{-2}. Black arrows highlight position of peaks in r_y due to elastic inter-LL transitions that arise when the electron velocity approaches the Landau velocity.

[1] M.T. Greenaway *et al*., *Nature Communications* **12**, 6392 (2021)

Probing the charge density wave phase in sulfur with Raman spectroscopy and first principles calculations

Andreas Hermann[1], Owen Moulding[2,3], Israel Osmond[2], Lewis J Conway[1,4], Sam Cross[2], Jonathan Buhot[2], and Sven Friedemann[2]

[1]School of Physics and Astronomy, The University of Edinburgh UK, [2]HH Wills Laboratory, Bristol University, UK, [3]Institut Néel Grenoble, France, [4]Department of Materials Science & Metallurgy, University of Cambridge, UK

Charge density waves (CDW's) are modulations of the electron density and atomic positions with a periodicity different from – and often incommensurate with – the underlying crystalline lattice. CDW's affect various collective phenomena in condensed matter systems, causing metal-insulator transitions, and affecting superconductivity in 2D materials and the cuprates. Sulfur is one of the few elements that exhibits a charge density wave, which is present between 83 and 153 GPa, the highest transition pressures of any elemental CDW phase. Previous x-ray diffraction measurements confirmed the CDW S-IV phase as an incommensurate modulation of a body-centered monoclinic crystal structure [1,2].

Raman spectroscopy is an alternative probe of the CDW state, as the displacement mode of the atomic positions is always Raman-active. While the CDW mode has been detected in several elemental CDW phases [3], none have covered the entire stability range of a CDW phase. Here, we present Raman measurements of sulfur up to 155 GPa, tracking the CDW mode across the entire S-IV range, accompanied by first principles total energy calculations.

We find that the CDW mode in S-IV retains a finite frequency up to the transition to S-V, suggesting a weakly first order transition when the CDW breaks down. We show that only by combining the CDW displacement mode with a monoclinic lattice distortion of the rhombohedral S-V phase, the CDW phase is stabilised over the latter.

Our work suggests that the formation of CDW states can be more complex than hitherto assumed, e.g. *via* interactions with lattice degrees of freedom, but also demonstrates the potential of spectroscopic measurements in combination with electronic structure calculations to unravel those interactions.

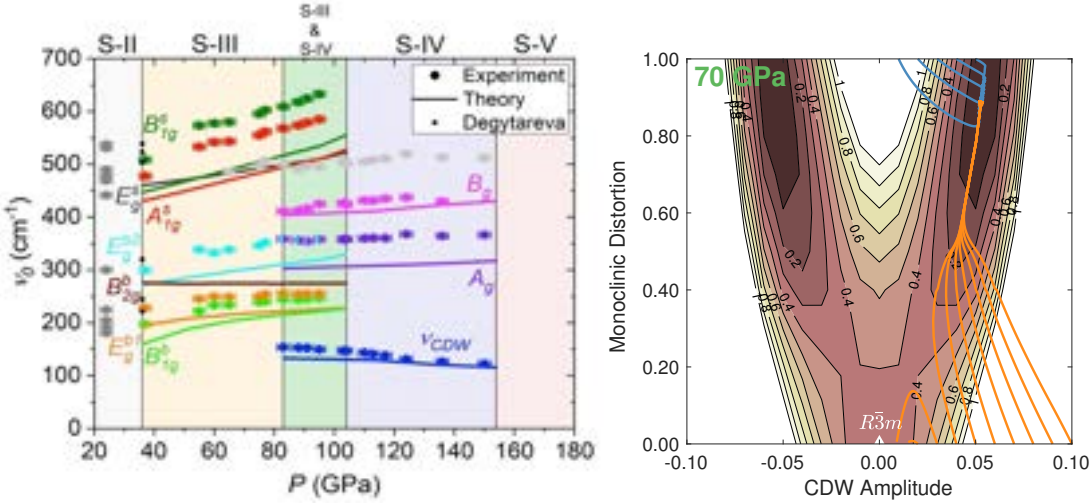

Fig. 1. (a) Raman modes from S-III to S-V; symbols/lines are measured/computed frequencies; CDW amplitude mode is shown in dark blue; (b) Computed potential energy surface for sulfur along the CDW displacement mode (horizontal axis) and lattice distortion (vertical axis); dark/light regions are energy minima/maxima; colored lines follow gradients and lead to either S-IV (global minimum) or S-V (metastable local minimum).

[1] O. Degtyareva, *et al.*, Phys. Rev. B **71**, 214104 (2005)
[2] C. Hejny, *et al.*, Phys. Rev. B **71**, 020101(R) (2005).
[3] T. Kume, *et al.*, Phys. Rev. Lett. **94**, 065506 (2005).

Topological transition from continuous monitoring of a free-fermion system

Graham Kells[1,2], Dganit Meidan[3], and Alessandro Romito[4]

[1]Dublin City University, School of Physical Sciences, Ireland,
[2]Dublin Institute for Advanced Studies, School of Theoretical Physics, Ireland,
[3]Department of Physics, Ben Gurion University of the Negev, Israel,
[4]Department of Physics, Lancaster University, LA1 4YB United Kingdom

Quantum measurements have been recently exploited as a tool to induce phase transitions between different steady state phases of many-body systems. Transitions between different entanglement scaling phases or different topological ordered phase have been studied in quantum circuits with unitary and projective gates [1]. Such transitions can be induced by continuous measurement too, for which analytical treatments and large system size numerical implementation are possible in free fermion models. Here we study a free fermion model where two sets of non-commuting continuous measurements induce a transition between area-law entanglement scaling phases of distinct topological order [3].

We find that, in the presence of unitary dynamics, the two topological phases are separated by a region with sub-volume scaling of the entanglement entropy and that the transition universality class of the measurement-only model differs from that in interacting models with stroboscopic dynamics and projective measurements. We further show that the phase diagram is qualitatively captured by an analytically tractable non-Hermitian Hamiltonian model obtained via post-selection. By the introduction of a partial-post-selection continuous mapping, we show that the topological distinct phases of the stochastic measurement-induced dynamics are uniquely associated with the topological indices of the non-Hermitian Hamiltonian (cf. Fig. 1). Our results mark a clear distinction between the topological phase transition induced by projective and continuous measurements, and open a door to the construction of topological invariants for stochastic quantum dynamics.

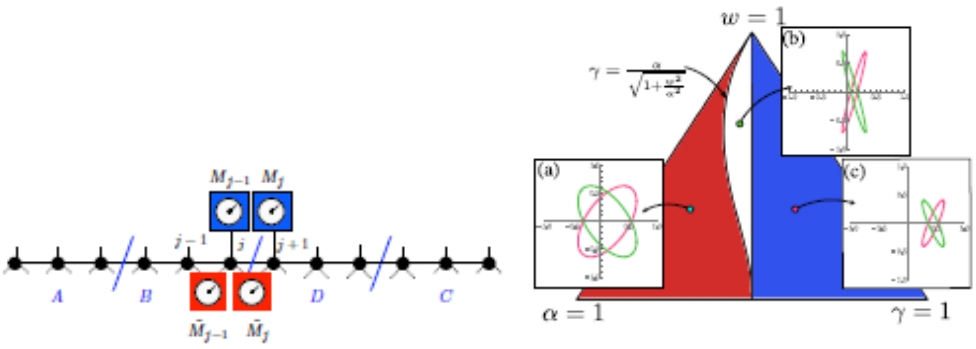

Fig. 1: Left. scheme of fermions hopping on a 1-d chain under local measurements of densitys (blue) and "Kitaev"-pairing operators (red). Right. Corresponding phase diagram from the associated non-Hermitian Hamiltonian showing topologically non-trivial (red) and trivial (blue) phases separated by a logarithmic scaling entanglement phase (white).

[1] Y. Li, X. Chen, and M. P. A. Fisher, Phys. Rev. B 98, 205136 (2018); A. Chan, R. M. Nandkishore, M. Pretko, and G. Smith, Phys. Rev. B 99, 224307 (2019); B. Skinner, J. Ruhman, and A. Nahum, Phys. Rev. X 9, 031009 (2019); M. Szyniszewski, A. Romito, and H. Schomerus, Phys. Rev. B 100, 064204 (2019).

[2] G. Kells, D. Meidan, A. Romito, arXiv: 211209787 (2021).

ARPES: A test for modelling gated twistronic graphenes

Andrew Mcellistrim[1], James E. Nunn[2,3], Astrid Weston[1], Matthew D. Watson[3], Abigail J. Graham[2], Aitor Garcia-Ruiz[1], Roman V. Gorbachev[1], Marcin Mucha-Kruczynski[4], Vladimir I. Fal'ko[1], Cephise Cacho[3], Neil R. Wilson[2].

[1]National Graphene Institute, University of Manchester, Manchester, M13 9PL, UK. [2]Department of Physics, University of Warwick, Coventry, CV4 7AL, UK. [3]Diamond Light Source, Harwell Science and Innovation Campus, Didcot, OX11 0DE, UK. [4]Department of Physics, University of Bath, Claverton Down, Bath, BA2 7AY, UK.

Twisted graphene multilayers are an established playground for strongly correlated, many-electron physics; such as superconductivity and Mott insulators [1-3]. Theoretically, the study of these began with the seminal work of Bistritzer and MacDonald, on twisted bilayer graphene [4]. Thus far, these systems have been mainly studied by transport and scanning tunnelling microscopy measurements. Motivated by experimental observations, we present a theoretical model for angle-resolved photoemission spectroscopy (ARPES) of Twisted monolayer on bilayer graphene (tMBLG), that is verified alongside experimental results. We hope to present ARPESs potential for furthering the understanding of these emerging systems.

Our work begins with a continuum model to describe interlayer coupling in tMBLG [4]. Next, we consider the conventional methods [5] for converting our graphenes systems wave functions into ARPES intensity plots. Following this, we consider the additional effects due to the interaction Hamiltonian for the photoemission process, the polarisation of the light [6,7] and the photon energy used. Lastly, we present the effect of gating and the subsequent interlayer screening visualised with ARPES intensity plots. We use this information to study the change to the systems dispersion curves in the presence of gating. Additionally, we study the interatomic coupling which has not been previously shown at lower angles ($\theta<5^o$) where interlayer coupling is highest and there is band hybridization that can lead to the formation of tunable van Hove singularities [8].

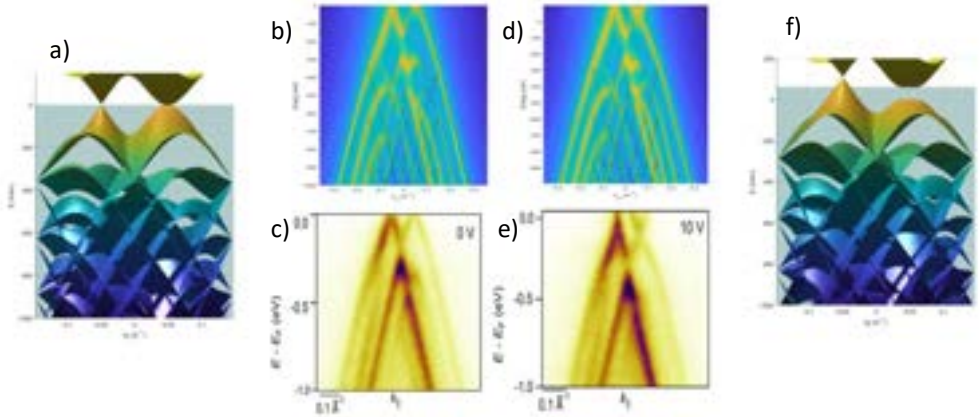

Fig. 1. a), f) Band structures of tMBLG at 3.3° with back gate voltage set to 0, 10V respectively. b), c) ARPES intensity plots of tMBLG at 3.3° with back gate voltage set to 0V. b) is from simulation and c) is from experiment. d), e) same as b), c) but for back gate voltage set to 10V.

[1] Yuan Cao et al., Nature 556.7699, pp. 43–50, Mar. 2018.
[2] Yuan Cao et al., Nature 556.7699, pp. 80–84, Mar. 2018.
[3] Xiaobo Lu et al., Nature 574.7780, pp. 653–657, Oct. 2019.
[4] Rafi Bistritzer and Allan H. MacDonald, PNAS 108.30, pp. 12233–12237, July 2011
[5] M. Mucha-Kruczyński et al., Phys. Rev. B 77, p. 195403, May 2008.
[6] Choongyu Hwang et al., In: Phys. Rev. B 84, p. 125422Sept. 2011.
[7] Jihang Zhu et al., Phys. Rev. B 103, p. 235146, June 2021.
[8] J. J. P. Thompson et al., Nature Communications 11.1, July 2020.

Cascade of Fermi surface reconstructions inside the CDW phase of $TiSe_2$

Owen Moulding[1,2], Roemer Hinlopen[1], Charles J Sayers[3], Enrico Da Como[3], Felix Flicker[4], Jasper van Wezel[5] and Sven Friedemann[1]

[1]*HH Wills Physics Laboratory, University of Bristol, BS8 1TL Bristol, UK*

[2]*Max Planck Institute for Chemical Physics of Solids, Nöthnitzer Straße 40, 01187 Dresden, Germany*

[3] *Department of Physics, University of Bath, Bath BA2 7AY, United Kingdom*

[4]*School of Physics and Astronomy, Cardiff University, The Parade, Cardiff CF24 3AA, UK*

[5]*Institute of Physics, University of Amsterdam, 1098 XH Amsterdam, The Netherlands*

The Fermi surface reconstruction induced by a charge density wave (CDW) has drawn interest for a long time. Recently, observations of CDW correlations in cuprates and nickelates [1,2] have sparked new interest in CDW phases. Several scenarios for the relation to superconductivity have been proposed in high-temperature superconductors [3].

The transition metal dichalcolgenides have been instrumental in the development of CDW models as well as studies of Fermi surface reconstruction [4] and the interplay of CDWs with superconductivity. Here, we study the Fermi surface evolution of $TiSe_2$ with pressure over the entire CDW phase. Our quantum oscillation experiments reveal not only a reconstruction upon entering the CDW phase, but also a remarkable cascade of repeated reconstructions within the CDW phase indicated by sharp changes in the observed frequencies.

To interpret these results we conducted DFT calculations to model the pressure evolution of the Fermi surface, finding good agreement outside the CDW phase where the Fermi surface is unreconstructed. Introducing the CDW gap into a tight-binding model inspired by recent ARPES results [5] we evolve the Fermi surface inside the CDW phase and find a good agreement with our measurements. We expect these findings to be relevant to understanding Fermi surface reconstruction induced by CDW phases more broadly, as well as the emergence of superconductivity in $TiSe_2$ which appears to be linked to the appearance of a large Fermi surface pocket. These results will help the quantitative understanding of CDW and superconducting phases.

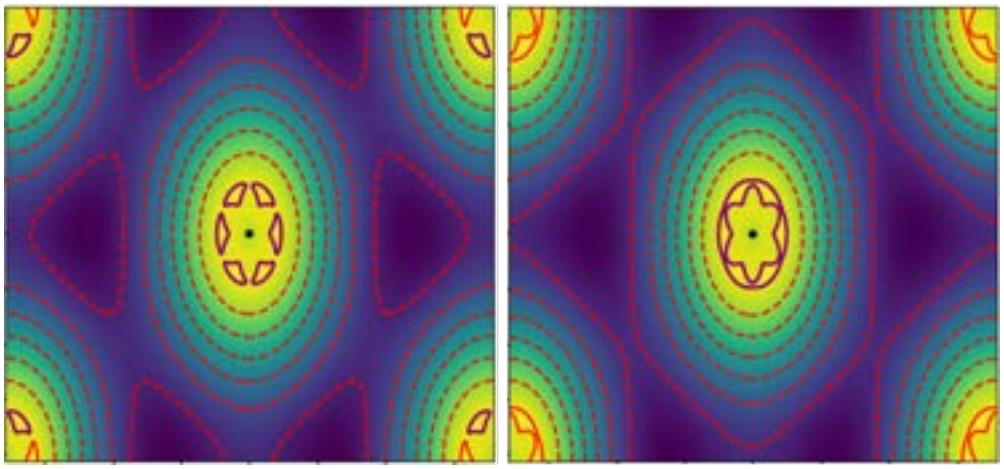

Fig 1: Fermi surface reconstruction within our model upon increasing pressure within the CDW phase.

[1] C. C. Tam, *et al.* Nature Commun. 13, 570 (2021).
[2] W. Tabis, *et al.,* Nature Commun. 5, 5875 (2014).
[3] Ramshaw, B. J. *et al. Science* **348**, 317–320 (2015).
[4] T. M. Rice and G. K. Scott, Phys. Rev. Lett. 35, 2 (1975).
[5] M. D. Watson, *et al.*, Phys. Rev. Lett. 122, 076404 (2019).

Measurement-induced entanglement transitions

Marcin Szyniszewski[1], Oliver Lunt[1,2], and Arijeet Pal[1]

[1]Department of Physics, University College London, Gower Street, London, WC1E 6BT, UK, [2]School of Physics and Astronomy, University of Birmingham, Birmingham, B15 2TT, UK

In the recent few years, the topic of measurement-induced entanglement transitions garnered significant interest [1,2]. This novel type of transition generically occurs (see Fig. 1) when the scrambling unitary evolution is opposed by local measurements, causing the entanglement entropy to change behaviour from extensive (volume law) to sub-extensive (area law). Initially proposed as a toy model similar to many-body localisation transition, now is understood to have tight connections to quantum error correction, and can be used to illuminate entanglement production within certain quantum systems.

In this talk, I will review the topic of entanglement transitions based on a few illustrative examples [2-5]: (1) 1D and 2D Clifford circuits with projective measurements, and (2) free fermions in a random field under continuous measurements. I will show how certain monitored models can be mapped to classical percolation problems, which gives an intuitive understanding behind the transition. Finally, I will draw a crude landscape of groups of universality classes within monitored quantum circuits and identify specific properties, which could be used to deduce which group a particular circuit falls into. This not only brings us closer to a generic understanding of these transitions, but also helps identify important characteristics easily accessible in experimental setups, particularly, in quantum computing.

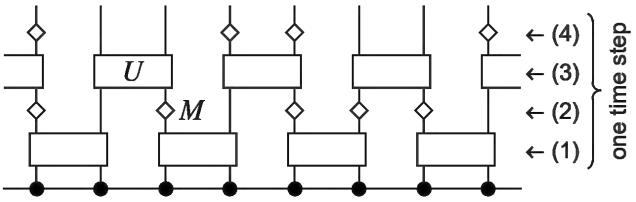

Fig. 1. Example of a monitored quantum circuit. Evolution starts at the bottom of the diagram with a product state, which is then subject to scrambling unitary evolution *U* and local measurements *M*.

[1] Y. Li, X. Chen, M.P.A. Fisher, Phys. Rev. B 98, 205136 (2018); A. Chan, R.M. Nandkishore, M. Pretko, G. Smith, Phys. Rev. B 99, 224307 (2019); B. Skinner, J. Ruhman, A. Nahum, Phys. Rev. X 9, 031009 (2019); Y. Li, X. Chen, M.P.A. Fisher, Phys. Rev. B 100, 134306 (2019).
[2] M. Szyniszewski, A. Romito, H. Schomerus, Phys. Rev. B 100, 064204 (2019).
[3] M. Szyniszewski, A. Romito, H. Schomerus, Phys. Rev. Lett. 125, 210602 (2020).
[4] O. Lunt, M. Szyniszewski, A. Pal, Phys. Rev. B 104, 155111 (2021).
[5] T. Boorman, M. Szyniszewski, H. Schomerus, A. Romito, Phys. Rev. B 105, 144202 (2022).

Evolution of the electronic structure in twisted bilayer transition metal dichalcogenides.

Sumanti Patra[1], Poonam Kumari[1], and Priya Mahadevan[1]

[1]S. N. Bose National Centre for Basic Sciences, India

We have examined the evolution of the electronic structure in twisted bilayers of $MoSe_2$ within ab-initio electronic structure calculations, assuming that the moire potential to be small perturbation to the untwisted limit. In order to examine twisting induced modifications in the electronic structure, we have projected the calculated band structure of the moire cell onto the primitive cell direction which represents the untwisted limit. We found that for large twist angles such as 19.03^o, the low energy electronic structure is identical to the untwisted limit. However, significant deviations have been found for small twist angle near zero degrees such as 3.48^o and also for twist angle near sixty degrees such as 56.52^o where large patches of different high symmetry stackings have been found in the Moire cell. This leads to enhanced interlayer interactions and hence strong perturbation which leads to a flat split off sub band formation [1] of the highest occupied valence band which has bandwidth of 19meV for 3.48^o and vanishingly small bandwidth for 56.52^o. This band is found to be localised in real space as well as momentum space. Examining the electronic structure of twisted bilayer WSe_2 at small twist angles, flat band formation is again seen. The unusual tunability of the electronic structure by an external electric field will also be discussed.

[1] S. Patra, P. Kumari, P. Mahadevan, Phys. Rev. B **102**, 205415 (2020).

Incommensurate time crystals in non-unitary quantum circuits and the link to complex-temperature statistical mechanics

Chris Hooley[1], Sankhya Basu[2], Daniel Arovas[3], Sarang Gopalakrishnan[4], and Vadim Oganesyan[2]

[1]University of St Andrews, UK, [2]City University of New York, USA, [3]University of California San Diego, USA, [4]Penn State University, USA

We present a quantum circuit with measurements and postselection [1] that exhibits a panoply of space- and/or time-ordered phases from ferromagnetic order to spin-density waves to time crystals. Unlike the time crystals that have been found in unitary models, those that occur here are incommensurate with the drive frequency. The period of the incommensurate time-crystal phase may be tuned by adjusting the circuit parameters. We demonstrate that the phases of our quantum circuit, including the inherently nonequilibrium dynamical ones, correspond to complex-temperature equilibrium phases of the exactly solvable square-lattice anisotropic Ising model.

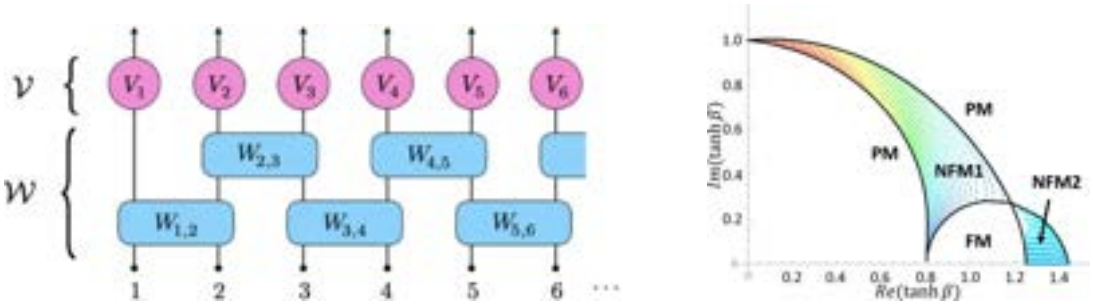

Fig. 1. Left: A sketch of our non-unitary quantum circuit. Right: The phase diagram of the circuit. Phases NFM1 and NFM2 are critical phases exhibiting incommensurate modulations in time and space respectively.

[1] S. Basu, D. P. Arovas, S. Gopalakrishnan, C. A. Hooley, and V. Oganesyan, Phys. Rev. Research **4**, 013018 (2022).

(Invited) Professor Monica Craciun

Title: Engineering the properties of 2D materials for emerging technologies

Abstract: Two-dimensional (2D) materials are emerging systems for applications in electronics and optoelectronics due to their exceptional properties such as high electrical conductivity, optical transparency and mechanical flexibility. These properties can be enhanced or tailored to fit specific device functionalities by chemical functionalization or by combining them in hetero-structures with other materials. In this talk, I will give an overview of our latest developments in engineering 2D materials for applications in novel electronics, photonics and optoelectronics devices. Examples includes the electrical tuning at room temperature of optically active interlayer excitons in 2D semiconductors [Nature Nanotechnology 16, 888 (2021)] and the photo-assisted selective oxidation of the 2D semiconductor HfS2 resulting in its conversion to the high-k dielectric HfOx. This has also enabled the first experimental electrical detection of the inverse charge funnel effect in a strained 2D semiconductor [Nat Comms 9, 1652 (2018)] and the development of nano-scale devices such as transistors, photosensors, light emitting diodes and memories embedding high-k 2D oxides [Sci Adv 5, eaau0906 (2019)].

(Invited) Philip Moll

Field-switchable chiral transport in the Kagome superconductor CsV_3Sb_5

The family AV_3Sb_5 (A=K,Rb,Cs) has shifted into the research focus recently as the chemically clean compounds offer access to a series of electronic correlated states, ranging from charge ordering, superconductivity to rotational symmetry breaking (chirality, nematicity). In addition, time-reversal-symmetry breaking in this has been proposed by muon spectroscopy, despite the absence of large magnetic moments. Furthermore, a mirror-symmetry breaking is observed by scanning tunnelling microscopy (STM), that curiously switches between the enantiomers upon reversing the direction of an applied magnetic field. We probe the out-of-plane transport signatures by Focused Ion Beam machining of micro-wires from cross-sections of the thin, plate-like crystals. These experiments present CsV_3Sb_5 as a rather remarkable correlated conductor, with two unusual properties: First, the in-plane magnetoresistance just above the CDW transition (T~94K) is unmeasurably small, yet it suddenly increases by orders of magnitude once the sample enters the low-temperature state. This highlights the appearance of small, closed 3D Fermi surfaces at the CDW formation, a result of its 3D nature despite the layeredness of the material. Second, under finite magnetic field a strong non-reciprocal transport is observed that points towards a chiral state of the conductor, with an unusually strong coupling of this chiral object to the conduction process. Unlike all other chiral conductors, the enantiomer is not statically selected by the crystal structure, but can be reversed by reversing the field direction – in a phenomenology reminiscent of the STM observations. This points to a strong coupling of a chiral object in the charge ordered state of CsV_3Sb_5 to magnetic fields, in line with the observations of time-reversal symmetry breaking and the consecutive proposals of exotic correlated states such as loop currents.

[1] X. Huang et al., arXiv:2201.07780 (2022)

[2] C. Guo et al., arXiv:2203.09593

James McIver, Independent Max Planck Research Group Leader
Max Planck Institute for the Structure and Dynamics of Matter (MPSD), Hamburg, Germany

Title: Ultrafast optoelectronic probes of quantum materials

Abstract: Ultrafast optoelectronic circuits offer new opportunities for investigating the electrical response of microstructured quantum materials and heterostructures on femtosecond timescales and at terahertz frequencies. Based on waveguides and laser-triggered photoconductive switches, these circuits can be used to directly probe the ultrafast flow of electrical currents in materials [1], or perform near-field spectroscopy on length scales orders of magnitude smaller than the diffraction limit [2]. In this talk, I will show how using this circuitry we observed an anomalous Hall effect in graphene driven by a femtosecond pulse of circularly polarized light [3]. The dependence of the anomalous Hall effect on a gate potential used to tune the Fermi level revealed multiple features that reflect the formation of photon-dressed ('Floquet-engineered') topological band structure [4], similar to the band structure originally proposed by Haldane [5]. This included an approximately 60 meV wide conductance plateau centered at the Dirac point, where a gap of equal magnitude was predicted to open. We found that when the Fermi level was tuned within this plateau, the anomalous Hall conductance saturated around 1.8 ± 0.4 e^2/h.

In the second part of the talk, I will share our progress on using these ultrafast circuits to perform near-field time-domain terahertz spectroscopy on graphene heterostructures, where we observe a coherent plasmonic response that can be tuned with electrostatic gating. This near-field technique, which we are extending to mK temperatures and strong magnetic fields, could be used to investigate a wide range of topological and strongly correlated phenomena in microstructured quantum materials and heterostructures that often fall on the gigahertz-terahertz energy scale.

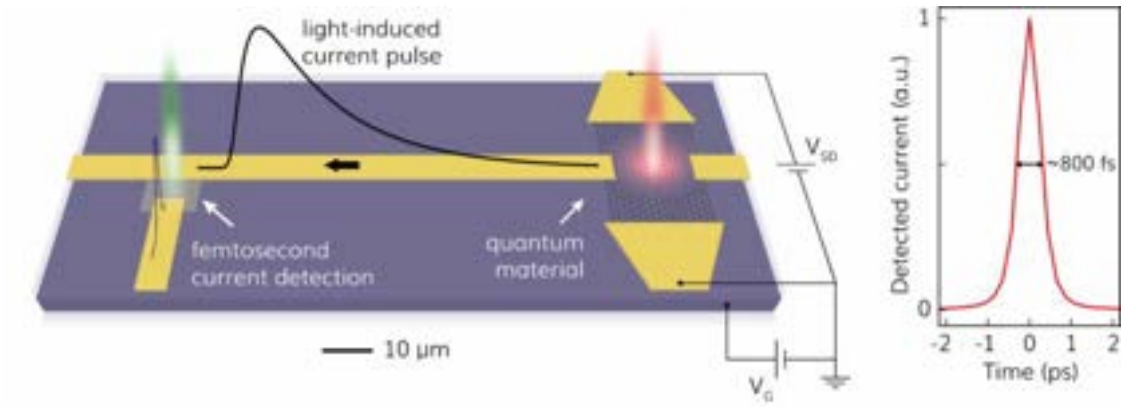

Figure: An ultrafast optoelectronic device architecture based on waveguides and laser-triggered photoconductive switches enables the ultrafast transport properties of quantum materials to be probed on sub-picosecond timescales.

[1] D.H. Auston, *Appl. Phys. Lett.* **26**, 101–103 (1975)
[2] Z. Zhong *et al*., *Nature Nano.* **3**, 201-205 (2008)
[3] J.W. McIver *et al*., *Nature Physics* **16**, 38 (2020)
[4] T. Oka & H. Aoki. *Phys. Rev. B* **79**, 081406 (2009)
[5] F.D.M. Haldane, *Phys. Rev. Lett.* **61**, 2015 (1988)

A study of the Interaction Between H_2, H-ions, SnS_2, and SnS as a Means to Produce SnS_2/SnS Heterostructures

James Felton[1], Elena Blundo[2], Dr. Zakhar Kudrynskyi[1], Dr. Sanliang Ling[1], Dr. Jonathan Bradford[1], Dr. Giorgio Pettinari[3], Prof. Antonio Polimeni[2], Prof. Peter Beton[1], Prof. Gavin Walker[1], and Prof. Amalia Patanè[1]

[1]University of Nottingham, United Kingdom, [2]Sapienza Università di Roma, Italy, [3]Institute for Photonics and Nanotechnologies (CNR-IFN), Italy

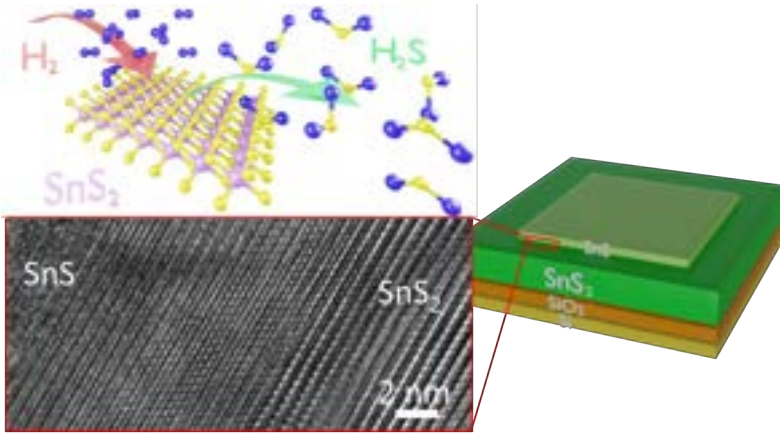

Fig. 1. A schematic of the reaction process and produced heterostructure alongside cross-sectional TEM of the SnS_2/SnS interface

The desire to improve the materials in hydrogen technology related applications and to find methods to process and utilise the unique properties of two-dimensional (2d) materials is driving research into the interactions between these materials and hydrogen. The mechanisms that govern this interaction are diverse and underpin a range of complex behaviours, from the passivation of electrical conductivity by hydrogen to proton exchange in atomically thin membranes essential for fuel cells and photo-catalysis for hydrogen generation. In addition, the ubiquity of H_2 as a processing gas in the semiconductor industry, and its ability to be produced renewably by water electrolysis makes finding methods of processing 2d materials with H_2 desirable.

In addressing these challenges, our work reports on the unique phenomena that arise from the interaction of hydrogen with the 2d semiconductor tin-disulphide (SnS_2), a material that can be produced at low-cost and is non-toxic with applications in electronics, optoelectronics and thermoelectrics. Here, we exploit the ability of hydrogen to bond with sulphur to induce a controlled chemical conversion of SnS_2 into semiconducting-SnS or metallic-Sn. This structural diversity is driven by hydrogen and is made possible by the ability of Sn to bind to S in different oxidation states. These conversions are successfully applied to form SnS_2/SnS heterostructures with uniform layers, atomically flat interfaces and well-aligned crystallographic axes.

Our approach is scalable and offers a route for engineering materials properties at the nanoscale for semiconductor technologies based on earth-abundant elements, such as Sn and S. From our extensive experience of hydrogen interaction with many 2d materials, including metal chalcogenides and well-established studies on metal dichalcogenides, such as MoS_2, it is astonishing that our simple approach yields such high-quality materials and heterostructures.

Two gap time reversal symmetry breaking superconductivity in non-centrosymmetric $LaNiC_2$ single crystals

Shyam sundar[1,6], S R Dunsiger[2], S Gheidi[1], K S Akella[1], A M Côté[1], H U Özdemir[1], N R Lee-Hone[1], D M Broun[1], E Mun[1], F Honda[3], Y J Sato[3], T Koizumi[3], R Settai[4], Y Hirose[4], I Bonalde[5], and J E Sonier[1]

[1]Department of Physics, Simon Fraser University, Canada, [2]CMMS, TRIUMF, Canada, [3]IMR, Tohoku University, Japan, [4]Department of Physics, Niigata University, Japan, [5]Instituto Venezolano de Investigaciones Científicas, Venezuela, [6]Present: University of St. Andrews, UK.

Non-centrosymmetric superconductors lack an inversion center in their crystal structure, one of the typical symmetries for the formation of Cooper pairs. The absence of inversion symmetry strongly influences the allowed Cooper pairing states. Here, we report a muon spin rotation/relaxation (μSR) study of $LaNiC_2$ single crystals. Earlier zero-field μSR measurements on a polycrystalline $LaNiC_2$ sample revealed the onset of spontaneous magnetic fields at T_c [1]. This finding signifies the breaking of time-reversal symmetry (TRS) in the superconducting phase, which is compatible with a non-unitary triplet-pairing state [1]. However, thermodynamic measurements of $LaNiC_2$ have provided evidence for conventional BCS s-wave pairing [2], point nodes in the gap function [3] and even two-gap superconductivity [4]. Consequently, the nature of the superconducting energy-gap structure in this compound has remained unsettled.

Our detailed μSR investigation of $LaNiC_2$ was carried out on a sample in single crystal form. From measurements that probe the magnetic field distribution in the vortex state, we have simultaneously determined the behaviors of the absolute value of the magnetic penetration depth and the vortex core size. The magnetic field dependence of these two quantities unambiguously demonstrates the presence of two nodeless superconducting energy gaps [5]. In addition, we have confirmed broken TRS in the superconducting phase of $LaNiC_2$ [5]. These two results suggest that Cooper pairing in $LaNiC_2$ is characterized by an interorbital equal-spin pairing model introduced to unify the pairing states of $LaNiC_2$ and the centrosymmetric superconductor $LaNiGa_2$.

[1] A. D. Hillier et al. Phys. Rev. Lett. 102, 117007 (2009).

[2] V. K. Pecharsky et al., Phys. Rev. B 58, 497 (1998).

[3] W. H. Lee et al., Physica C 266, 138 (1996).

[4] J, Chen et al., New J. Phys. 15, 053005 (2013).

[5] Shyam Sundar et al., Phys. Rev. B 103, 014511 (2021).

Spread of Fermi-edge singularity in time and space as time delayed interaction and impact on RKKY type coupling and decoherence between quantum states

Bernd Braunecker and Conor Jackson

University of St Andrews

Fermi-edge singularity and Anderson's orthogonality catastrophe are paradigmatic examples of non-equilibrium many-body physics in conductors, appearing after a quench is created by the sudden change of a localized potential. Although the global response of these effects has been studied since more than half a century [1,2], the spatially and temporally resolved spread has received little attention.

We investigate here this spread under the aspect of transmitting a long ranged interaction, reminiscent of the RKKY interaction, but with the inclusion of the full many-body propagation over space and time [3]. We furthermore make a link to the requirements of quantum information processing and examine the possibility of using the quench to couple two distant quantum states through a quantum wire, as shown in the Figure below. To this end we also formulate the Fermi-edge quench in an open quantum system language by treating the quench as a correlated bath response acting on the reduced density matrix of a discrete quantum system.

Through this formalism we show that the Fermi-edge quench has the dual effect of building up and decohering entanglement between the quantum state. Maintaining coherence between the distant states is indeed only possible with finely tuned interaction between the discrete states and the conductor. Thus the triggering of Fermi-edge quenches in any device used for quantum processing should generally be avoided. As this is in opposition to desired ultra-fast quantum operations it should be taken into consideration when designing quantum gates.

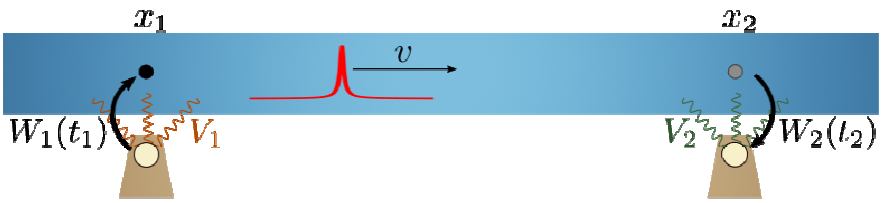

Fig. 1. Representation of the propagating Fermi-edge signal in a conductor coupling two quantum states at positions x_1 and x_2, analysed at times t_1 and t_2 [3].

[1] G. D. Mahan, Phys. Rev. **163**, 612 (1967).
[2] P. W. Anderson, Phys. Rev. **164**, 352 (1967).
[3] C. Jackson and B. Braunecker, Phys. Rev. Res. **4**, 013119 (2022).

Synthesis of MoS_2 and ZnS Thin Films via Aerosol-Assisted Chemical Vapor Deposition

Nilanthy Balakrishnan[1], Lewis Adams[1], and Peter D. Matthews[1]
[1] School of Chemical and Physical Sciences, Keele University, Keele, Staffordshire, ST5 5BG, United Kingdom

Transition metal dichalcogenides (TMDCs) are versatile two-dimensional (2D) materials that have unique optical and electronic properties. Amongst them, molybdenum disulfide (MoS_2) and zinc sulfide (ZnS) have attracted attention due to their semiconductor nature. Remarkably, MoS_2 shows a thickness-dependent bandgap that ranges from 1.2 eV for bulk (indirect bandgap) to 1.9 eV for monolayer (direct bandgap). Furthermore, ZnS exhibits a similar property with a large bandgap from 3.26 eV to 3.7 eV. Band gap of these materials laying from the near infrared to visible and ultraviolet range of the electromagnetic spectrum potentially make them suitable for photodetectors and photovoltaics [1]. Various deposition techniques such as, physical vapor deposition (PVD) and chemical vapor deposition (CVD) have been successful growth methods of monolayer MoS_2 [2]. However, these methods have had limited success in the synthesis of crystalline 2D ZnS thin films. Moreover, there are still great challenges on scalable production in terms of large-area uniform growth.

Here we demonstrate that the epitaxial growth, by an Aerosol-Assisted Chemical Vapor Deposition (AACVD) method, [3] results in large area coverage (~1 cm^2) of MoS_2 on sapphire and Silicon dioxide (SiO_2) substrates. The morphology and thickness of MoS_2 can be tuned by precursor concentration and/or growth temperature allowing for the engineering of different structures such as, nanorods, snowflake-like structures (Figure 1) and 2D layers as thin as 40 nm. The AACVD method is also successful in the synthesis of ZnS thin films of 400 nm thickness. The growth of 2H-MoS_2 and Wurtzite ZnS was confirmed by X-ray diffraction (XRD), Raman and electron dispersive X-ray spectroscopies. XRD analysis indicates that the MoS_2 structures, grown on SiO_2, are under strain compared to those grown on sapphire substrates. However, the type of the substrate and/or the substrate induced strain does not affect the growth of different morphologies [4]. On the other hand, ZnS crystalline growth can only be successfully achieved on smooth surfaces such as, sapphire and exfoliated Indium selenide layers on SiO_2 indicating substrate dependency [4]. The successful growth of 2H-MoS_2 and Wurtzite ZnS offer the prospect for large-area device fabrication that exploit distinctive optical and electronic properties.

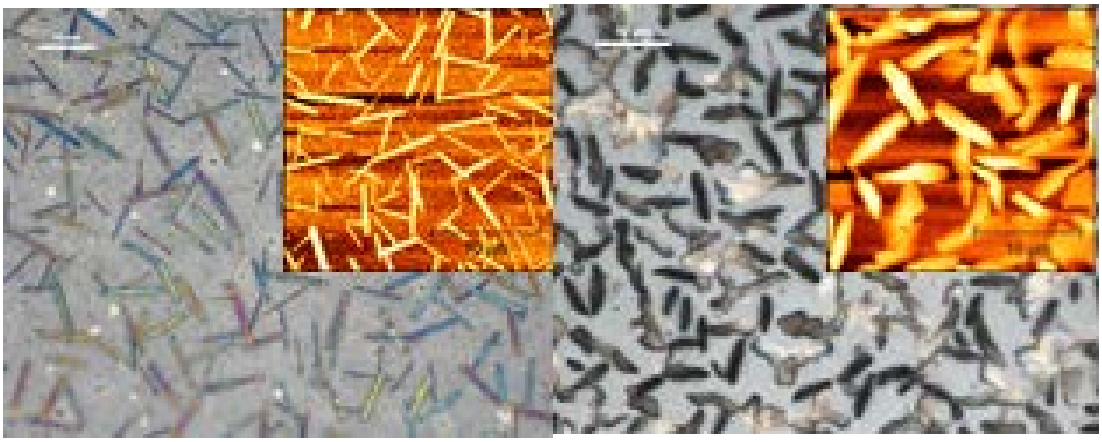

Fig. 1. Optical and AFM image of MoS_2 nanorods (left) and snowflake-like structures (right) on glass substrates.

[1] J. Zhu *et al.*, RSC Adv., **112**, 110604 (2016).
[2] Y. Xie *et al.*, Nanotechnology, 28, 084001 (2017).
[3] A. A.Tedstone *et al.*, Chem. Mater., 9, 3858 (2017).
[4] L. Adams *et al.*, unpublished.

!"#$%&'() '*+$#,*$&&-(,#."*'.(+-/0'1'/,/(,#(/"/2'#.'.(34/'2+/4#(5"#*0,4#/(

!"#$%&'%&($)*%!+&,-.#"/&O12%3#.44"+&"*5&63./&O"3$"*$!#

!7*$8%3/$49&.:&6;%4%3+&7*$4%5&<$*)5.#+&"7*$8%3/$49&.:&="3/">+&?.@"*5&

,-%& 1.AB@$*)&.:& /AB%31.*5A14$*)& /9/4%#/&4.& #%1-"*$1"@& 3%/.*"4.3/& $/& "*& %#%3)$*)& :$%@5+& >$4-& $#B@$1"4$.*/& /B"**$*)&:3.#& B3%1$/$.*& #%"/A3%#%*4& 4.& 4-%& A*5%3/4"*5$*)& .:& -$)-& 4%#B%3"4A3%& /AB%31.*5A14$8$49C&6;B%3$#%*4"@&/$)*"4A3%/&.:&4-$/&1.AB@$*)&-"8%&/.&:"3&D%%*&/#"@@+&/%@5.#+&"*5&.:4%*& 3%@$"*4& .*& -$)-& :3%EA%*19& FG& %@%143.*$1/C& H*& /4"3I& 1.*43"/4+& $*& 4-$/& >.3I& >%& A*8%$@& /43.*)& %@%143.#%1-"*$1"@&%::%14/&$*&BA3%@9&2G&1A33%*4JD$"/%5&/A/B%*5%5&!./%B-/.*&KA*14$.*/&:.3#%5&D9&"& #%1-"*$1"@&3%/.*"4.3&/A/B%*5%5&D%4>%%*&/AB%31.*5A14$*)&1.*4"14/&LM$)CNL"OO&PN+QRC&H*&4-$/&/9/4%#&4-%& %@%143.*$1&1A33%*4/&1"*&D%&1.AB@%5&4.&#%1-"*$1"@&#.4$.*&8$"&4-%&'.3%*4S&:.31%&5A%&4.&"*&$*JB@"*%& #")*%4$1&:$%@5&4.&$*5A1%&#%1-"*$1"@./1$@@"4$.*/&PTRC&

=%&/4A59&4-$/&/9/4%#&8$"&4-%&UG(!&#.5%@&PVR&"*5&/-.>&D.4-&"*"@94$1"@@9&"*5&*A#%3$1"@@9&4-"4&4-$/& 1.AB@$*)&B3.5A1%/&"&#%1-"*$1"@@9&$*5A1%5&-9/4%3%/$/&@..B&$*&4-%&KA*14$.*W/&2G&HX&1-"3"14%3$/4$1C&=%& A*8%$@&-.>&4-$/&*%>&-9/4%3%/$/&#"9&D%&%;B@.$4%5&4.&"11%//&"@")%&#%1-"*$1"@@9&$*5A1%5&(-"B$3.J@$I%& PYR&8.@4")%&B@"4%"A&LM$)CNLDOO+&%;4%*5$*)&.8%3&"&1A33%*4&3"*)%&.:&"BB3.;$#"4%@9&-"@:&4-%&KA*14$.*W/& 13$4$1"@&1A33%*4+&AB.*&>-$1-&#%1-"*$1"@&3%/.*"*1%&$/&B.*4"*%.A/@9&%;1$4%5C&&

ZA#%3$1"@&%;B%3$#%*4/&"4&/43.*)&1.AB@$*)&3%8%"@&"&3"*)%&.:&/A55%*&#%1-"*$1"@@9&$*5A1%5&3%43"BB$*)& %8%*4/+&4-"4&#"9&1A34"$@&4-%&#%1-"*$1"@&B@"4%"A&.3&B3%8%*4&"11%//&%*4$3%@9C&F*"@94$1"@&$*8%/4$)"4$.*& B3.8$5%/&D.4-&"&EA"@$4"4$8%&%;B@"*"4$.*&:.3&4-%&":.3%#%*4$.*%5&D%-"8$.3/+&"*5&EA"*4$4"4$8%& 3%@"4$.*/-$B/&D%4>%%*&13$4$1"@&1.AB@$*)&/43%*)4-/&"*5&4-%&#%1-"*$1"@&3%/.*"*1%&:3%EA%*19&"*5&EA"@$49& :"14.3+&%*"D@$*)&5%8$1%&1-"3"14%3$S"4$.*C&=%&#B-"/$S%&4-"4&.A3&B3%5$14$.*/&1"*&D%&3%"@$S%5&A/$*)&.*@9& 2G&1A33%*4&D$"/&"*5&8.@4")%&#%"/A3%#%*4/+&>$4-&#")*%4$1&:$%@5/&"*5&4%#B%3"4A3%/&"44"$*"D@%&$*& 1.##%31$"@&139./4"4/C&&

&

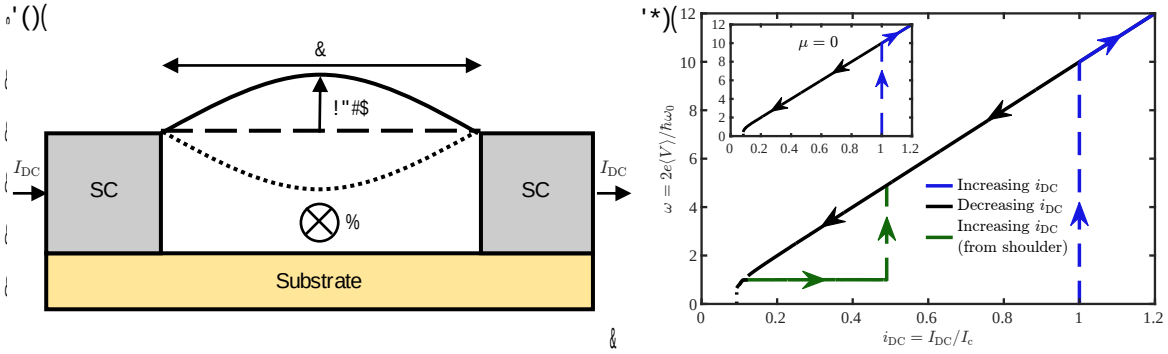

&

!"#$%&$!"#$!%&'()#*+&!,-!#!./.0(12(2!3,.(0'.,1!4/1&*+,15!6'(!-7,8!,-!&/99(1*!*'9,/:'!*'(!8(#;!7+1;!09,2/&(.!#! <,9(1*=!-,9&(!2/(!*,!*'(!)#:1(*+&!-+(72!!>!&#/.+1:!)(&'#1+&#7!2+.07#&()(1*!,-!*'(!8(#;!7+1;5!"?$!@/)(9+&#7!AB! &'#9#&*(9+.*+&!,-!#!./.0(12(2!4/1&*+,1>!9(C(#7+1:!#1*!)(&'#1+&#7!07#*(#/D'E.*(9(.+.!7,,0!2/(!*,! .E1&'9,1+=#*+,1!8+*'!.0,1*#1(,/.7E!(F&+*(2!)(&'#1+&#7!,.&+7#*+,1.5!A1.(*C!AB!&'#9#&*(9+.*+&!+1!*'(!#?.(1&(!,-!) (&'#1+&#7!&,/07+1:5!!

PNR&& [C&2C&!./%B-/.*+&?-9/C&'%44C&6+&QYN&LN\]QOC&
PQR&& ZC&O$SA*.+&[C&Z$%@/%*+&"*5&^C&2A+&Z"4C&G.##A*C&7+&N&LQ_NTOC&
PTR&& (C&64"I$+&MC&<.*/1-%@@%+&`C&OC&[@"*4%3+&aC&`"#")A1-$+&"*5&aC&(C&!C&8"*&5%3&b"*4+&Z"4C&G.##A*C&7+& Nc_T&LQ_NTOC&
PVR&& ,C&O12%3#.44+&aC&`C&2%*)+&FC&H/"1//.*+&"*5&6C&O"3$"*$+&?-9C&U%8+&[&89+&NVYQ]&LQ_NcOC&
PYR&& (C&(-"B$3.+&?-9/+&U%8C&'%44C&66+&c_&LN\]TOC!!

Non-equilibrium thermoelectric transport across normal metal-Quantum Dot-Superconductor hybrid system within the Coulomb blockade regime

Sachin Verma[1] and Ajay Singh[1]

[1] Department of Physics, Indian Institute of Technology, Roorkee, Uttarakhand, 247667, India

We have investigated the non-equilibrium steady-state electric and thermoelectric transport properties of a quantum dot (QD) coupled to the normal metallic and s-wave superconducting reservoirs (N–QD–S) within the Coulomb blockade regime. Using non-equilibrium Keldysh Green's function formalism, initially, various model parameter dependences of thermoelectric transport properties are analysed within the linear response regime. It is observed that the single-particle tunnelling close to the superconducting gap edge can generate a relatively large thermopower and figure of merit. Moreover, the Andreev tunnelling plays a significant role in the suppression of thermopower and figure of merit within the gap region. Further, within the non-linear regime, we discuss two different situations, i.e., the finite voltage biasing between isothermal reservoirs and the finite thermal gradient in the context of thermoelectric heat engine. In the former case, it is shown that the sub-gap Andreev heat current can become finite beyond the linear response regime and play a vital role in asymmetric heat dissipation and thermal rectification effect for low voltage biasing. The rectification of heat current is enhanced for strong on-dot Coulomb interaction and at low background thermal energy. In the latter case, we study the variation of thermovoltage, thermopower, maximum power output, and corresponding efficiency with the applied thermal gradient. These results illustrate that hybrid superconductor–QD nanostructures are promising candidates for the low-temperature thermal applications.

The research work can be found in the reference:

[1] Sachin Verma and Ajay Singh, **Journal of Physics: Condensed Matter 34,** 155601, ***(2022)***

Probing light-driven superconductors with ultrafast resonant inelastic x-ray scattering

Matteo Mitrano[1]

[1]Department of Physics, Harvard University, USA

Ultrafast optical excitation, especially when resonant to specific lattice modes, has recently emerged as a powerful means to control and induce new functionalities in quantum materials. One of the most ambitious goals is to selectively drive structural or electronic degrees of freedom to bring about nonequilibrium superconductivity at temperatures far above the equilibrium critical temperature T_c. While this phenomenon has been observed in a variety of systems ranging from copper oxides to organic molecular metals, the microscopic physics of these dynamics is still largely unexplored. By focusing on the paradigmatic example of light-driven $La_{2-x}Ba_xCuO_4$, I will show how the newly developed technique of time-resolved resonant inelastic X-rays scattering (trRIXS) provides an unprecedented route to probe the finite-momentum excitation spectrum of these transient phases (see Fig. 1) [1,2,3]. Furthermore, I will discuss how intense fields are conducive to a dynamical renormalization of the Hubbard U in the CuO_2 plane [4] and how these electronic changes can affect the finite-momentum spin fluctuation spectrum detected in trRIXS experiments [5].

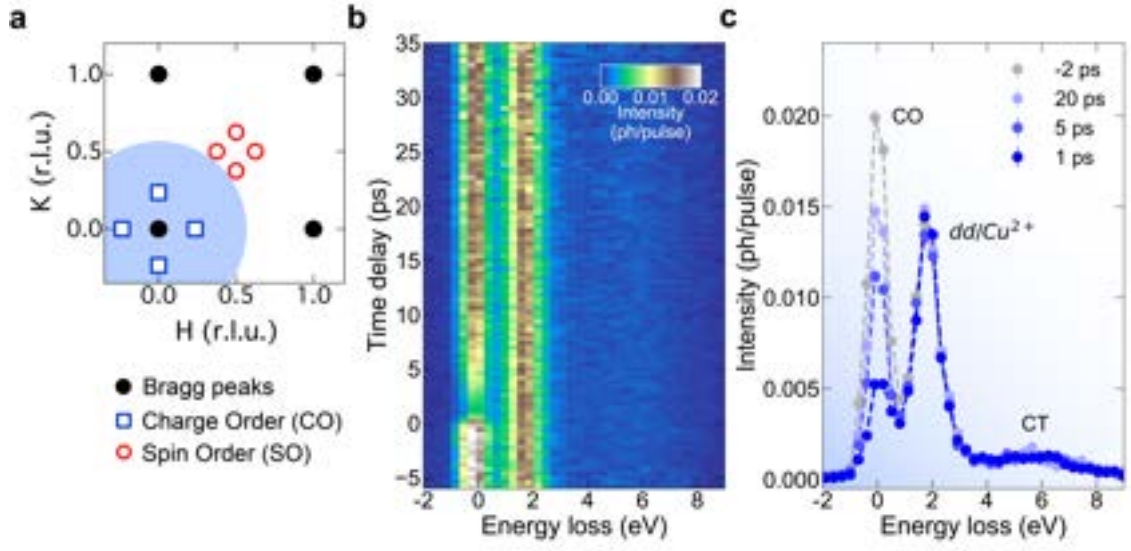

Fig. 1. Charge order melting in $La_{2-x}Ba_xCuO_4$. **a** Reciprocal space map of structural Bragg peaks, charge order (CO) and spin order (SO) peaks in $La_{2-x}Ba_xCuO_4$. The blue area represents the maximum momentum transfer achievable at the Cu L-edge (931 eV). The location of peaks in momentum space is denoted by the Miller indices (H,K,L) and expressed in reciprocal lattice units (r.l.u.); **b** Time-resolved resonant inelastic X-ray scattering (trRIXS) spectra of photoexcited $La_{1.875}Ba_{0.125}CuO_4$ at Q_{CO} = (0.236; 0, 1.5) r.l.u. at the Cu L-edge for variable pump-probe time delay; **c** trRIXS spectra for a selection of time delays showing a prompt melting of the CO, while higher energy features of the inelastic spectrum remain unaffected. From [3].

[1] M. Mitrano, *et al.*, Sci. Adv. **5**, eaax3346 (2019).
[2] M. Mitrano, *et al.*, Phys. Rev. B **100**, 205125 (2019).
[3] M Mitrano & Y. Wang, Commun. Phys. **3**, 184 (2020).
[4] D. R. Baykusheva, *et al.,* Phys. Rev. X **12**, 011013 (2022).
[5] Y. Wang, *et al.*, Commun. Phys. **4**, 212 (2021).

Liam Turnpenny, Kristian Reed-Spargo, and Adelina Ilie

Department of Physics/University of Bath, UK

Transition metal dihalides are a less studied class of layered semiconductors that are predicted to exhibit a plethora of magnetic/spin textured and multiferroic properties that depend whether they are in single, few-layer or bulk form. Here we focus on NiI_2: this is predicted to be ferromagnetic in the monolayer limit [1] and shown to undergo a phase transition to helimagnet order with ferroelectric polarization in the bulk [2].

In this work we show successful growth of NiI_2 on Au(111) by molecular beam epitaxy in an ultra-high vacuum environment, and its characterization predominantly via atomically-resolved scanning tunneling microscopy and spectroscopy (STM/STS) at low-temperature. Single layer NiI_2 forms predominantly, accompanied by bi- and tri-layer islands depending on the growth conditions. A beneficial, decoupling "buffer" layer exists at the interface with the Au(111) substrate.

Electronic characterization using STS demonstrates the semiconductor nature of the single- to three-layer NiI_2 systems; and the presence of a predicted magnetic band deriving from the Ni d orbitals, together with its evolution with the number of layers. From the latter, information about the interlayer coupling is also derived. Finally, atomic-scale defects and domain grain boundaries in this material are identified and their electronic fingerprints obtained. Links to magnetic properties are discussed.

[1] A.S. Botana, M.R. Norman, Phys. Rev. Mat. , 044001 (2019).
[2] T. Kurumaji, *et al.*, Phys. Rev. B. , 014429 (2013).

Quantum oscillations in heavy-fermion ferromagnet $YbNi_4P_2$ over many Zeeman induced Lifshitz transitions

Will Broad[1], Sven Friedemann[1], Owen Moulding[1], Takaki Muramatsu[1], Kristin Kliemt[2] and Cornelius Krellner[2]

[1]HH Wills Physics Laboratory University of Bristol, UK, [2]Physikalisches Institut, Johann Wolfgang Goethe-Universität, Frankfurt am Main, Germany

$YbNi_4P_2$ is a heavy-fermion Kondo-lattice metal situated near a very rare ferromagnetic quantum critical point (FM QCP) [1]. Understanding the nature of this ferromagnetism requires knowledge of the Fermi surface; it has been speculated that this FM QCP is due to a quasi-1D Fermi surface [2]. At the same time, the strongly renormalised bandstructure is readily modified by relatively small magnetic fields, with nine Lifshitz transitions (abrupt topological changes in the Fermi surface) below 20 T due to Zeeman energy shifts [3].

Here we present quantum oscillations in resistivity and Hall effect of $YbNi_4P_2$ up to 35T, including detailed rotation and mass studies. We present analysis over several of these Lifshitz transitions, observing frequency changes and appearances/disappearances using moving window FFT and Landau indexing. Notably, we observe large frequencies $\sim$6 kT indicative of large Fermi surfaces due to Kondo hybridisation gaps near the Fermi level, and large cyclotron masses $\sim 7\ m_0$ and $\sim 12\ m_0$ from the heavy fermions.

To work towards the zero field Fermi surface of $YbNi_4P_2$, we model the bandstructure of the non-heavy fermion reference compound $LuNi_4P_2$ then extract the expected frequencies at a variety of rigid-band shifts. With these predictions we gain insight in to the shape of the Fermi surface observed, and the Lifshitz transitions it undergoes. Finally, we consider a few scenarios for Lifshitz transitions and, through the use of several toy models, how the measured frequencies should evolve a function of field.

[1] A. Steppke *et al.*, Science **339**, 6122:933-936 (2013).
[2] M. Brando *et al.*, Rev. Mod. Phys. **88**, 025006 (2016).
[2] H. Pfau *et al.*, Phys. Rev. Letters **119**, 126402 (2017).

Spin Transport in Boundary-Driven Tilted Systems: Ferromagnetic Domains and Giant Rectification

Juan José Mendoza-Arenas[1], Stephen R. Clark[1]

[1]H. H. Wills Physics Laboratory, University of Bristol, United Kingdom

The recent prediction [1,2] and experimental implementation [3] of Stark many-body localization has led to a massive interest on the physics of insulating states in clean tilted systems. Motivated by these advances, we study the high-temperature transport properties of a spin-1/2 XXZ chain in the presence of a tilted potential, driven to a nonequilibrium configuration by unequal reservoirs at its boundaries. In the noninteracting limit we describe an exact solution for the spin current and magnetization profile, and show that at maximal driving a size-dependent tilt induces an insulating state characterized by ferromagnetic domains of opposite polarization pinned to the edges of the system. Furthermore, we develop a perturbative solution that provides a physical picture for the emergence of this state. Based on this approach and on numerical calculations, we show that turning on nearest-neighbor interactions leads to a transport asymmetry, enhancing the domains and thus decreasing the current for forward boundary driving and degrading the domains for reverse driving. Finally, we discuss how strong current resonances emerge in the latter case for particular interaction strengths, as a result of large coherences at avoided crossings of Hamiltonian eigenstates. These results lead to a novel mechanism for inducing giant rectification, which can be implemented in state-of-the-art quantum simulators.

[1] E. Van Nieuwenburg *et al*., Proc. Natl. Acad. Sci. USA **116**, 9269 (2019).
[2] M. Schulz *et al*., Phys. Rev. Lett. **122**, 040606 (2019).
[3] W. Morong *et al*., Nature **599**, 393 (2021).

Behavior of Li-ion on the surface of Ti_3C_2–T (T = O, S, Se, F, Cl, Br) MXene: Diffusion barrier and conductive pathways

Konstantina A. Papadopoulou[1], David Parfitt[1], Alexander Chroneos[1,2], and Stavros-Richard G. Christopoulos[1]

[1]Faculty of Engineering, Environment and Computing, Coventry University, Priory Street, Coventry CV1 5FB, United Kingdom
[2]Department of Materials, Imperial College London, London SW7 2BP, United Kingdom

After obtaining Ti_3C_2 MXene structures terminated with O, S, Se, F, Cl, and Br, we calculate the energy barrier for Li-ion diffusion on the surface of each MXene, being the first to report on the Li-ion diffusivity in Cl and Br terminated Ti_3C_2. We find that the $Ti_3C_2Cl_2$ MXene has the lowest diffusion barrier, substituting the $Ti_3C_2S_2$ reported in the literature so far. In addition, a study on the adsorption energies indicates that the top binding position is the most stable adsorption position for the Li-ion. Furthermore, it is shown that the adsorption energy depends on the electronegativity of the termination atoms, as well as the distance between the terminations, the Li, and the surface Ti-atoms. Finally, we show that the bond valence sum method provides an indication of the transition state of the Li-ion and can serve as a comparison tool for the diffusion barriers of different structures.

Fig. 1. (a) CMQM (Condensed Matter and Quantum Materials) 2020 Conference banner; (b) The venue for the meeting in London.

Atomic-scale imaging of emergent order at a magnetic-field-induced Lifshitz transition

Carolina A Marques, [1] Luke C Rhodes, [1] Izidor Benedičič, [1] Masahiro Naritsuka, [1] Aaron B Naden, [2] Zhiwei Li, [3] Alexander C Komarek, [3] Andrew P Mackenzie, [3,1] Peter Wahl [1]

[1]SUPA, School of Physics and Astronomy, University of St Andrews, St Andrews, UK
[2]School of Chemistry, University of St Andrews, St Andrews, UK
[3]Max Planck Institute for Chemical Physics of Solids, Dresden, Germany

Strongly correlated phases, such as superconductivity, metamagnetism and electronic nematicity are often found in close proximity to a quantum critical point. To understand how such phases arise, are stabilised and clarify the role of quantum fluctuations and how to manipulate them, we require detailed knowledge about the low energy electronic structure of these systems on a sub-millielectronvolt energy scale.

One example of such a system which shows evidence for a quantum critical point is the layered perovskite $Sr_3Ru_2O_7$, which is known to undergo a series of metamagnetic transitions and exhibits a pronounced transport anisotropy suggesting a breaking of C_4 symmetry at a magnetic field of 8 T. Using ultra-low temperature scanning tunnelling microscopy, we find that the surface layer of $Sr_3Ru_2O_7$ already exhibits a strongly C_2 symmetric electronic structure, even at zero magnetic field, Fig. 1. Under the application of out-of-plane field, we find that the surface undergoes a Lifshitz transition at 11 T, accompanied by the emergence of a zig-zag charge stripe order. Our results reveal that the surface layer of $Sr_3Ru_2O_7$ exhibits strikingly similar, yet distinct, phenomena compared to the bulk material, which can be used to uncover the physics of a metamagnetic quantum critical point. Our results allow us to track the changes in the low energy electronic structure as a function of magnetic field across the Lifshitz transition.

Additionally, we also compare and contrast the electronic structure uncovered for the surface of $Sr_3Ru_2O_7$ with the surface electronic structure of the unconventional superconductor Sr_2RuO_4[2,3], highlighting the phenomenal impact of minor octahedral rotations and bilayer interactions in the stabilisation of unconventional superconductivity.

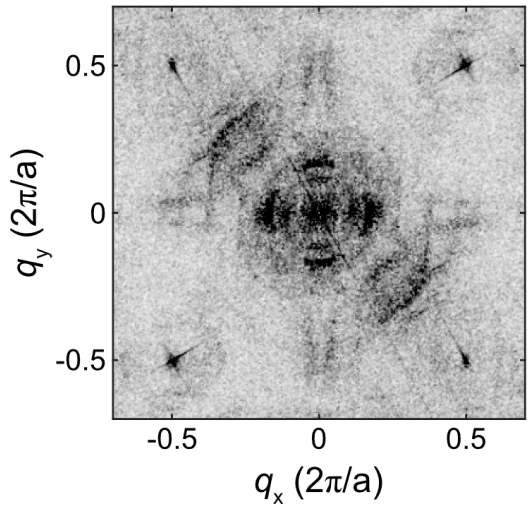

Fig. 1. Fourier transform of a differential conductance spectroscopic map at -0.3 mV, showing highly C2 symmetric quasiparticle interference patterns.

[1] C. A. Marques *et al.*, arXiv:2202.12351 (2022)
[2] C. A. Marques *et al.*, Adv. Mater. 33, 2100593 (2021)
[3] A. Kreisel *et al.*, npj Quantum Mater. 6, 100 (2021)

Quantum many-body scars have extensive multipartite entanglement

Jean-Yves Desaules[1], Francesca Pietracaprina[2], Zlatko Papić[1], John Goold[2], Silvia Pappalardi[3]

[1]University of Leeds, United Kingdom, [2]Trinity College Dublin, Republic of Ireland , [3]Laboratoire de Physique de l'Ecole Normale Supérieure, Paris, France

Recent experimental observation of weak ergodicity breaking in Rydberg atom quantum simulators has sparked interest in quantum many-body scars - eigenstates which evade thermalisation at finite energy densities due to novel mechanisms that do not rely on integrability or protection by a global symmetry. A salient feature of quantum many-body scars is their sub-volume bipartite entanglement entropy. In this work we demonstrate that exact many-body scars also possess extensive multipartite entanglement structure. We show this analytically, through a scaling of the quantum Fisher information density, which is found to be extensive for scarred eigenstates in contrast to generic thermal states. Furthermore, we numerically study signatures of multipartite entanglement in the PXP model of Rydberg atoms, showing that extensive quantum Fisher information can be generated dynamically by performing a global quench experiment. Our results identify a rich multipartite correlation structure of scarred states with significant potential as a resource in quantum enhanced metrology.

Identifying the CDW ground state and its associated gap(s) in topographic STM images

Á. Pásztor,[1] A. Scarfato,[1] F. Flicker,[2] J. van Wezel,[3] D.R. Bowler,[4] Ch. Renner,[1]

[1]Department of Quantum Matter Physics, University of Geneva, 24 Quai Ernest-Ansermet, CH-1211 Geneva 4, CH

[2]School of Physics and Astronomy, Cardiff University, Cardiff CF24 3AA, UK

[3]Amsterdam and Delta Institute for Theoretical Physics, University of Amsterdam, Science Park 904, 1098XH Amsterdam, NL

[4]London Centre for Nanotechnology and Department of Physics and Astronomy, University College London, London WC1E 6BT, UK

Charge density waves (CDWs) are the subject of renewed interest to understand their structure, their formation mechanism(s) and their interplay with other quantum phases such as superconductivity and magnetism. Many models developed over the years often fail to fully describe specific experimental data sets, with embodiments of the classic Peierls Fermi surface nesting scenario being the exception rather than the rule. We will present recent scanning tunneling microscopy investigations, which provide new insight into the CDW gap, including its multiband nature. We will address the ongoing challenge in measuring the CDW gap by tunneling spectroscopy and in identifying the CDW ground state in topographic STM images. Not every periodic charge modulation imaged by STM is a CDW, and identifying the CDW gap in tunneling spectra remains highly controversial.

Á. Pásztor, A. Scarfato, M. Spera, F. Flicker, C. Barreteau, E. Giannini, J. v. Wezel and C. Renner, *Multiband charge density wave exposed in a transition metal dichalcogenide*, Nature Communications **12**, 6037 (**2021**)

M. Spera, A. Scarfato, Á. Pásztor, E. Giannini, D. R. Bowler and C. Renner, *Insight into the Charge Density Wave Gap from Contrast Inversion in Topographic STM Images*, Physical Review Letters **125**, 267603 (**2020**)

Á. Pásztor, A. Scarfato, M. Spera, C. Barreteau, E. Giannini and C. Renner, *Holographic imaging of the complex charge density wave order parameter*, Physical Review Research **1**, 033114 (**2019**)

Relating spin-polarized STM imaging and inelastic neutron scattering in the van-der-Waals ferromagnet Fe_3GeTe_2

Olivia R. Armitage[1], Christopher Trainer[1], Harry Lane[2,3], Luke C. Rhodes[1], Edmond Chan[2,4], Izidor Benedičič[1], J. A. Rodriguez-Rivera[5,6], O. Fabelo[4], Chris Stock[2] and Peter Wahl[1]

[1]University of St Andrews, United Kingdom, [2]University of Edinburgh, United Kingdom
[3]ISIS Pulsed Neutron and Muon Source, United Kingdom, [4]Institute Laue-Langevin, France,
[5]National Institute of Standards and Technology, USA, [6]University of Maryland, USA

Van-der-Waals (vdW) ferromagnets have enabled the development of heterostructures assembled from exfoliated monolayers with spintronics functionalities, making it important to understand and ultimately tune their magnetic properties at the microscopic level. Information about the magnetic properties of these systems comes so far largely from macroscopic techniques, with little being known about the microscopic magnetic properties. Here, we combine spin-polarized scanning tunneling microscopy and quasi-particle interference imaging with neutron scattering to establish the magnetic and electronic properties of the metallic vdW ferromagnet Fe_3GeTe_2. By imaging domain walls at the atomic scale, we can relate the domain wall width to the exchange interaction and magnetic anisotropy extracted from the magnon dispersion as measured in inelastic neutron scattering, with excellent agreement between the two techniques. From comparison with Density Functional Theory calculations we can assign the quasi-particle interference to be dominated by spin-majority bands. We find a dimensional dichotomy of the bands at the Fermi energy: bands of minority character are predominantly two-dimensional in character, whereas the bands of majority character are three-dimensional. We expect that this will enable new design principles for spintronics devices.

Field effect in superconductors: Reality or Delusion?

I. Golokolenov[1,2,3], A. Guthrie[1], S. Kafanov[1], Yu. A. Pashkin[1], and V. Tsepelin[1]

[1]Department of Physics, Lancaster University, Lancaster, LA1 4YB, United Kingdom, [2] P. L. Kapitza Institute for Physical Problems of RAS, Moscow, 117334, Russia; [3]National Research University Higher School of Economics, Moscow 101000, Russia

There was a lot of controversy recently caused by the claims that the field effect exists in superconductors [1-4]. The effect was attributed to the observed suppression of the critical current in superconducting and proximized normal-metal nanowires under intense electric fields. On the other hand, a number of papers published last year provide a different explanation of the observed effect as being due to the local suppression of superconductivity by energetic quasiparticles injected at high gate voltages [5-7].

In my talk, after a brief introduction, I will present our results on studying the properties of superconducting coplanar quarter-wavelength waveguide resonators [7]. The resonators were formed in a vanadium film and grounded through a gated nanoscale constriction about 50 nm wide and 50 nm long. We have found that at high enough gate voltage, $|V_g| > 25$ V, the resonance frequency starts to fall, which is accompanied by the decrease of the quality factor and increase of the low-frequency noise. At the same time, the leakage current between the gate and constriction grows rapidly and perfectly follows the Fowler-Nordheim model of electron field emission from a metal electrode [8]. The effect is bipolar and can be explained by the injection of high-energy quasiparticles resulting in weaker superconductivity and suppression of the critical current of the constriction. This interpretation, also proposed in the publications by other groups [5,6], refutes the existence of the field effect in superconductors [1-4].

[1] G. De Simoni et al., Nat. Nanotechnol. **13**, 802 (2018).
[2] F. Paolucci et al., Nano Lett. **18**, 4195 (2018).
[3] G. De Simoni et al., ACS Nano **13**, 7871 (2019).
[4] F. Paolucci et al., Phys. Rev. Appl. **11**, 024061 (2019).
[5] M.F. Ritter et al., Nat. Commun. **12**, 1266 (2021).
[6] L.D. Alegria et al., Nat. Nanotechnol. 10.1038/s41565-020-00834-8 (2021).
[7] I. Golokolenov et al., Nat. Commun. **12**, 2747 (2021).
[8] R.H. Fowler and L. Nordheim, Proc. R. Soc. Lond. A **119**, 173 (1928).

Light-tunable charge-density wave orders in monolayer $MoTe_2$ and WTe_2

Giovanni Marini[1] and Matteo Calandra[1,2,3]

[1]Italian Institute of Technology, Italy, [2]University of Trento, Italy, [3]Sorbonne Université, France

Designing and manipulating broken symmetry states with laser light is an appealing perspective as it can lead to the discovery of hidden states and enable control over a broad range of material properties. In this respect, few layer transition metal dichalcogenides are an ideal class of materials for ultrafast investigations for two reasons: first, the metallic compounds belonging to the family very often host competing orders and second, their insulating counterparts have typical gaps in the 1-2.5 eV range, ideal for laser manipulation. In this work we demonstrate that ultrafast optical pumping can unveil hidden charge orders in group VI monolayer transition metal ditellurides. By using a suitable form of constrained density functional theory[1], we show that irradiation of the insulating 2H phases stabilizes multiple transient charge density wave orders with light-tunable distortion, periodicity, electronic structure and bandgap. Moreover, optical pumping of the semimetallic 1T' phases generates a transient charge ordered metallic phase composed of 2D diamond clusters. For each transient phase we identify the critical fluence at which it is observed and the specific optical and Raman fingerprints to directly compare with future ultrafast pump-probe experiments. Our work demonstrates that charge density waves can be stabilized even in insulating 2D transition metal dichalcogenides by ultrafast laser irradiation[2].

This project has received funding from the European Union's Horizon 2020 research and innovation programme Graphene Flagship under grant agreement No 881603.

[1] G. Marini and M.Calandra, Phys. Rev. B **104**, 144103 (2021)
[2] G. Marini and M.Calandra, Phys. Rev. Lett. **127**, 257401 (2021)

3D electronic structure in the potential Kitaev Quantum Spin Liquid, α-RuI_3

A. Louat[1], M. D. Watson[1], T. K. Kim[1], D. Ni[2], R. J. Cava[2], C. Cacho[1]

[1]Diamond Light Source, Harwell Campus, Didcot OX11 0DE, UK

[2]Department of Chemistry, Princeton University, Princeton, NJ 08544, USA

Quantum Spin Liquids are an exciting class of material with localized and entangled spin 1/2 electronic states, with great interest for quantum computing application. Among them the Kitaev QSL are characterized by a honeycomb lattice showing no magnetic order at very low temperature. In general, the promising family of compounds are the magnetically frustrated quasi-2D systems. The well-known α-$RuCl_3$ is a Mott insulator with a zig-zag antiferromagnetic transition [1]. Recently, single crystals of a cousin material, α-RuI_3 has been synthetized. In this isostructural compound no long-range magnetic ordering was found down to at least 0.35 K [2].

In this study we investigate the 3D band structure of α-RuI_3 measured by micro-ARPES with a spatial resolution of 4 µm. The high symmetry cuts (fig. 1) show clear evidence of metallic states and significant broadening of the bands at higher binding energies attributed to the strong electron correlations. The bulk Fermi Surface is characterized by an electron pocket dispersing around the GA axis and 6-hole pockets at the edge of the BZ. Our DFT calculation with SOC and k_z broadening agree reasonably well with the measurements. The "spiral" features of the Fermi Surface are a direct consequence of the reduced symmetry of the R-3 phase of α-RuI_3. The detailed photon energy dependence study shows a strong k_z variation indicating that the interlayer stacking order plays a key role in the electronic structure of the α-RuI_3.

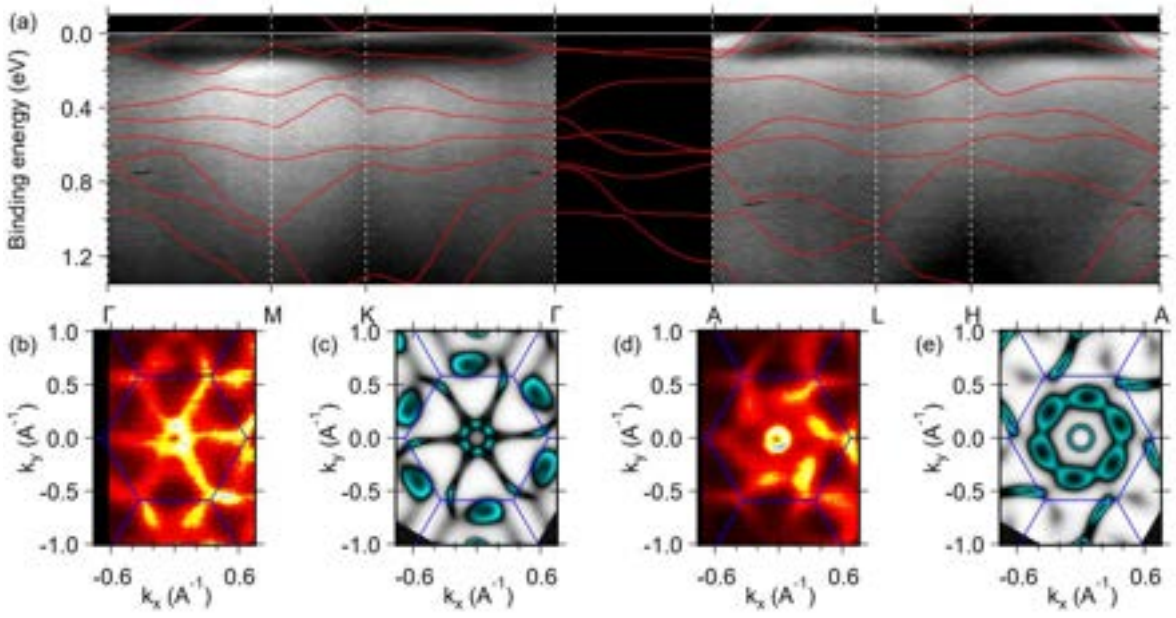

Fig. 1. (a) Experimental band dispersion of RuI3 along ΓMKΓALHA path. The red lines are DFT with SO band dispersion (b) and (d) Experimental Fermi surfaces at k_z=0 and c*/2 respectively. The blue hexagon is the simplified Brillouin zone. (c) and (e) Fermi surfaces extracted from DFT with k_z broadening at k_z=0 and c*/2 respectively.

[1] Sears, J. A. et al. Magnetic order in α-RuCl3: a honeycomb-lattice quantum magnet with strong spin-orbit coupling. Phys. Rev. B 91, 144420–144424 (2015).

[2] Ni, D.et al. Honeycomb-Structure RuI3, A New Quantum Material Related to α-RuCl3. Advanced Materials, 2106831 (2022).

Three-fold way of entanglement dynamics in monitored quantum circuits

T. Kalsi, A. Romito, and H. Schomerus

Lancaster University, UK

We investigate the measurement-induced entanglement transition in quantum circuits built upon Dyson's three circular ensembles (circular unitary, orthogonal, and symplectic ensembles; CUE, COE, and CSE) [1]. We utilise the established model of a one-dimensional circuit evolving under alternating local random unitary gates and projective measurements performed with tunable rate, which for gates drawn from the CUE is known to display a transition from extensive to intensive entanglement scaling as the measurement rate is increased. By contrasting this case to the COE and CSE, we obtain insights into the interplay between the local entanglement generation by the gates and the entanglement reduction by the measurements. For this, we combine exact analytical random-matrix results for the entanglement generated by the individual gates in the different ensembles, and numerical results for the complete quantum circuit. These considerations include an efficient rephrasing of the statistical entangling power in terms of a characteristic entanglement matrix capturing the essence of Cartan's KAK decomposition, and a general result for the eigenvalue statistics of antisymmetric matrices associated with the CSE.

[1] T. Kalsi, A. Romito, H. Schomerus (2022), arXiv:2201.12259.

Band hybridisation at the charge density wave transition in monolayer $TiTe_2$

Tommaso Antonelli[1], Warda Rahim[2], Matthew D. Watson[1], Akhil Rajan[1],

David O. Scanlon [2] and Phil D. C. King [1,*]

[1] SUPA, School of Physics and Astronomy, University of St Andrews, St Andrews KY16 9SS, UK

[2] Department of Chemistry and Thomas Young Centre, University College London, 20 Gordon Street, London, WC1H 0AJ, UK

Reducing the thickness of a material to its 2D limit can have dramatic consequences for its collective electronic states such as magnetism, superconductivity, and charge and spin ordering. An extreme case is $TiTe_2$, where a charge density wave (CDW) has recently been observed to emerge in the single-layer compound, while it is not found in multi-layer crystals [1]. The origin of this phase transition and its 2D-3D crossover remain poorly understood, opening questions regarding the CDW physics across the broader materials family. Using temperature-dependent angle-resolved photoemission spectroscopy (ARPES) we investigate how the band structure evolves across the CDW transition in ML $TiTe_2$ [2]. Our study reveals the band hybridisation between the back-folded conduction and valence bands occurring in the distorted phase, which in turn provides an electronic incentive to stabilise the CDW. Using a minimal Hamiltonian-based approach, we demonstrate how the corresponding energy gain is almost completely suppressed in bulk $TiTe_2$, due to its three-dimensional electronic band structure and a band-inverted orbital character compared to the monolayer. Our study provides a natural basis for understanding CDW state in $TiTe_2$, and brings critical new insights into how to engineer collective states in 2D materials.

[1] Chen et al., Nat. Commun., 2017, 8, 516
[2] T. Antonelli et al., arXiv:2203.15560

Real-space spectral simulation of quantum spin models: Application to the Kitaev-Heisenberg model

Francisco M. O. Brito[1], Aires Ferreira[1]

[1]University of York, Heslington, York YO10 5DD, United Kingdom

The proliferation of quantum fluctuations and long-range entanglement presents an outstanding challenge for the numerical simulation of interacting spin systems with exotic ground states. I will present a Chebyshev iterative method [1] that gives access to the thermodynamic properties and critical behavior of frustrated quantum spin models with good accuracy. The computational complexity scales linearly with the Hilbert space dimension and the number of Chebyshev iterations used to approximate the eigenstates. I will show results obtained with this approach for the spin correlations of the Kitaev-Heisenberg model, a paradigmatic model of honeycomb iridates that exhibits a rich phase diagram including a quantum spin liquid phase. The results are benchmarked against exact diagonalization and a popular iterative method based on thermal pure quantum (TPQ) states. All methods accurately predict transitions between paramagnetic, stripy antiferromagnetic and spin-liquid phases for honeycomb layers with antiferromagnetic Heisenberg interactions. Our findings suggest that a hybrid Chebyshev-TPQ approach could open the door to previously unattainable studies of quantum spin models in two dimensions, namely α-$RuCl_3$ in proximity to graphene [2]. This system is promising for quantum computing since it may support bond-directional Kitaev spin interactions.

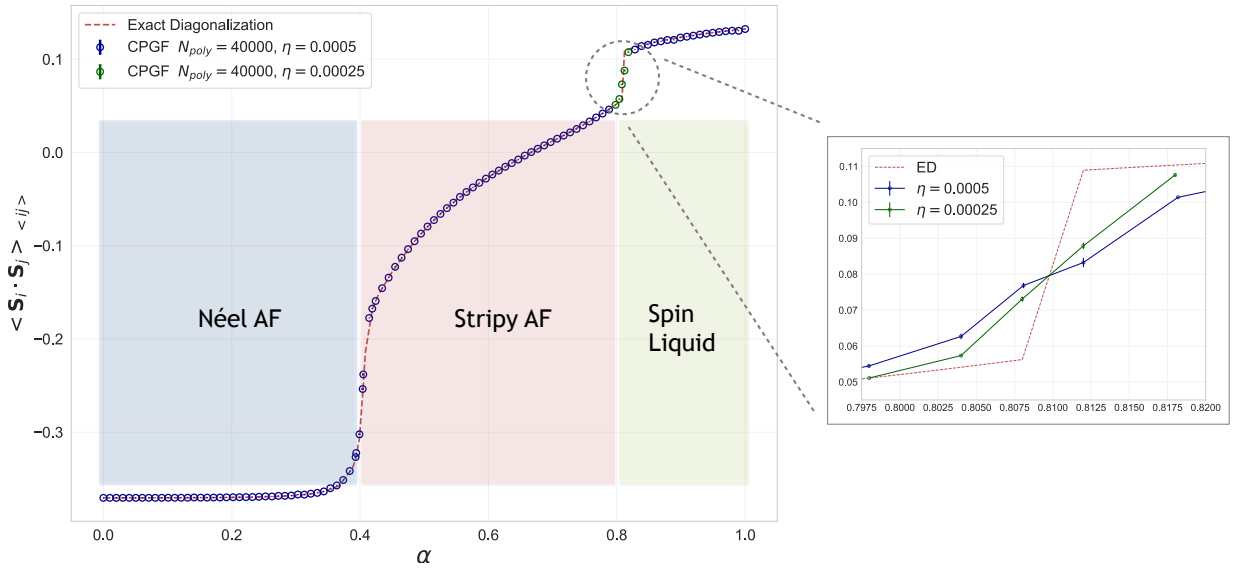

Fig. 1. (a) Nearest neighbor spin correlation for the ground state of a 24-site Kitaev-Heisenberg model on the honeycomb lattice with periodic boundary conditions, displaying two phase transitions.

[1] Aires Ferreira and Eduardo R. Mucciolo, C Authorc, Phys. Rev. Lett. **115**, 106601 (2015).
[2] Sananda Biswas, Ying Li, Stephen M. Winter, Johannes Knolle, and Roser Valentí, Phys. Rev. Lett. **123**, 237201 (2018).

Theory of Strongly Interacting Light-Matter Hybrids in Moiré Materials

Nigel Cooper

University of Cambridge, United Kingdom

The ability to tune the optical, electronic, and transport properties in van der Waals heterostructures has opened the door for the engineering, realisation, and detection of intriguing complex many-body phases of matter. Much attention has focused on the electronic properties, which show novel quantum phases arising from strong interactions and provide a new testbed for quantum simulation. However, these materials also hold interesting opportunities to study new hybrid quantum states of light and matter.

In twisted bilayers of transition-metal dichalcogenides the emergent moiré periodicity has significant effects on the nature of the excitons – the bound electron-hole pairs which dominate the coupling to light. In general these excitons are hybrids of the intra-layer excitons formed by an electron and hole in the same layer and inter-layer excitons with an electron and a hole belonging to different layers. Hybrid excitons have attracted much attention as they possess tuneable features of both intra- and inter-layer character, and have strong mutual repulsion due to the dipole moment from their inter-layer component.

I will describe theoretical predictions of the nature of the many-body states of polaritons formed by combining these strongly interacting hybrid excitons with a microcavity. These show that the very strong optical non-linearities arising from the interactions between the hybrid excitons can lead to features with no parallel in conventional two-dimensional polariton gases based on semiconductor quantum wells. When the cavity is driven coherently, the steady-state exhibits a bi-stability which, in contrast to two-dimensional polariton gases, is modulated by a discretised pattern, reminiscent of the equilibrium Mott insulating phase. When the excitons are pumped incoherently, the strong correlations can cause the system to act as a multi-photon laser, akin to that of Rydberg and multi-level atoms.

Work based on: A. Camacho-Guardian and N. R. Cooper, arXiv:2108.06177 & unpublished.

Aharonov-Bohm oscillations on a kagomé network of Lifshitz transition trajectories as a precursor of Brown-Zak fermions in graphene superlattices.

Sergey Slizovskiy[1],Folkert K. de Vries[2], Petar Tomić[2], Aitor Garcia-Ruiz[1], Giulia Zheng[2], Peter Rickhaus[2], Thomas Ihn[2], Klaus Ensslin[2], Vladimir Fal'ko[1]

National Graphene Institute,University of Manchester, UK and ETH, Zurich, Switzerland. Author A Name[1], Author B Name[2], and Author C Name[1]

[1] *University of Manchester, UK*, [2] *ETH, Zurich, Switzerland*

Brown-Zak magnetic minibands for electrons are common for metals with a rational value of magnetic field flux, $\phi = \phi_0 p/q$, piercing the unit cell of a crystal [1]. Here, we study how this ultra-quantum phenomenon, usually, attributed to strong magnetic fields emerges at low magnetic fields and moderate temperatures from the interplay between peculiar dynamics and interference of electrons at the fundamental Lifshitz transition (LT), realised using moiré superlattice miniband in twistronic graphene. We show that precursors of Brown-Zak minibands appear in the form of Aharonov-Bohm oscillations of conductivity produced by electrons propagating along entwining paths with a kagomé network topology, Fig.1(left). We report the observation of coinciding features in the vicinity of LT for both twisted tetralayer graphene and in highly aligned graphene - hexagonal boron nitride heterostructures. In particular, the maximal amplitude of conductance oscillations is located in the vicinity of LT, displacing from the LT by the amount growing linearly in the magnetic field Fig.1 (right). These findings are naturally explained by the topology of interfering paths [2]. The considerations can be also generalized to bands of Brown-Zak fermions, explaining "secondary" oscillations at non-integer inverse fluxes ϕ_0/ϕ.

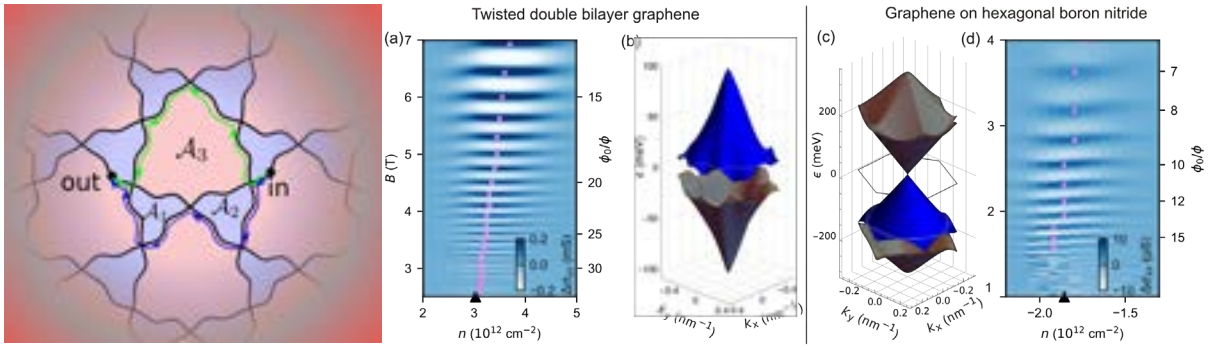

Fig. 1. left: At the LT, ballistic trajectories of electrons in a magnetic field form a kagome network. Green and blue lines exemplify the shortest paths responsible for quantum magneto-oscillations at the LT. Due to magnetic breakdown, electrons scatter at the intersections of chiral paths (linked to the saddle points in the band dispersion). **Right:** The shift of the oscillations maxima in twisted double bilayer graphene (a,b) and graphene aligned to boron nitride (c,d). Pink dots are the maxima of the oscillations, bending away from LT. The LT density is indicated with the solid triangle.

[1] R. K. Kumar, X. Chen, G. Auton, A. Mishchenko, D. A. Bandurin, S. V. Morozov, Y. Cao, E. Khestanova, M. B. Shalom, A. Kretinin, et al., Science **357**, 181 (2017).

[2] **(manuscript in preparation)**

Novel hysteresis effects in the charge density wave compound 1*T*-$TaS_{2-x}Se_x$

Aimee Nevill[1], Ben Smith[1], Liam Farrar[2], Charles Sayers[3], Simon Bending[1], Sara Dale[1], Daniel Wolverson[1], Enrico da Como[1]

[1] Department of Physics, University of Bath, UK

[2] School of Physics and Astronomy, University of St Andrews, Scotland

[3] Department of Physics, Politecnico di Milano, Italy

The metallic transition metal dichalcogenide (TMD) compounds 1*T*-$TaS_{2-x}Se_x$ (where x = 0 to 2) have been the focus of much research in condensed matter physics, in part due to the variety of electronic phases that are seen as the stoichiometry x is varied. At low temperatures such phases include commensurate and incommensurate charge density waves (CDW's), superconductivity under pressure, and a Mott insulating state. This is particularly interesting as both TaS_2 and $TaSe_2$ have very similar crystal structure and CDW superstructures, yet exhibit these very different electronic properties.

We have prepared single crystals of 1*T*-$TaS_{1.2}Se_{0.8}$ using chemical vapour transport, and confirmed their quality using EDX and Raman spectroscopy. Electronic transport data will be presented showing CDW phases of varying commensurability and novel hysteresis effects in resistance that are revealed through repeated cooldown and warm-up cycles. The cooling rate and thickness dependence of these transitions will be discussed.

This work was supported by the EPSRC Centre for Doctoral Training in Condensed Matter Physics (CDT-CMP) grant EP/L015544 and Royal Society grant UF160272.

Matter-Wave Localization and Delocalization in an Optical Quasicrystal

Bo Song, Jr-Chiun Yu, Shaurya Bhave, Lee Reeve, Emmanuel Gottlob, Georgia Nixon, Ulrich Schneider

University of Cambridge

Disorder plays a crucial role in transport phenomena. For example, in the presence of sufficient disorder, the matter wave will interfere and remain localized rather than spreading, which results in the formation of a localized state known as Anderson insulator. Interestingly, increasing interactions between particles can revive the coherence of the localized state, leading to delocalization of the matter wave.

Here I will report on the observation of the disorder-driven localization, as well as the interaction-induced delocalization in a two-dimensional optical quasicrystal with ultracold quantum gases. The interplay of disorder and interactions profoundly shifts the localization transition between a superfluid and the so-called Bose glass – a localized phase of an interacting and disordered quantum system. Our study using optical quasicrystals opens a new avenue to exploring novel localization phenomenon such as the many-body localization transition in two dimensions.

Gate-dependent electronic structure of twisted monolayer-bilayer graphene revealed by μARPES

James E. Nunn[1,2], Astrid Weston[3], Andrew Mcellistrim[3], Matthew D. Watson[2], Abigail J. Graham[1], Aitor Garcia-Ruiz[3], Roman V. Gorbachev[3], Marcin Mucha-Kruczynski[4], Vladimir I. Fal'ko[3], Cephise Cacho[2], Neil R. Wilson[1].

[1]Department of Physics, University of Warwick, Coventry, CV4 7AL, UK. [2]Diamond Light Source, Harwell Science and Innovation Campus, Didcot, OX11 0DE, UK. [3]National Graphene Institute, University of Manchester, Manchester, M13 9PL, UK. [4]Department of Physics, University of Bath, Claverton Down, Bath, BA2 7AY, UK.

Since reports of superconductivity [1] and Mott-like insulator states [2] in magic angle twisted bilayer graphene (MATBG) in 2018, there has been huge interest in exploring 2D twistronic systems in the hopes of finding further exotic states and increasing our understanding of correlated phenomena. For MATBG, the moiré periodicity produced by the 1.1° twist between layers results in a flat band near the Fermi energy, whose filling can be controlled electrostatically by gate electrodes to give rise to the reported correlated states. These phenomena are not unique to twisted graphene bilayers, but also present in other twisted 'multilayer' graphene systems [3,4] such as twisted monolayer-on-bilayer graphene (TMBG). In this system, the flat bands exist over a wider range of twist angles [5] than in MATBG. With a wealth of transport data and modelling, there is a pressing need for electronic structure measurements to test the theoretically predicted changes in electronic structure that underpin these twistronic effects.

We use angle-resolved photoemission spectroscopy with micrometre-scale spatial-resolution (μARPES) to directly study the band structure of TMBG over a range of different twist angles. Experiments were performed at the I05 beamline of Diamond Light Source, using capillary mirror optics to gain spatial resolution alongside high energy and angular resolution, with control over the photon energy and polarization. The strength of the interlayer interactions can be discerned through measurement of the size of the gaps formed at avoided band crossings, which inform and constrain theoretical modelling. By *in situ* electrostatic gating, we can control the carrier density within the TMBG layers, changing between n- and p-type doping, and look for gate-dependent changes of the band structure (Fig. 1). The results demonstrate the importance of considering the field across the layers as well as the change in carrier concentration when a back gate voltage is applied.

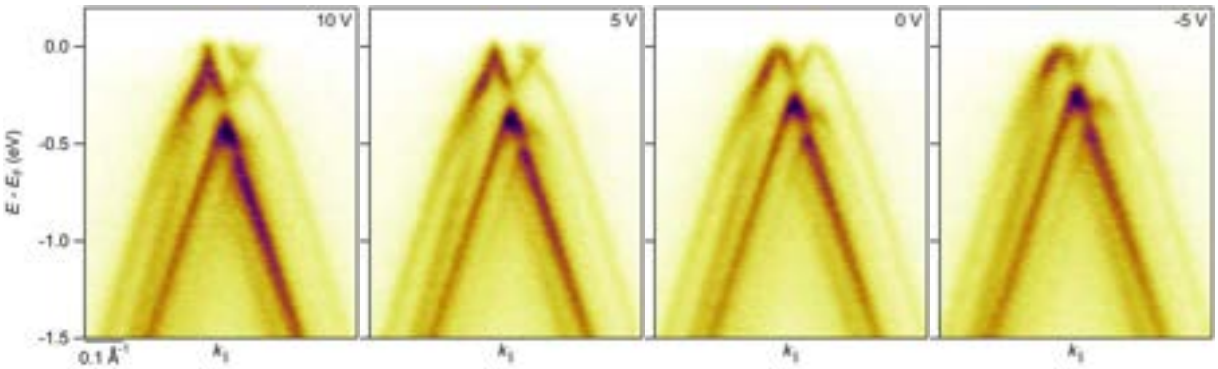

Fig. 1. Energy-momentum cuts through the monolayer and bilayer K points of 3.3° TMBG, taken over a range of back gate voltages.

[1] Y. Coa, *et al*., Nature **556**, 43-50 (2018).
[2] Y. Coa, *et al*., Nature **556**, 80-84 (2018).
[3] S. Chen, *et al*., Nat. Phys. **17**, 374-380 (2021).
[4] C. Chen, *et al*., Nat. Phys. **16**, 520-525 (2020).
[5] S. Xu, et al., Nat. Phys. **17**, 619-626 (2021).

Exploring the Charge Density Wave phase of 1T-$TaSe_2$: Mott system or band (semi)metal?

C. J. Sayers[1], D. Wolverson[2], E. Da Como[2], E. Carpene[3], Y. Zhang[4], C. E. Sanders[4], R. Chapman[4], A. Wyatt[4], G. Chatterjee[4], E. Springate[4]

[1]Dipartimento di Fisica, Politecnico di Milano, Italy

[2]Centre for Nanoscience and Nanotechnology, Department of Physics, University of Bath, UK

[3]IFN-CNR, Dipartimento di Fisica, Politecnico di Milano, Italy

[4]Central Laser Facility, STFC Rutherford Appleton Laboratory, UK

The nature of electronic correlations in Ta-based transition metal dichalcogenides (TMDs) is a fascinating, yet puzzling, topic in modern condensed matter physics. In the 1T-TaX_2 (X = S, Se) system, it is widely believed that the low-temperature charge density wave (CDW) phase directly leads to a Mott metal-insulator transition. However, the unusual conductive behavior of 1T-$TaSe_2$ down to cryogenic temperatures (T < 4K) remains controversial [1]. Previous investigations inferred that the occurrence of the Mott phase is limited to the surface only [2,3], however recent analysis on atomically thin 1T-$TaSe_2$ revealed that the Mott-like behavior, observed in the monolayer, is rapidly suppressed at larger thickness due to enhanced interlayer coupling and dielectric screening [4]. Here, we report combined time- and angle-resolved photoemission spectroscopy (trARPES) and theoretical investigations of the electronic structure of 1T-$TaSe_2$. Our experimental results reveal the existence of a transiently populated, weakly dispersive state lying a few hundreds of meV above the Fermi level, that could be ascribed to an upper Hubbard band (signature of the Mott phase). However, density functional theory (DFT) calculations demonstrate that its origin rests on the specific band structure induced by the CDW phase, without the need to invoke any strong electronic correlation effect.

[1] J. A. Wilson et al., Advances in Physics **50**, 1171 (2001).
[2] L. Perfetti et al., Phys. Rev. Lett. **90**, 166401 (2003).
[3] S. Colonna et al., Phys. Rev. Lett. **94**, 036405 (2005).
[4] Y. Chen et al., Nat. Phys. **16**, 218 (2020).

Rydberg exciton-polaritons in a Cu_2O microcavity

Konstantinos Orfanakis[1], Sai Kiran Rajendran[1], Valentin Walther[2,3], Thomas Volz[4,5], Thomas Pohl[6], and Hamid Ohadi[1]

[1]SUPA, School of Physics and Astronomy, University of St. Andrews, St. Andrews KY16 9SS, United Kingdom, [2]ITAMP, Harvard-Smithsonian Center for Astrophysics, Cambridge, MA, USA, [3]Department of Physics, Harvard University, Cambridge, MA, USA, [4]School of Mathematical and Physical Sciences, Macquarie University, Sydney, New South Wales, Australia, [5]ARC Centre of Excellence for Engineered Quantum Systems, Macquarie University, Sydney, New South Wales, Australia, [6]Center for Complex Quantum Systems, Department of Physics and Astronomy, Aarhus University, Aarhus, Denmark

Giant Rydberg excitons with principal quantum numbers as high as n = 25 have been observed in cuprous oxide (Cu_2O), a semiconductor where the exciton diameter can become as large as ~1 μm [1]. The giant dimension of these excitons results in excitonic interaction enhancements of orders of magnitude [2]. Rydberg exciton-polaritons, formed by the strong coupling of Rydberg excitons to cavity photons, are a promising route to exploit these interactions and achieve a scalable, strongly correlated solid-state platform. However, the strong coupling of these excitons to cavity photons has remained elusive. Here, by embedding a thin Cu_2O crystal into a Fabry-Pérot microcavity, we achieve strong coupling of light to Cu_2O Rydberg excitons up to n = 6 and demonstrate the formation of Cu_2O Rydberg exciton-polaritons [3]. These results pave the way towards realising strongly interacting exciton-polaritons and exploring strongly correlated phases of matter using light on a chip.

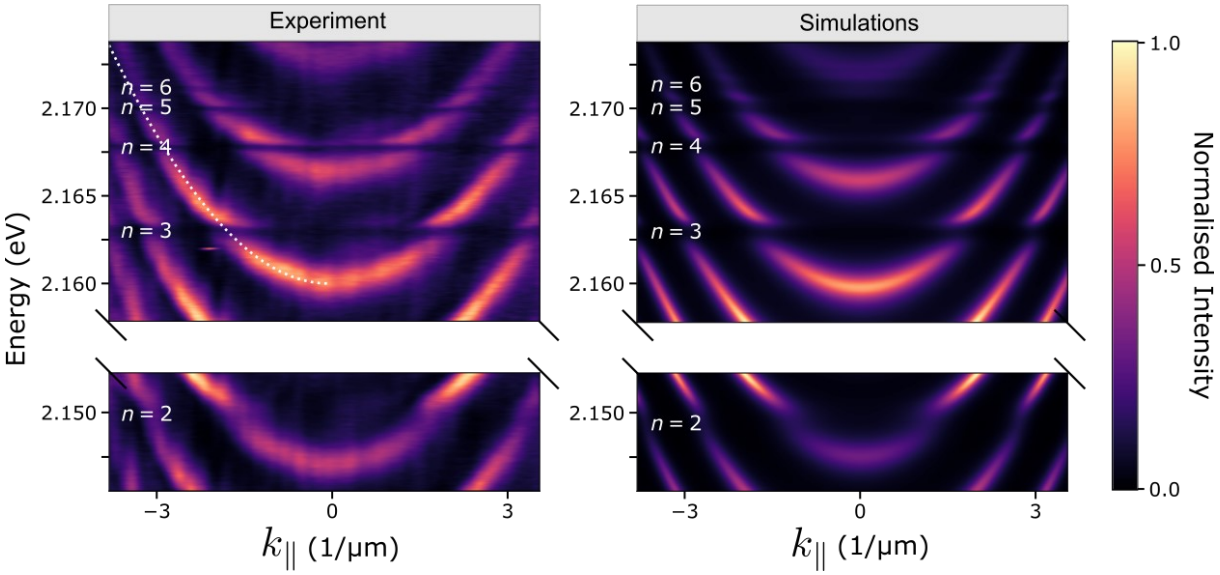

Fig. 1. Momentum-resolved transmission at 4 K from experiment (left) and TMM simulations (right).

[1] T. Kazimierczuk, *et al.*, Nature **514**, 343–347 (2014).
[2] J. Heckötter, *et al.*, Nature Communications **12**, 3556 (2021).
[3] K. Orfanakis, *et al.*, Nature Materials, In press (2022).

Tuning high-lying excitons comprising negative-mass electrons by twist angle in layered 2D semiconductors

Kai-Qiang Lin[1], Sebastian Bange[1], and John M Lupton[1]

[1]Institute of Experimental and Applied Physics, University of Regensburg, Regensburg, Germany

In the early days of 2D materials research, Novoselov and Geim pointed out that exfoliated 2D crystal monolayers of transition-metal dichalcogenides are "*essentially gigantic 2D molecules*" (PNAS 2005). A 2D crystal can be thought of as a huge molecular aggregate, a "J-aggregate", where microscopic transition dipole moments all add up to give optical transitions with extremely high oscillator strength. This phenomenon is exhibited by a simple effect: whereas the fluorescence of molecules tends to be quenched by energy transfer to metal-nanoparticle plasmons, the radiative rates in 2D materials can be so large that they become comparable to those of nanoparticle plasmons. Excitation energy is harvested from the metal to the semiconductor [1].

Electronic relaxation in molecules is famously described by Kasha's rule, stipulating that internal conversion leads to swift depopulation of any higher-lying excited states. Radiative relaxation therefore occurs from the lowest-energy state. But as with every rule, there are a few exceptions: under certain conditions, non-radiative energy dissipation is blocked, so that metastable bright excitons with energies far above the optical gap are formed [2]. While this phenomenon may seem conceptionally acceptable in a small molecule, with localized excited states, in a semiconductor crystal, such a high-lying exciton would entail an electron in an upper conduction band. We have now succeeded in identifying luminescence from such excitons in monolayer [3] and twisted-bilayer [4] crystals of WSe_2, with a transition energy of almost twice the bandgap and the PL spectrum extending out into the UV.

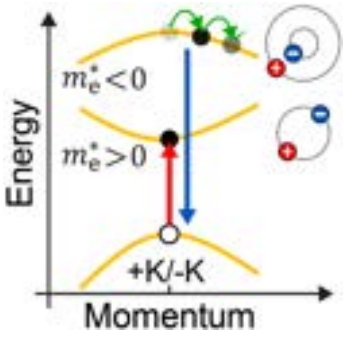

The obvious difference of 2D materials to molecules lies in the role of momentum space. The curvature of an upper conduction band can be negative, endowing the electron with negative effective mass. The spectrum of radiative exciton recombination, which can be as narrow as a few meV, then acquires a striking valley-selective phonon progression as the electron relaxes downwards in energy, emitting phonons.

Like in a molecular aggregate, excitons in two-dimensional semiconductors have large binding energies. Because of the existence of metastable higher-lying excitons, the overall excitonic structure of the material can be viewed as a quasi-atomic three-level system. Quantum interference then arises between the discrete excitonic transitions, giving rise to electromagnetically induced transparency [5]. Rabi flopping between states shows up as distinct features in the spectra of optical nonlinearities, such as of second-harmonic generation or four-wave mixing. Because the orbitals of the negative-mass electron protrude far into the chalcogenide atoms, PL and quantum interference involving the higher-lying exciton show an over tenfold greater susceptibility to twist angle in bilayers than the band-edge exciton does [6-7], opening up new opportunities for control of quantum-optical phenomena in the solid state.

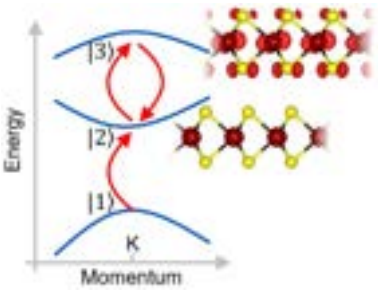

[1] Puchert *et al.*, Nature Nano. **12**, 637 (2017). [2] Chaudhuri *et al.*, Angew. Chem. Int. Ed. **52**, 13449 (2013). [3] Lin *et al.*, Nature Comm. **12**, 5500 (2021). [4] Lin *et al.*, Nature Comm. **12**, 1553 (2021). [5] Lin *et al.*, Nature Phys. **15**, 242 (2019). [6] Merkl *et al.*, Nature Mater. **18**, 691 (2019). [7] Merkl *et al.*, Nature Comm. **11**, 2167 (2020).

Cascade of charge density wave transitions in selenium doped 1T-TaS_2 probed with optics

X. Feng[1], J. Groefsema[1], A. Nevill[2], E. Da Como[2], E. van Heumen[1]

[1]Van der Waals-Zeeman Institute, University of Amsterdam, The Netherlands, [2]Department of Physics, University of Bath, United Kingdom

1T-TaS_2 is a unique material among the transition metal dichalcogenides (TMDC) in the sense that it undergoes a number of distinct charge density wave (CDW) transitions and ends in what has been suggested to be a strongly correlated phase at low temperature. In 1T-TaS_2 a light induced meta-stable state has previously been observed. We recently discovered that close to the Se concentration where the low-temperature strongly correlated phase gives way to superconductivity ($x \approx 0.8$ in 1T-$TaS_{2-x}Se_x$), a meta-stable charge density wave state (MS-CDW) can be reached by fast cooling through the low temperature CDW phase transition [1]. Our optical experiments indicate that this low temperature phase strongly resembles the CCDW phase of 1T-TaS_2, but a detailed study of the electronic properties is called for.

We have used bulk sensitive FT-IR spectroscopy to collect optical spectra of single crystalline 1T-$TaS_{2-x}Se_x$ (with $x \approx 0.8$ and $x \approx 1.0$) between 10 K and 400 K and over the photon energy range of 4 meV to 4 eV, which allows us to observe a series of different CDW phase transitions during cooling and warming cycles. We observe significant differences between the MS-CDW state, reached after cooling from 400 K and the normal CCDW that can be reached by subsequent heating and re-cooling.

I will present an analysis of the infrared active optical phonons and the different spectral signatures of the various CDW phases. By comparing the $x \approx 0.8$ and $x \approx 1.0$ crystals, more insight in this meta stable state will be provided.

[1] Nevill, Aimee, et al. "Novel hysteresis effects in the charge density wave compound 1T-$TaS_{2-x}Se_x$." Bulletin of the American Physical Society (2022).

Photon condensation in an arbitrary gauge cavity model

Dominic Rouse[1], Adam Stokes[2], and Ahsan Nazir[1]

[1]University of Manchester, UK, [2]Newcastle University, UK

There is a long history of `no-go' and counter theorems purporting that quantum models of many charges in a cavity cannot or can support a phase transition (PT) to a photon condensate (superradiant) state. At the heart of this debate is the role of gauge-relativity. For example, the Dicke model when derived in the Coulomb gauge does not possess a photon condensate state, although it does support a PT to a ferroelectric state. However, when derived in the multipolar gauge within the long wavelength approximation, this same model does show a superradiant PT. This difference is not a breakdown of gauge-invariance, rather it is a manifestation of this symmetry: subsystem definitions are gauge-relative and therefore so are subsystem dependent quantities like PTs. Crucially, the PT always occurs in the same parameter regime when expressed in terms of gauge invariant quantities.

Recently, a multimode cavity-jelium model was studied in the context of photon condensation. In Ref. [1] it was found that a PT to a photon condensate state was possible in the Coulomb gauge of the jelium model if the electromagnetic field could vary in space. The authors showed that the PT was caused by a magnetic instability and derived a criterion that the magnetic susceptibility of a material must satisfy for it to support a condensate state.

In this talk, we will build upon Ref. [1] by revisiting the jelium model using an arbitrary gauge theory in which the gauge-relativity of the condensation criterion is explicit. We find that in gauges other than the Coulomb gauge a condensate is caused by a combination of magnetic and electric instabilities. The relative contributions of the instability types, and the critical value which they must exceed, are gauge-relative.

[1] G. Andolina, et al., Phys. Rev. B, **102**, 125137 (2020).

Twist angle-dependent electronic, magnetic, and optical properties of $MnBi_2Te_4/CrGeTe_3$ Van der Walls heterostructure: a first principle study

S. Majumder[1], S. Kar[1], S. J. Ray[1]

[1]Department of Physics, Indian Institute of Technology Patna, Bihta 801103

By rotating (or twisting) the relative angle between a vertically stacked Van der Waals gave rise to a new area called 'Twistronics'. A variety of novel phenomena like superconductivity, orbital ferromagnetism, moire excitation, quantum anomalous Hall effect, strong electron correlation, photoluminescence, 1D topological channels, fractal quantum Hall effect have been reported for twisted bilayer heterostructures till now[1]. So, along with doping, straining, and proximity induced phenomena between two layers, 'Twistronics' provided another degree of freedom in the field of Van der Walls magnetic heterostructure. In this work, we theoretically investigated the electronic, magnetic, and optical properties of twisted Van der Walls heterostructure of $MnBi_2Te_4$ and $CrGeTe_3$. We have taken a total of four different VdW configurations with an interlayer angle between the layers: 0°, 10.89°, 17.48°, and 30° All the first-principle-based density functional theory (DFT) were performed using Atomistix Toolkit (ATK) software. We have used Strongly-Constrained and Appropriately-Normed (SCAN) functional as the exchange-correlation functional for electronic property calculation. Many reports showed that SCAN gave comparably better results than DFT/GGA+spin-orbit coupling+vdw and DFT/GGA+U approaches for transition metal dichalcogenide and 2D materials.

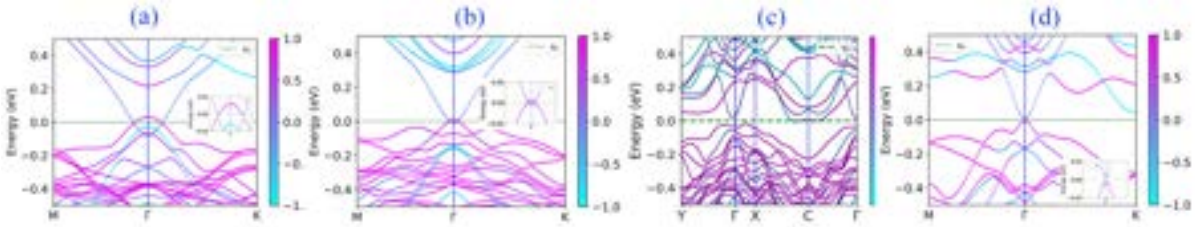

Fig. 1. (a) Spin projected bandstructure for heterostructure with interlayer rotation of (a) 0° (b) 10.89°, (c) 17.48°, and (d) 30° obtained by using SCAN functional.

A 16×16 supercell of the unit cell was taken as the basis for the Monte Carlo simulation which was run up to 10^5 iterations for better accuracy. We also estimated the exchange coupling between the layers. We found out that for the heterostructure with a twist angle of 0° the system is AFM in nature. In contrast, heterostructure with a twist angle of 10.89°, 17.48°, and 30° demonstrated ferromagnetic behavior with curie temperature of 12 K, 46 K, and 15 K. In the optical property estimation, we found the dielectric constant, absorption coefficient, refractive index and optical conductivity of the heterostructure to be heavily influenced by the $MnBi_2Te_4$ layer irrespective of the twist angle.

[1] Andrei, E. Y., & MacDonald, A. H. (2020). Graphene bilayers with a twist. Nature Materials, 19(12), 1265–1275.

[2] Fu, Y., & Singh, D. J. (2019). Density functional methods for the magnetism of transition metals: Scan in relation to other functionals. Physical Review B, 100(4).

[3] Ekholm, M., Gambino, D., Jönsson, H. J., Tasnádi, F., Alling, B., & Abrikosov, I. A. (2018). Assessing the scan functional for itinerant electron ferromagnets. Physical Review B, 98(9).

Lifshitz transition-induced tuning of charge density waves in 2H-$TaSe_2$

William Luckin[1], Yiwei Li[2,3], Juan Jiang[2,3,4], Surani M. Gunasekera[1], Dharmalingam Prabhakaran[5], Felix Flicker[6], Yulin Chen[5,2,3] and Marcin Mucha-Kruczynski[1,7]

[1]Department of Physics, University of Bath, UK, [2]School of Physical Science and Technology, ShanghaiTech University, PRC, [3]CAS-Shanghai Science Research Center, PRC, [4]Hefei National Laboratory for Physical Sciences at the Microscale, PRC, [5]Department of Physics, University of Oxford, UK, [6]School of Physics and Astronomy, Cardiff University, UK, [7]Centre for Nanoscience and Nanotechnology, University of Bath, UK

Because of the fundamental importance of the electrons in the vicinity of the Fermi surface (FS) for low-energy excitations, the shape of this surface has a significant impact on the properties of metals. This is particularly evident when, as a function of some external parameter like pressure, temperature , magnetic field or doping, the FS undergoes a change of topology resulting in a Lifshitz transition (also known as electronic topological transition) [1].

In contrast to the more conventional phase transitions described by the Landau theory, Lifshitz transitions do not involve symmetry breaking but still lead to observable singularities in thermodynamics, electron transport, sound propagation, and magnetic response as the system is tuned across special points in the electronic dispersion where the density of states (DoS) exhibits analytic (van Hove)singularities. The impact of van Hove singularities is especially significant in low dimensions,$d \leq 2$, where divergences in the DoS are possible at some of the critical points.

Here, we study the impact of a Lifshitz transition on a correlated many-body state by surface doping bulk 2H-$TaSe_2$ with potassium. Using angle-resolved photoemission spectroscopy, we map out directly the electronic dispersion in its low-temperature commensurate (3×3)charge density wave and how it changes as the previously unoccupied electronic states in the topmost layers are filled so that the chemical potential crosses a saddle point in the dispersion. Based on calculations of generalized susceptibility within a minimal two-band model and the symmetry of ARPES constant-energy maps, we conclude that the change in FS topology drives a change in the charge density order from a (3×3) to a (2×2) superlattice. This validates a theoretical model postulated for $TaSe_2$ almost half a century ago [2] and demonstrates the importance of saddle points in layered materials.

[1] I. M. Lifshitz, Anomalies of Electron Characteristics of a Metal in the High Pressure Region, Sov. Phys. JETP 11, 1130 (1960)
[2] T. M. Rice and G. K. Scott, New Mechanism for a Charge-Density-Wave Instability, Phys. Rev. Lett. 35,120 (1975).

Anisotropic diffusion and angle-resolved photoluminescence in transition metal dichalcogenide monolayers

J. J. P. Thompson[1], S. Brem[1], H. Fang[2], B. Han[3], C. Antón-Solanas[3], R. Schmidt[4] , S. Michaelis de Vasconcellos[4] , Saroj P. Dash[2], W. Wieczrorek[2], R. Bratschitsch[4] , C. Schneider[3] and E. Malic[1,2]

[1]Philips Universität Marburg, Germany, [2]Chalmers University of Technology, Sweden, [3]University of Oldenburg, Germany, [4]University of Münster, Germany

Atomically thin transition metal dichalcognides (TMDs) possess numerous unique electronic and optical properties, important for future technologies. One of the most fundamental of these properties is the formation of stable 2D excitons, which dominate the optoelectronic response. Energy transfer process, driven by these excitons, are crucial in light-harvesting technology such as solar cells, as well as for quantum information applications. The energy transport in technologically promising transition metal dichalcogenides is determined by exciton diffusion, which strongly depends on the underlying excitonic and phononic dispersion.

First, we propose [1] that angle-resolved photoluminescence can be used to probe the changes of the excitonic dispersion. The exchange-coupling leads to a unique angle dependence of the emission intensity for both circularly and linearly-polarised light. We show that these emission characteristics can be strongly tuned by an external magnetic field due to the valley-specific Zeeman-shift. We propose that angle-dependent photoluminescence measurements involving both circular and linear optical polarisation as well as magnetic fields should act as strong verification of the role of valley-exchange coupling on excitonic dispersion and its signatures in optical spectra.

Secondly, based on a fully microscopic theory we demonstrate that the valley-exchange interaction leads to an enhanced exciton diffusion due to the emergence of a linear excitonic dispersion and the resulting decreased exciton-phonon scattering [2]. Interestingly, we find that the application of an uniaxial strain can drastically boost the diffusion speed and even give rise to a pronounced anisotropic diffusion, which persists up to room temperature. We reveal that this behaviour originates from the highly anisotropic exciton dispersion in presence of strain, displaying parabolic and linear behaviour perpendicular and parallel to the strain direction, respectively. Our work demonstrates the possibility to control the speed and direction of exciton diffusion via strain and dielectric engineering. This opens avenues for more efficient and exotic

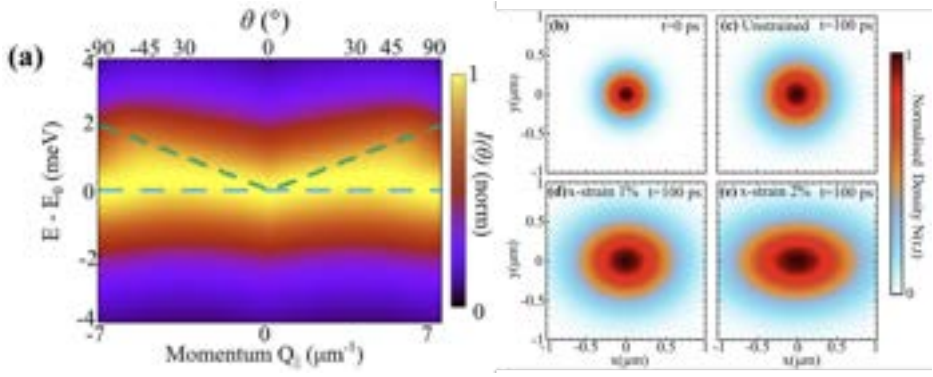

optoelectronic applications of atomically thin materials.

Fig. 1. (a) Angle resolved photoluminescence; (b-e) Anisotropic exciton diffusion.

[1] J. J. P. Thompson, *et al.*, Nanoscale Horiz. **7**, 77-84 (2021)
[2] J. J. P. Thompson *et al.,* 2D Mater. **9** 025008 (2022)

Electronic and magnetic structure of Fe_3Sn_2 characterised by scanning tunnelling microscopy.

Liam S. Farrar[1], Christopher Trainer[1], Christoph Heil[2], Lilian Prodan[3], Vladimir Tsurkan[3], Mohamed A. Kassem[4], Istvan Kezsmarki[3], Peter Wahl[1]

[1]University of St Andrews, UK. [2]Graz University of Technology, Austria. [3]Universität Augsburg, Germany. [4]Assiut University, Egypt.

Fe_3Sn_2 is a ferromagnetic material which consists of layers of honeycomb Sn sandwiched between bilayers of Kagome-like Fe-Sn. The Kagome lattice consists of a two-dimensional network of corner sharing triangles which are expected to host exotic quantum magnetic states [1]. The Sn layer, structurally equivalent to stanene, is also of interest due to its similarity to graphene and the predictions of topological insulating behaviour in the monolayer form [2].

In this talk I will present recent work on the characterisation of both the Kagome and stanene layers of Fe3Sn2 using low-temperature scanning tunnelling microscopy (STM) and scanning tunnelling spectroscopy (STS). We identify large (> 500x500 nm) regions of each termination, as well as regions of mixed terminations in which we observe nanoscale wires and islands of stanene. The atomic character of each surface is identified by comparison between density function theory calculations, topographic images (Fig. 1), quasi-particle interference, and work function measurements. Utilising out-of-plane magnetic fields up to 14 T, we characterise the field dependence of the quasiparticle excitations of both layers. By performing spin-polarised STM, we demonstrate imaging magnetic domain walls, providing atomically resolved information about the magnetism.

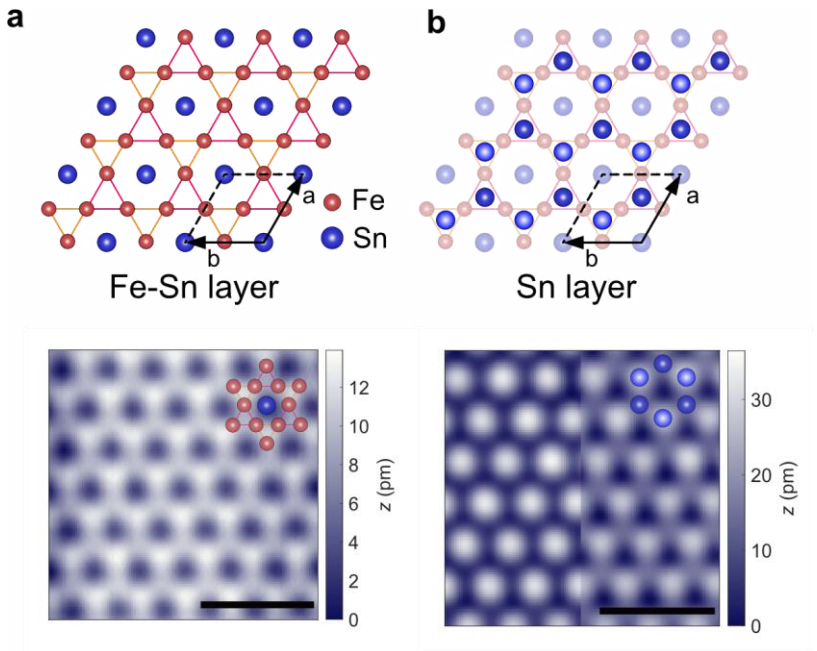

Fig. 1. (a) Crystal structure of the Fe-Sn layer (top), experimentally resolved lattice (bottom, *V* = 80 mV, *I* = 1 nA). (b) Crystal structure of the Sn layer (top), experimentally resolved lattice (bottom, [left] *V* = -80 mV, *I* = 1 nA, [right] *V* = 80 mV, *I* = 1 nA). The scalebar corresponds to 1 nm.

[1] Mekata, M. Kagome: the story of the basketweave lattice. Phys. Today, **56**, 12 (2003)
[2] Ezawa, M. Monolayer topological insulators: silicene, germanene, and stanene. J. Phys. Soc. Japan, **12**, 121003, (2015)

Electromagnetic response of composite Dirac fermions in the half-filled Landau level

Johannes Hofmann[1]

[1]Department of Physics, Gothenburg University, 41296 Gothenburg, Sweden

An effective field theory of composite Dirac fermions was proposed by Son [Phys. Rev. X 5, 031027 (2015)] as a theory of the half-filled Landau level with explicit particle-hole symmetry. In this talk, I will present recent results on the electromagnetic response of this Son-Dirac theory on the level of the random phase approximation (RPA), where particular attention is paid to the effect of an additional composite- fermion dipole term that is needed to restore Galilean invariance. We find that once this dipole correction is taken into account, spurious interband transitions and collective modes that are present in the response of the unmodified theory either cancel or are strongly suppressed. We demonstrate that this gives rise to a consistent theory of the half-filled Landau level valid at all frequencies, at least to leading order in the momentum. In addition, the dipole contribution modifies the Fermi- liquid response at small frequency and momentum, which is a prediction of the Son-Dirac theory within the RPA that distinguishes it from a separate description of the half-filled Landau level by Halperin, Lee, and Read within the RPA.

Fig. 1. (a) CMQM (Condensed Matter and Quantum Materials) 2020 Conference banner; (b) The venue for the meeting in London.

[1] J. Hofmann, Phys. Rev. B **104**, 115401 (2021)

Van der Waals interfaces in multilayer heterojunctions for ultraviolet photodetection

Mustaqeem Shiffa[1], Shihong Xie[1,2], Mujahid Shiffa[1], Zakhar R. Kudrynskyi[1], Oleg Makarovskiy[1], Zakhar D. Kovalyuk[3], Wenkai Zhu[2], Kaiyou Wang[2] and Amalia Patane[1]

[1]School of Physics and Astronomy, University of Nottingham, United Kingdom.
[2]State Key Laboratory of Superlattices and Microstructures, Institute of Semiconductors, Chinese Academy of Sciences, China.
[3]Frantsevich Institute for Problems of Materials Science, The National Academy of Sciences of Ukraine, Ukraine.

Advances in semiconductor technologies have led to the miniaturisation and improvement of light sensing devices for a range of applications. However, development of efficient ultraviolet (UV) light detectors remains technologically challenging, with most devices exhibiting low photoresponsivity, high power consumption and/or other drawbacks[1]. Performance is typically limited by the physical properties of the semiconductors used, such as the low penetration depth of UV light in silicon. Van der Waals (vdW) semiconductors and their *pn*-junctions offer an alternative solution. They possess strong optical properties and their thin *pn*-junction regions and layered crystal structures open doors for new approaches to device engineering. Here, we report on a multi-layer junction that combines single layer graphene and vdW semiconductors (*p*-GaSe and *n*-In_2Se_3) with strong optical absorption in the UV range (fig. 1a).[2] The junctions have a high photoresponsivity in forward and reverse bias, of up to ~10^2 A W^{-1} under optical excitation with visible and UV light (fig. 1b-e). The photoresponse differs from that of a traditional *pn*-junction diode as it is governed by charge transport across thin layers and light-current conversion at three vdW interfaces (*e.g.* the graphene/GaSe, GaSe/In_2Se_3, and In_2Se_3/graphene interfaces, as shown in fig. 1c-e). The type-II band alignment at the GaSe/In_2Se_3 interface and electric field at the three vdW interfaces suppress carrier recombination, leading to enhanced photoresponsivity and detectivity beyond conventional UV-enhanced silicon detection technology.

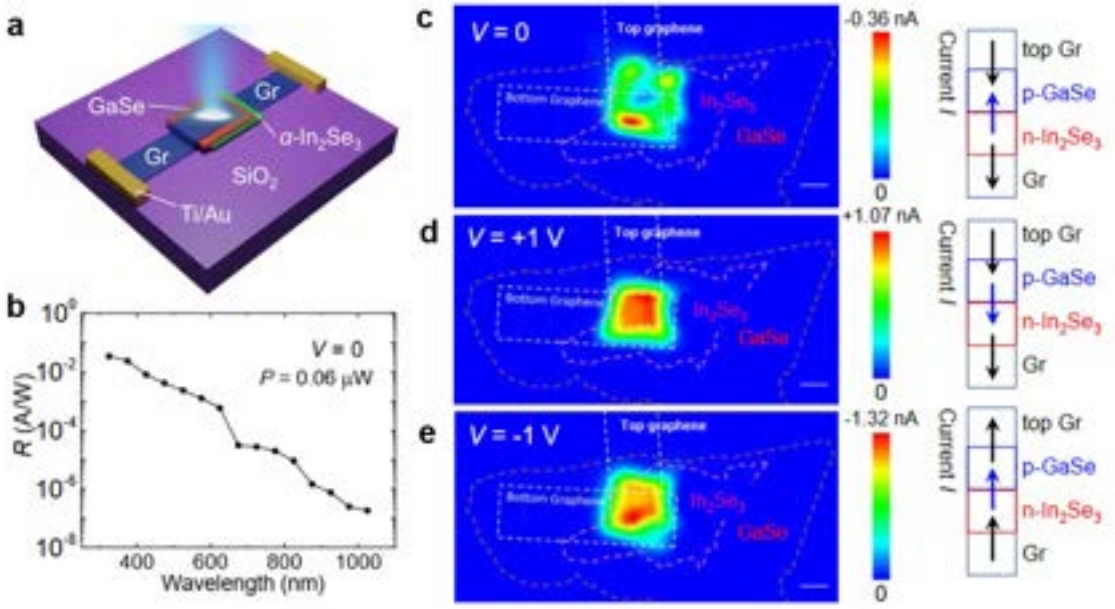

Fig. 1. (a) i. Schematic of a graphene contacted *p*-GaSe/*n*-In_2Se_3 junction. (b) Wavelength-dependence (λ = 325 – 1025 nm) of the photoresponsivity (*R*) of a graphene contacted *p*-GaSe/*n*-In_2Se_3 junction (GaSe/In_2Se_3 thickness ~ 30/30 nm) at T = 300 K and V = 0. (c-e) Photocurrent (*ΔI*) maps at (c) V = 0, (d) + 1 V and (e) -1 V. The laser beam (*λ* = 425 nm and *P* = 15 μW) has a spot size of about 1 μm. Scale bar: 10 μm. The right insets illustrate the direction of the current across the three interfaces of the heterostructure.

[1] Li, Q. *et al.*, npj 2D Mater. Appl. 5, 36 (2021).
[2] Xie et al. unpublished (2022)

Magnetic properties of sputtered and electrodeposited nickel/nanoporous-GaN composites

Yonatan Calahorra[1]

[1]Department of Materials Science and Engineering, Technion – IIT, Haifa, Israel

Adding Magnetic functionality to semiconductors opens up a wide variety of applications, from magnetic and current sensors, through magnetically controlled devices to spintronics [1]. Due to its increasing role in electronics and optoelectronics, GaN is an interesting candidate for such coupling [2]. Here we describe the realization and magnetic characterization of nickel/nanoporous-GaN composites of 0-3 and 2-2 connectivity. Studying both electrodeposited and sputtered nickel, the results show an intricate interplay between the process parameters (pore size, deposition method) and the resulting magnetic properties as reflected in temperature dependent magnetization measurements and magnetic force microscopy (MFM).

Conductive layers of n-doped GaN were electrochemically etched to form controlled nanoporous structures. Subsequently, two nickel deposition methods were studied: electrodeposition - using the remaining GaN material as a working electrode, and sputtering directly onto the porous surface (see Figure 1). No thermal treatment was used. Materials (x-ray diffraction and scanning electron microscopy; XRD,SEM) and magnetic characterization (Temperature dependent vibrating sample magnetometry, VSM, and MFM) were used to study characterize the resulting composites [3].

In general, the porous substrate was found to allow stress relaxation in 2-2 layers (made using either methods) and infiltration of nickel into the nanopores - only for electrodeposition. The crystalline properties, and in agreement the magnetic properties s.a. squareness and saturation magnetization, of electrodeposited samples were found superior to sputtering. Furthermore, the sputtered layers of 100-300 nm were found to exhibit transcritical characteristics (in VSM loops) and corresponding perpendicular magnetic anisotropy in MFM.

Overall, the use of nanoporous-GaN as an active and controllable template for deposition of nickel was demonstrated, and the process details were found to significantly influence the magnetic properties of the composites.

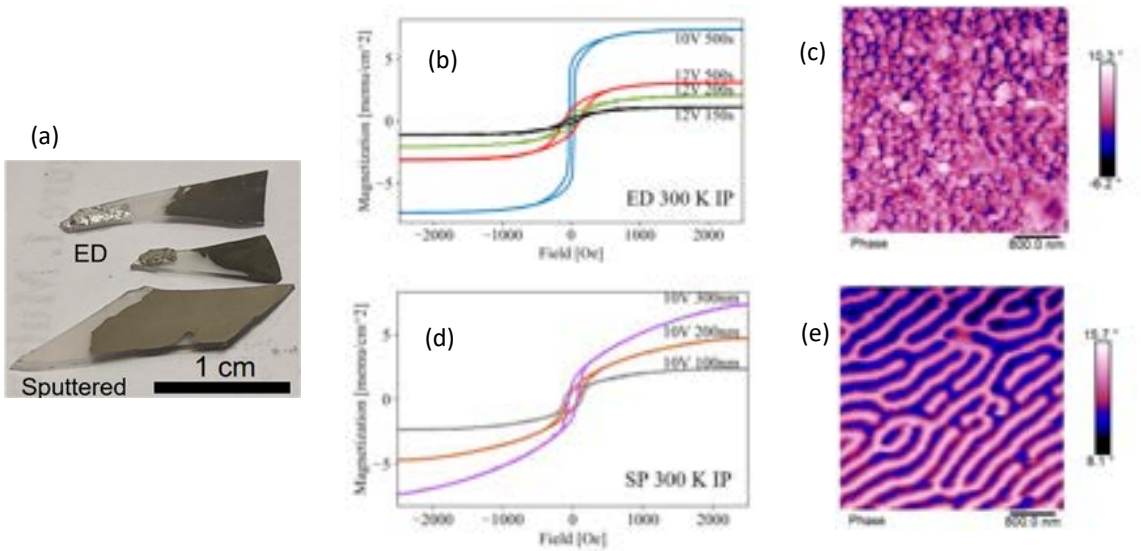

Fig. 1. (a) Appearance of the composites; (b,d) VSM of electrodeposited (ED) and sputtered (SP) samples; (c,e) MFM signal of in-plane poled ED and SP samples.

[1] T. Dietl and H. Ohno, Rev. Mod. Phys. 86(2014) 187.

[2] C. J. Humphreys. Solid-State Lighting. MRS Bulletin, 33(2008) 459–470.

[3] Y. Calahorra et al. arXiv:2102.02904 (2021)

Very high-energy collective states of partons in fractional quantum Hall liquids

Ajit C. Balram[1], Zhao Liu[2], Andrey Gromov[3] and Zlatko Papic[4]
[1]*Institute of Mathematical Sciences, HBNI, CIT Campus, Chennai 600113, India*
[2]*Zhejiang Institute of Modern Physics, Zhejiang University, Hangzhou 310027, China*
[3]*Brown Theoretical Physics Center & Department of Physics, Brown University, Providence, RI 02912, USA*
[4] *School of Physics and Astronomy, University of Leeds, Leeds LS2 9JT, United Kingdom*

The low energy physics of fractional quantum Hall (FQH) states -- a paradigm of strongly correlated topological phases of matter -- to a large extent is captured by weakly interacting quasiparticles known as composite fermions (CFs). In this paper [1], based on numerical simulations and effective field theory, we argue that some high energy states in the FQH spectra necessitate a different description based on parton quasiparticles. We show that Jain states at filling factor $\nu=n/(2pn\pm1)$ with integers n, $p\geq2$, support two kinds of collective modes: in addition to the well-known Girvin-MacDonald-Platzman (GMP) mode, they host a high energy collective mode, which is interpreted as the GMP mode of partons. We elucidate observable signatures of the parton mode in the dynamics following a geometric quench. We construct a microscopic wave function for the parton mode, and demonstrate agreement between its variational energy and exact diagonalization. Using the parton construction, we derive a field theory of the Jain states and show that the previously proposed effective theories follow from our approach. Our results point to partons being "real" quasiparticles which, in a way reminiscent of quarks, only become observable at sufficiently high energies.

*This work is supported by the Leverhulme Trust Research Leadership Award RL-2019-015.

[1] Ajit C. Balram, Zhao Liu, Andrey Gromov, and Zlatko Papic, arXiv:2111.10395 [to appear in Physica Review X]

Controlling hot electron cooling dynamics in graphene/hBN van der Waals heterostructures

Jake Dudley Mehew[1], Alexander Block,[1] Jaime Díez Mérida,[2] Rafael Luque Merino,[2] Dmitri K. Efetov,[2] and

Klaas-Jan Tielrooij[1]

[1]Catalan Institute of Nanoscience and Nanotechnology (ICN2), CSIC and BIST, 08193 Barcelona, Spain, [2] ICFO-Institut de Ciencies Fotoniques, The Barcelona Institute of Science and Technology, 08860 Castelldefels, Barcelona, Spain

Van der Waals heterostructures allow for the layer-by-layer design of complex material systems in which new physics and novel device properties can be studied. For instance, topological and correlated phases of matter emerge through precise control of twist angle. Furthermore, these enhanced properties will benefit electronic and optoelectronic applications providing that the nature of heat flow at the nanoscale is well understood. [1,2,3,4]

In this work, we study hot electron cooling dynamics at pn-junctions electrostatically formed in heterostructures of mono- and bi-layer graphene encapsulated in hexagonal boron nitride (hBN). Using time-resolved photocurrent measurements, we find that the cooling time constant varies from 1 to 100´s picoseconds as we modify the number of graphene layers, Fermi level and lattice temperature.

These results are particularly relevant for applications in thermal management, photonics, and high-speed electronics as well as fundamental studies of emergent quantum effects including the Dirac fluid regime [4].

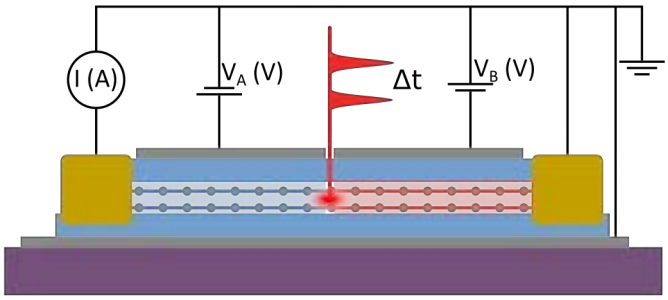

Fig. 1. Schematic of experimental setup. Graphene top gates (VA and VB) define the pn-junction in hBN encapsulated bilayer graphene. Ultrafast pulses illuminate the nanoscale junction generating a photocurrent.

[1] Dong Sun et al, Nat. Nano., 7 (2012) 114
[2] Matt W. Graham et al, Nat. Physics, 9 (2013) 103
[3] Klaas-Jan Tielrooij et al, Nat. Nano., 13 (2018) 41
[4] Alexander Block et al, Nat. Nano., 16 (2021) 1195

Excitonic vs Mott insulator in carbon nanotubes: A proposed experimental test

Giacomo Sesti[1,2], Daniele Varsano[2], Elisa Molinari[1,2] and Massimo Rontani[2]

[1]UNIMORE, Italy, [2]CNRNANO, Italy

Transport studies on ultraclean, nominally metallic carbon nanotubes have revelead that a residual intrinsic gap is always present, despite band theory predicting a metallic behaviour. Many-body interactions are commonly associated with the opening of the residual gap. Two fundamentally different scenarios have been proposed: a Mott phase[1], driven by the short-range part of Coulomb interaction, and an excitonic phase[2], linked to the long-range part of Coulomb interaction. Despite the two phases having different symmetry properties, a conclusive experiment has been missing so far. Here we propose as a unique fingerprint of the excitonic insulator phase the presence of a cusp in the evolution of the gap with the axial magnetic field, close to the gap mimimum.

On the contrary, the Mott phase exhibits a featureless, rounded profile. The non-analytic spike originates from the extreme sensitivity of electron-electron interactions to the Aharonov-Bohm gap modulation. This is demonstrated on the basis of a newly developed model for screening[3] adapt for tubes of different size and chirality, capable to replicate first-principles computation of the electron-electron interaction in nanotubes.

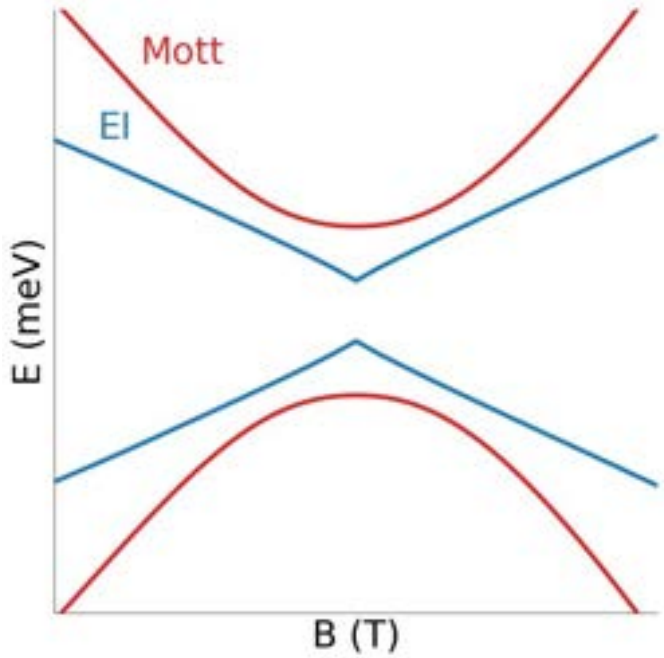

Fig. 1. Dispersion of the gap with the magnetic field close to the gap minimum at the Dirac field in the Excitonic Insulator phase and in the Mott insulator phase of a carbon nanotube. If not for many-body effects, the gap would close at the Dirac field.

[1] Deshpande et al., *Science* 323, 106 (2009)
[2] Varsano et al., *Nat. Comm*. 8, 1461 (2017)
[3] Sesti et al., *Phys. Rev. B* in press, also on arXiv https://doi.org/10.48550/arXiv.2201.10199

Comparison of Simulation and Experimental Results of Travelling Wave JPA's in the Three Wave Mixing Regime

Searbhán Ó Peatáin[1,2], Tom Dixon[2], Phil Meeson[3], Jonathan Williams[2], Sergey Kafanov[1] and Yuri Pashkin[1]

[1]Lancaster University, UK,
[2]NPL, UK
[3]Royal Holloway University of London, UK

Josephson Parametric Amplifiers (JPA's) have found widespread use in the amplification of low level signals for many years due to their ability for high amplification with quantum limited noise, although they suffer from an inherent gain-bandwidth trade-off. For modern applications in qubit read out and axion detection a wide bandwidth amplification is required which can be achieved by incorporating the Josephson element in a transmission line. These Travelling Wave JPA's (TWJPA's) have been shown to work in two regimes, three or four wave mixing, with varying degrees of success. The three wave mixing regime promises larger dynamic range and easier separation of signal tone from pump and parasitic tones than four wave mixing [1,2]. However, experimental results have not yet managed to replicate the promises of theory and novel amplifier designs and technologies have been proposed to counter this problem [3].

We present here our recent simulation results of different schemes of TWJPA completed in open-source WRspice along with Coupled Mode Equation solutions. These results are then compared with experimental results and the discrepancies discussed, with special attention given to the importance of impedance matching for a successful device [4].

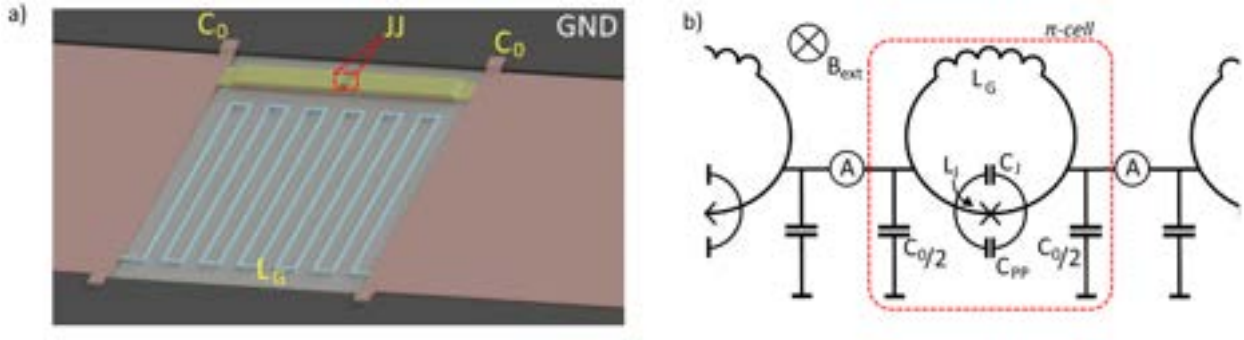

Fig. 1. (a) Sketch of an example RF-SQUID structure often used in proposed TWJPA's implementing three wave mixing and b) its complementary lumped element model.

* This work was supported by the STFC.

[1] A. B. Zorin et al., Phys. Rev. Appl. 6, 034006 (2016).

[2] T. Dixon, J. Williams, P. J. Messon, et al., Phys. Rev. Appl. 14, 034058 (2020).

[3] M. Esposita, N. Roch, et al., Appl. Phys. Lett. 119, 120501 (2021).

[4] S. O Peat´ain, Yu. Pashkin, et al., arXiv:2112.07766 (2021).

Scattering a diffracted electron wave from nanoscale potential barriers on graphene: a novel approach

Dylan Jones, Marcin Mucha-Kruczynski, and Adelina Ilie

Department of Physics, University of Bath, U.K.

Following its discovery, it was found that graphene's electrons exhibit the Klein tunneling effect. This prompted excitement around the tunneling/scattering behaviours of graphene electrons from electrostatic potentials of various geometries. One avenue of research was the use of on-sheet scattering from nanoscale circular potential barriers / circular quantum dots (CQDs) in graphene-based circuitry applications [1, 2]. The main results of these theoretical works were the predictions of anisotropic electron flow in the scattered probability current from the CQD following the scattering of a plane wave. However, these predicted scattering effects would not be measurable in a realistic device setting since a plane wave corresponds to current injection from a large electrode whose lateral is much greater than the CQD; local perturbations to the total current density would be dominated by the incident current field.

Within the framework of the low-energy, single-valley continuum approach we model the scattering of a *diffracted* electron plane wave from a CQD on the surface of graphene. The diffracted wave is modelled by solving the spinor Helmholtz equation [3] through calculation of the derived graphene Green's matrices. Then, the scattering problem at the CQD boundary is solved through partial wave analysis as in [1, 2]. Calculation of the resulting probability current densities shows that tunable anisotropic scattering in the far-field *can* be realised following the scattering of a diffracted graphene electron wave, unlike the case of simple plane wave scattering.

Our findings open the door for the design and realisation of a multi-terminal device based on the anisotropic distribution of scattered current from a CQD on graphene. In such a device, the Fermi wavelength, and hence the scattering from the dot, could be controlled by the switching of a gate voltage. This work also permits the detailed device behaviour, i.e., conductances through the multiple terminals, to be modelled using tight-binding simulations.

[1] Heinisch RL, Bronold FX, Fehske H., 2013. Mie scattering analog in graphene: Lensing particle confinement, and depletion of Klein tunneling. Phys. Rev. B., 87(15)

[2] Schulz, C., Heinisch, R.L. and Fehske H., 2014. Electron flow in circular graphene quantum dots. arXiv preprint arXiv:1412.2539

[3] Hillion, P., 1978. The spinor Helmholtz equation. Journal of Mathematical Physics, 19(1), pp.264-269

Asymmetric dual Bloch point domain walls in cylindrical magnetic nanowires

J. Askey[1], M. Hunt[1], W. Langbein[1], and S. Ladak[1*]

[1]School of Physics and Astronomy, Cardiff University, Cardiff, CF24 3AA, United Kingdom

Cylindrical magnetic nanowires have been studied extensively due to the presence of domain walls with novel topology and outstanding dynamic properties. In soft magnetic systems, where shape anisotropy aligns the magnetization along the wire axis, and for radii above 50nm, two topologically distinct walls have been previously identified [1]. The Bloch point wall (BPW) has a circulating spin structure around the circumference and contains a single Bloch point within the centre of the wire cross-section. In contrast, asymmetric transverse walls (ATW) have a circulating spin structure on the surface, and contain two topological defects, a vortex and an anti-vortex on the wire surface, connected through a vortex tube through the wire volume. In this study we have numerically investigated the domain wall spin textures for Nickel nanowires of radii 50nm to 120nm. Beyond reproducing the known BPW and ATW topology, we discover a new domain wall type which contains aspects of both walls. This new domain wall type, which we call asymmetric dual Bloch point wall (ADBPW), has surface vortices similar to an ATW, and two Bloch-points adjacent to the internal vortex tube. Time-resolved simulations investigating the stability of the ADBPW show its field-driven transformation into a BPW via the ejection of a single Bloch point at the surface and subsequent annihilation of surface vortices.

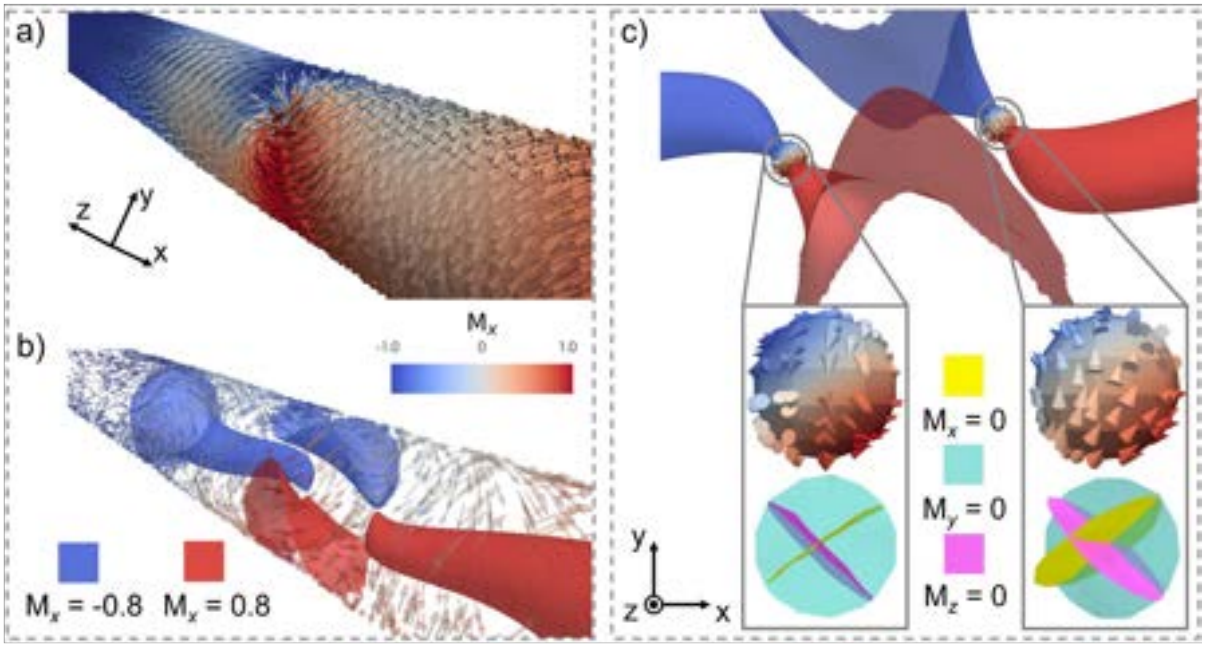

Fig. 1. (a) Surface spin texture of asymmetric dual Bloch point wall (ADBPW). (b) Isosurfaces of axial magnetization where two Bloch points (BPs) are found at the transitions between blue (negative) and red (positive) surfaces. (c) Rotated view of isosurfaces in (b), with spherical regions plotted at the transition regions. Grey boxes show zoomed views of the regions, where the intersection of the $M_x = M_y = M_z = 0$ isosurfaces confirm existence of the BPs at these regions. The BPs are of same type and have opposite circulations.

[1] C. A. Ferguson, et al., Magnetism and Magnetic Materials **381**, 457 (2015).

Detection of Rashba-Edelstein effect using a Josephson junction

Tapas Ranjan Senapati, Ashwin Kumar K*, Kartik Senapati
tapas.senapati@niser.ac.in, kartik@niser.ac.in
School of Physical Sciences, National Institute of Science Education and Research (NISER), an OCC of Homi Bhabha National Institute, Bhubaneswar, Odisha, India
*BITS, Pilani, Goa, India

Abstract:

At the interface of heavy metals (with large spin-orbit coupling) and normal metal the interaction of Pauli spin matrices $\boldsymbol{\sigma}$ with the momentum vector $\boldsymbol{k}$ leads to the splitting of spin contours at the Fermi level, usually known as the Rashba effect. Edelstein [2] first recognized that a charge current at such a Rashba interface would naturally lead to a non-zero spin accumulation at the interface due to the shifting of Fermi contours along the direction of current. Inversely, spin injection to a Rashba interface can generate a charge current at the interface. This Inverse Rashba-Edelstein effect has been recently demonstrated [3] experimentally.

In this work we have attempted to utilize the extreme phase sensitivity of a Josephson junction to look for signatures of the Rashba-Edelstein (RE) effect at the heavy metal/normal metal (Pt/Cu) interface. Since the RE effect produces a net spin accumulation (polarization) at the Pt/Cu interface, a Josephson junction realized across such an interface would see a net magnetic moment due to the spin polarization. Therefore, the Fraunhoffer pattern (magnetic field dependence of critical current or, equivalently, the magnetic field dependence of the voltage across the junction at a fixed current bias) of the Josephson junction should show a field shift corresponding to the effective magnetic moment. In this experiment, using Nb superconducting electrodes on Pt/Cu bilayers, we have realized planar Josephson junctions to study this effect. We indeed observe a shift in the Fraunhoffer pattern of the junctions which changes direction when the magnetic field direction is reversed. We also found that the magnitude of the shift in the Fraunhoffer pattern depends on the thickness of the Pt layer in the Pt/Cu bilayer. This effect is also verified in a SQUID device of identical structure.

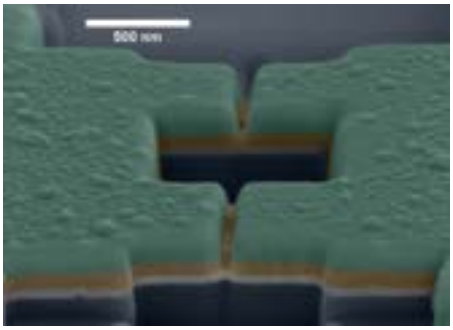

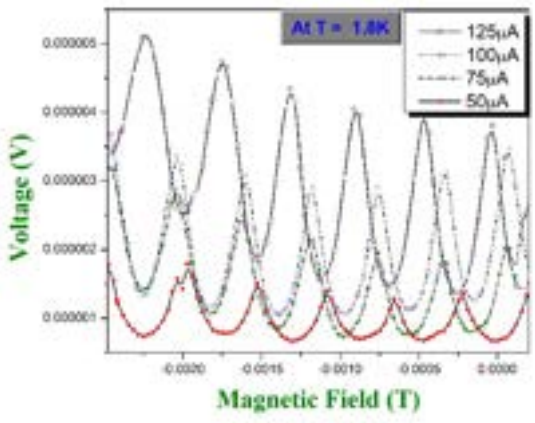

References:

[1] S. Maekawa et al., (eds) Spin Currents (Oxford University Press, 2012).

[2] V. M. Edelstein, Solid State Commun. 73, 233–235 (1990).

[3] J.C. Rosas Sánchez et al.,. Nat Commun 4, 2944 (2013).

Investigating ballistic charge transport and spin injection via 1D graphene/FM junctions

Daniel Burrow, Jesus C. Toscano-Figueroa, Noel Natera-Cordero, Chris R. Anderson, Victor H. Guarochico-Moreira, Thomas Thomson, Irina Grigorieva, Ivan J. Vera-Marun

University of Manchester, UK.

Despite its great promise for spintronics, experimental values for spin transport parameters extracted from graphene are currently significantly below theoretical predictions. Our group recently reported encouraging results from a novel spintronic device architecture constituting a fully encapsulated single layer graphene channel that employs one-dimensional (1D) ferromagnetic (FM) contacts (Fig. 1a) [1]. Encapsulation of the channel in hexagonal boron nitride preserves the quality of the graphene, resulting in high charge mobilities, while use of 1D contacts mitigates many of the problems associated with tunnel contacts, such as doping and Fermi level pinning [2, 3]. Additionally, the geometry of the contact area places transport across the junction in the ballistic regime. This not only allows for achieving sizeable contact resistance without the need for tunnel barriers, but also allows for studying previously unexplored phenomena such as quantized conductance across the 1D graphene/FM junction. Recent results from our novel device architecture have focussed on transport through these junctions, at low temperature. Bias spectroscopy measurements demonstrate conductance through the junction quantized in fractions of the conductance quantum - indicating a transmission factor T ≈ 0.5 (Fig. 1b). Furthermore, application of an out-of-plane magnetic field leads to better defined quantization, resulting from a transition into the quantum Hall regime [4]. Finally, in our spin transport experiments we observe an electrically tuneable spin polarization reversal, implying a spin split density of states in the graphene region adjacent to the FM contact, which occurs due to the magnetic proximity effect. Quantized conductance in a nanoscale 1D FM contact, in the absence of a fabricated graphene nanoconstriction, is a previously unreported result, and could offer a path to ballistic spintronics.

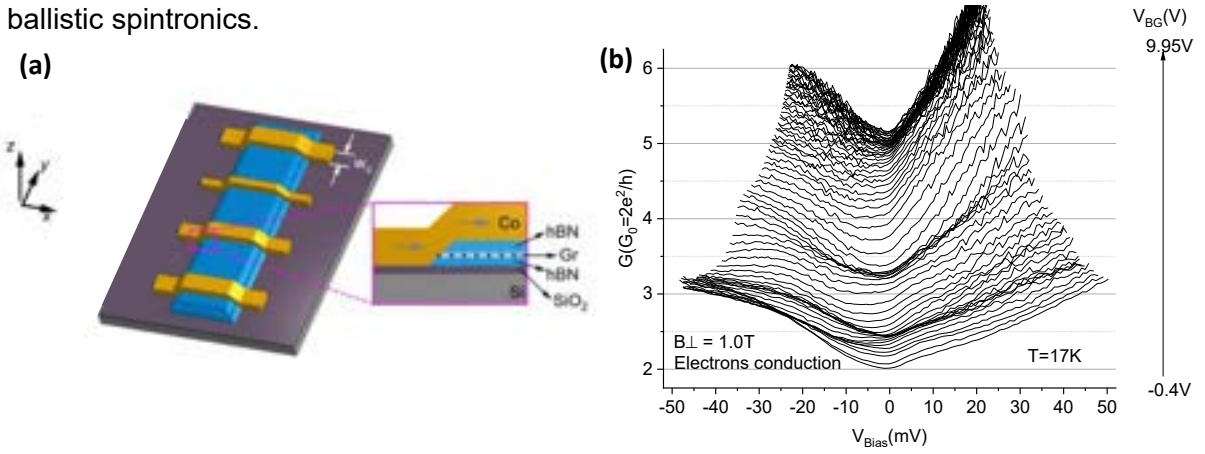

Figure 1: (a) 3D schematic and 2D cross section (inset) of the device architecture. Figure adapted from [1]. **(b)** Bias spectroscopy conductance measurement of a 1D contact, for electron transport ($V_{BG} > V_{neutrality}$) under an applied out-of-plane magnetic field B = 1 T.

[1] Guarochico-Moreira, V. H., et al. (2022). Nano Letters, 22(3), 935–941.

[2] Wang, L., et al. (2013). Science, 342(6158), 614–617.

[3] Xu, J., et al. (2018). Nature Communications, 9(1), 2869.

[4] Tombros, N., et al. (2011). Nature Physics, 7(9), 697–700.

Exceptional points and exceptional behavior in quantum metamaterials

O. I. R. Fox and C. A. Downing

Department of Physics and Astronomy, University of Exeter, United Kingdom

Symmetry underpins our understanding of physical law. Open systems, those in contact with their environment, can provide a platform to explore an important dual symmetry: parity-time (PT) symmetry. That is when swapping left and right, as well as the direction of time, leaves the system essentially unchanged. The condition of combined space and time reflection symmetry has immediate utility for open quantum systems, where there is balanced loss into and gain from the surrounding environment.

In such circumstances, the fact that the resultant Hamiltonian is non-Hermitian may be disconcerting at first glance. While the eigenvalues of a Hermitian Hamiltonian are always real, the Hermicity condition is actually more stringent than is strictly necessary. It was shown by Bender and co-workers [1] that non-Hermitian Hamiltonians which obey parity-time PT symmetry can both admit real eigenvalues and describe physical systems. This brilliant realization has led to many recent advances [2], especially in essentially classical systems, which are intrinsically linked to topological physics [3].

However, the exploitation of PT symmetric physics in truly quantum systems is much less mature. Here we consider a general quantum metamaterial built from qubits [4]. We discuss how the concept of PT symmetry may be generalized for quantum systems, and how this leads to a variety of flavours of exceptional point (which mark the borders between trivial and nontrivial regimes). When passing through these quantum exceptional points (see Fig. 1), we demonstrate some remarkable observable consequences, including for unconventional quantum transport throughout the metamaterial. We also suggest some experiments which should be able to tease out the differences between exceptional points in classical and quantum systems, which may be important in the development of future quantum devices.

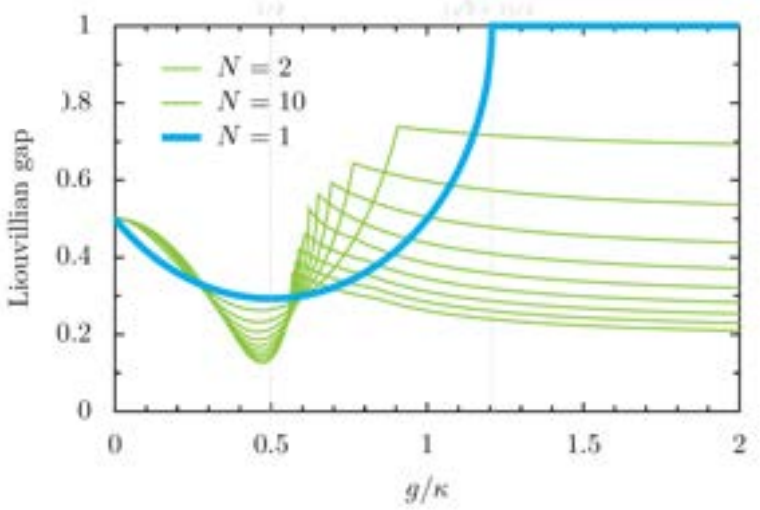

Fig. 1. The Liouvillian gap as a function of coupling strength (in units of the gain-loss rate). The cyan line shows the result for a qubit, and the green lines for oscillators with an increasing number of energy levels N. In the limit of N tending towards infinity, the Liouvillian gap closes at an exceptional point, suggesting a dissipative phase transition. Adapted from Ref. [4].

[1] C. M. Bender and S. Boettcher, Phys. Rev. Lett. **80**, 5243 (1998).
[2] E. J. Bergholtz, J. C. Budich and F. K. Kunst, Rev. Mod. Phys. **93**, 15005 (2021).
[3] C. A. Downing and V. A. Saroka, Commun. Phys. **4**, 254 (2021).
[4] O. I. R. Fox and C. A. Downing *(in preparation, 2022)*.

Spin-to-charge conversion effects in van der Waals heterostructures

C.K. Safeer[1,2], J. Ingla Aynes[1], F. Herling[1], N. Ontoso[1], L. Hueso[1], F. Casaonva[1].

[1] CIC nanoGUNE, San Sebastian, Spain
[2] Physics department, University of Oxford, Oxford, UK

Graphene has been known as an excellent material for long-distance spin transport due to its weak spin-orbit coupling (SOC). However, the same reason makes graphene an adverse candidate for different spintronics applications in which strong SOC is required, such as the Datta and Das spin transistor proposal or spin-charge interconversion applications. It has recently been predicted theoretically that SOC can be induced in graphene so that spin-orbit phenomena such as spin Hall effect (SHE) or Rashba-Edelstein effect can be obtained. In our work, by using van der Waals heterostructure-based lateral spin valve [1], we experimentally demonstrated the first unambiguous measurement of spin-to-charge conversion (SCC) due to SHE in graphene via spin-orbit proximity with transition metal dichalcogenides (TMD), MoS_2[2] and WSe_2 [3] as shown in figure 1. We extended similar experiments in graphene combined with an insulator, Bi_2O_3[4]. Then we demonstrated gate tuneable SHE in graphene with SCC efficiency larger than in some of the best SCC materials such as topological insulators [3]. Using a similar approach, we performed another experiment using Weyl semimetal $MoTe_2$ and observed large multidirectional SCC [5]. Here, due to the low symmetry of MoTe2 crystal, we detect, along with the conventional SCC, an unconventional SCC where the spin polarization and the charge current are parallel. Our finding enables the simultaneous conversion of spin currents with any in plane spin polarization in one single experimental configuration. In summary, all these different experiments spread light into the understanding of spin-orbit effects in van der Waal materials such as graphene, TMDs, and Weyl semi metals. These exceptional effects obtained by the unique properties of 2D materials open exciting opportunities in a variety of future spintronic applications.

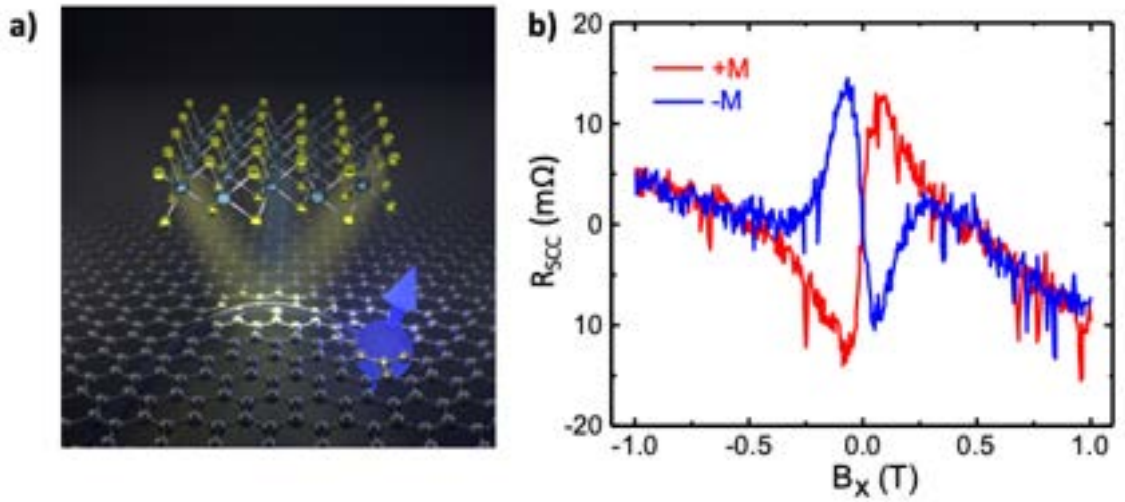

Fig. 1: a) Schematic representation of spin Hall effect in graphene due to spin-orbit proximity from transition metal dichalcogenides **b)** Spin-to-charge conversion signals due to spin Hall effect measured in graphene/MoS_2 heterostructure [1].

[1] C. K. Safeer, et al. *2D Materials*, 9, 6, 015024 (2021).
[2] C. K. Safeer, et al. *Nano Letters*, 19, 2, 1074-1082 (2019).
[3] F. Herling, C.K. Safeer et al. *APL Materials*, 8, 071103 (2020).
[4] C. K. Safeer, et al. *Nano Letters*, 20, 6, 4573-4579 (2020).
[5] C. K. Safeer, et al. *Nano Letters*, 19, 12, 8758-8766 (2019).

Probing valley-dependent spin splitting at the surface of magnetic VNb_3S_6 using angle-resolved photoemission spectroscopy

B. Edwards[1], O. Dowinton[2], A. Hall[3], P. Murgatroyd[1], S. Buchberger[1], G. Siemann[1], E. Abarca Morales[1], T. Antonelli[1], A. Rajan[1], A. Zivanovic[1], G. Balakrishnan[3], M. S. Bahramy[2] and P. D. C. King[1]

[1]SUPA, School of Physics and Astronomy, University of St Andrews, United Kingdom
[2]Department of Physics and Astronomy, University of Manchester, United Kingdom
[3]Department of Physics, University of Warwick, United Kingdom

Intercalating guest atoms into the van der Waals gaps of transition-metal dichalcogenides has emerged as a powerful route to tune their already flexible material properties. In superconducting NbS_2 [1], intercalating magnetic (M=V,Cr,Co,Fe) ions leads to the development of long-range magnetic orders hosting non-trivial spin textures. For a critical composition of MNb_3S_6, the intercalated atoms arrange periodically in a superstructure, making the crystal non-centrosymmetric [2,3,4]. Upon cooling, the intercalated ions order magnetically: in VNb_3S_6, for example, a nearly antiferromagnetic state is found, with recent studies reporting that out-of-plane spin canting leads to a net uncompensated moment [5,6].

Here, we use angle-resolved photoemission spectroscopy to investigate the surface electronic structure of VNb_3S_6. Upon sample cleavage, both V and NbS_2 surface terminations are obtained, randomly distributed across the sample. Whilst the disordered nature of the surface intercalates [7] leads the V surface termination to display a broadened band structure, the NbS_2 surface termination exhibits clear features for a range of dispersive states which are derived from the surface NbS_2 layer. These are shifted in energy as compared to the bulk, due to self-doping at the polar surface. Excitingly, we observe a valley-dependent splitting of the Nb-derived conduction bands developing below the magnetic ordering temperature. We find this to be natural consequence of spin–valley locking in the surface layer of NbS_2 [8] when proximity coupled to the underlying magnetic intercalate layer. These results reflect a strong interplay between spin-orbit mediated and magnetic exchange splittings, offering a method to control valley spin polarization.

[1] I. Guillamon *et al.*, Phys. Rev. Lett. **101**, 166407 (2008).
[2] S. S. P. Parkin and H. Friend, Philos. Mag. B **41**, 65 (1980).
[3] Y. Kousaka *et al.*, Methods Phys. Res., Sect. A **600**, 250 (2009).
[4] Y. Togawa *et al.*, Phys. Rev. Lett. **108**, 107202 (2012).
[5] K. Lu *et al.*, Phys. Rev. Mat. **4**, 054416 (2020).
[6] A. E. Hall *et al.*, Phys. Rev. B **103**, 174431 (2021).
[7] N. Sirica *et al.*, Phys. Rev. B **94**, 075141 (2016).
[8] L. Bawden *et al.*, Nature Commun. **7**, 11711 (2016).

Topological Photonic Crystal Fibre

Nathan Roberts[1], Guido Baardink[1], Josh Nunn[1,2], Peter J Mosley[1], and Anton Souslov[1]

[1]University of Bath, UK, [2]ORCA Computing, UK

Topological photonics is a burgeoning field that ties the physical properties of light propagation to unchanging topological invariants. These invariants can be exploited to engineer photonic topological band structures that give rise to disorder-resistant band gaps [1] and back-scattering-free propagation [2]. Despite recent progress in this field, it remains a challenge to create scalable waveguides in which light is both confined by a sub-micron architecture and topologically protected.

Here we fabricate photonic crystal fibre in which light propagation is inextricably tied to a topological invariant (see Fig. 1A and Ref. [3]). Our fibre enables the propagation of topologically protected supermodes over millions of wavelengths, hundreds of times greater than planar waveguide devices [4]. By curling up a Su-Schrieffer-Heeger chain and embedding it within a periodic cladding of glass and air, the fibre becomes characterised by a winding number invariant. This invariant gives rise to protected edge modes, which we experimentally observe in Fig. 1B. After performing a direct measurement of the winding number invariant, we demonstrate bending as a topological switch. This global geometric perturbation is inaccessible to rigid waveguide substrates and highlights the unique flexibility of our fibre platform (see Fig. 1C).

In conclusion, we have used a combination of finite-element simulation and topological design to fabricate photonic crystal fibre that supports topologically protected supermodes. We have experimentally observed the invariant that characterises the fibre and investigated the effects of fibre bending. Our fibre presents a step towards using topological design to enable scalable, robust quantum communication, immune to symmetry preserving disorders. Based on our results, we envision a make-to-order approach for topological band engineering inside long, thin optical fibre.

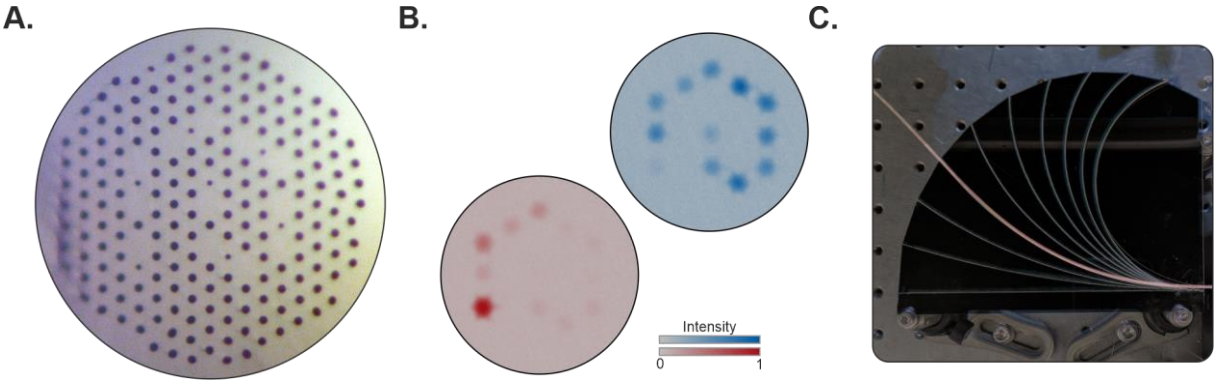

Fig. 1. (A) Cleaved end face of fibre; (B) Experimental demonstration of topological bulk (blue) and edge (red) modes; (C) Demonstration of fibre bending.

[1] M. C. Rechtsman, *et al.*, Nature **496**, 196-200 (2013).
[2] Z. Wang, *et al.*, Phys. Rev. Lett. **100**, 1-4 (2008).
[3] N. Roberts, *et al.*, arXiv preprint, arXiv:2201.10584 (2022).
[4] Y. Wang, *et al.*, Phys. Rev. Lett. **122**, 193903 (2019).

REPORT

2D MATERIALS

Out-of-equilibrium criticalities in graphene superlattices

Alexey I. Berdyugin[1,2]*†, Na Xin[1,2]†, Haoyang Gao[3], Sergey Slizovskiy[1,2], Zhiyu Dong[3], Shubhadeep Bhattacharjee[1,2], P. Kumaravadivel[1,2], Shuigang Xu[1,2], L. A. Ponomarenko[1,4], Matthew Holwill[1,2], D. A. Bandurin[1,2], Minsoo Kim[1,2]‡, Yang Cao[1,2], M. T. Greenaway[5,6], K. S. Novoselov[2], I. V. Grigorieva[1], K. Watanabe[7], T. Taniguchi[8], V. I. Fal'ko[1,2,9], L. S. Levitov[3], Roshan Krishna Kumar[1,2,10]*, A. K. Geim[1,2]*

In thermodynamic equilibrium, current in metallic systems is carried by electronic states near the Fermi energy, whereas the filled bands underneath contribute little to conduction. Here, we describe a very different regime in which carrier distribution in graphene and its superlattices is shifted so far from equilibrium that the filled bands start playing an essential role, leading to a critical-current behavior. The criticalities develop upon the velocity of electron flow reaching the Fermi velocity. Key signatures of the out-of-equilibrium state are current-voltage characteristics that resemble those of superconductors, sharp peaks in differential resistance, sign reversal of the Hall effect, and a marked anomaly caused by the Schwinger-like production of hot electron-hole plasma. The observed behavior is expected to be common to all graphene-based superlattices.

The electric response of metallic systems is routinely described by a Fermi surface displacement in momentum space, established through a balance between acceleration of charge carriers and their relaxation caused by scattering (*1*). The displacement is usually small, so that the drift velocity v_d is minute compared with the Fermi velocity v_F. In theory, if inelastic scattering is sufficiently weak, it should be possible to shift the Fermi surface so far from equilibrium that all charge carriers within the topmost, partially filled bands start streaming along the applied electric field E. The field would then start producing extra carriers through interband transitions (*2*), allowing electronic bands under the Fermi energy to contribute to the charge flow. Such an extreme out-of-equilibrium regime has never been achieved in metallic systems because Ohmic heating, phonon emission, and other mechanisms greatly limit v_d (*3*–*5*).

A rare exception is semimetallic graphene. At high carrier densities n, the drift velocity in graphene is limited by phonon emission (*6*, *7*), similar to other metallic systems. However, at low n, thermal excitations can create a relativistic plasma of massless electrons and holes, the "Dirac fluid." Its properties in thermodynamic equilibrium were in the focus of recent research (*8*–*12*), but the behavior at high biases represents an uncharted territory. Yet close to the Dirac point, even a small E can shift the entire Fermi surface and tap into a supply of carriers from another band (*13*, *14*). This can trigger processes analogous to the vacuum breakdown and Schwinger particle-antiparticle production in quantum electrodynamics, in which they are predicted to occur at enormous fields of ~10^{18} V m^{-1} (*15*). Because such E are inaccessible, it is enticing to mimic the Schwinger effect and access the resulting out-of-equilibrium plasma in a condensed matter experiment (*13*, *14*, *16*). Certain nonlinearities observed near graphene's neutrality point (NP) were previously attributed to the creation of electron-hole (e-h) pairs by means of a Schwinger-like mechanism (*13*, *14*), but the expected intrinsic behavior was obscured by low mobility, charge inhomogeneity, and self-gating effects (*6*, *17*).

We used graphene-based superlattices to identify an out-of-equilibrium state that sharply develops above a well-defined critical current j_c. The current marks an onset of the Schwinger pair production and a transition from a weakly dissipative fluid-like flow to a strongly dissipative e-h plasma regime. The out-of-equilibrium Dirac fluid is realized at surprisingly small E, thanks to the narrow electronic bands and low v_F characteristic of graphene superlattices (*18*, *19*). The resulting dual-band transport leads to striking anomalies in longitudinal and Hall resistivities. Counterintuitively, an apparent drift velocity in this regime exceeds v_F. With hindsight, we show that the current-induced critical state can be reached even in standard graphene, by using extra-high currents allowed by the point contact geometry.

The studied superlattices were of two types: graphene crystallographically aligned on top of hexagonal boron nitride (G/hBN) (*20*–*23*) and small-angle twisted bilayer graphene (TBG) (*24*–*28*). The superlattices were encapsulated in hBN, to ensure high electronic quality, and shaped into multiterminal Hall bar devices by using the standard fabrication procedures (*29*). The devices were first characterized by measuring their longitudinal resistivity ρ as a function of n as shown in Fig. 1, A to C, for three representative devices. The twist angles θ were determined from measurements of Brown-Zak oscillations (*30*); for TBG, θ was intentionally chosen away from the magic angle to avoid many-body states (*27*, *28*). Aside from the familiar peak in ρ at zero doping, satellite peaks indicating secondary NPs were observed at n that agreed well with the θ values (*20*–*22*, *26*). For G/hBN superlattices, the low-energy electronic spectrum is practically identical to that of monolayer graphene (*18*), and the spectral reconstruction occurs only near and above the edge of the first miniband (Fig. 1D, top). By contrast, all minibands in TBG are strongly reconstructed (Fig. 1D, bottom) (*19*). At low biases (Fig. 1, A to C, and fig. S1), our devices exhibited transport characteristics similar to those reported previously for G/hBN and TBG superlattices (*20*–*22*, *26*).

Next, we studied high-bias transport using current densities j up to 0.1 mA μm^{-1}, limited only to avoid device damage. Unless stated otherwise, all the reported measurements were carried out at the bath temperature T = 2 K. The superlattices exhibited qualitatively similar current-voltage (I-V) characteristics (Fig. 1, E to G), which were nearly linear at $j <$ 0.01 mA μm^{-1} and then rapidly switched into a high-resistance state so that the differential resistivity dV/dI showed a pronounced peak at a certain critical current j_c. The behavior was universal, found in all our devices (more than 10) (figs. S3 and S6), if the Fermi energy was tuned inside narrow minibands (that is, away from the main NP in the case of G/hBN). The I-V characteristics in Fig. 1, E to G, strongly resemble the superconducting response, despite electron transport being ballistic at low j and viscous at moderate currents (*31*); ρ always remained finite, although could be as low as <0.01 kilohms, a few orders of magnitude smaller than dV/dI above j_c. Further details are provided in Fig. 2 by showing dV/dI as a function of n, where the narrow white arcs indicate peaks in dV/dI. Considerable similarities

[1]School of Physics and Astronomy, University of Manchester, Manchester M13 9PL, UK. [2]National Graphene Institute, University of Manchester, Manchester M13 9PL, UK. [3]Massachusetts Institute of Technology, Cambridge, MA 02139, USA. [4]Department of Physics, University of Lancaster, Lancaster LA1 4YW, UK. [5]Department of Physics, Loughborough University, Loughborough LE11 3TU, UK. [6]School of Physics and Astronomy, University of Nottingham, Nottingham NG7 2RD, UK. [7]Research Center for Functional Materials, National Institute for Materials Science, 1-1 Namiki, Tsukuba 305-0044, Japan. [8]International Center for Materials Nanoarchitectonics, National Institute for Materials Science, 1-1 Namiki, Tsukuba 305-0044, Japan. [9]Henry Royce Institute for Advanced Materials, Manchester M13 9PL, UK. [10]Institut de Ciencies Fotoniques (ICFO), Barcelona Institute of Science and Technology, 08860 Castelldefels, Barcelona, Spain.
*Corresponding author. Email: alexey.berdyugin@manchester.ac.uk (A.I.B); roshankrishnakumar90@gmail.com (R.K.K.); geim@manchester.ac.uk (A.K.G.)
†These authors contributed equally to this work.
‡Present address: Department of Applied Physics, Kyung Hee University, Yong-In 17104, South Korea.

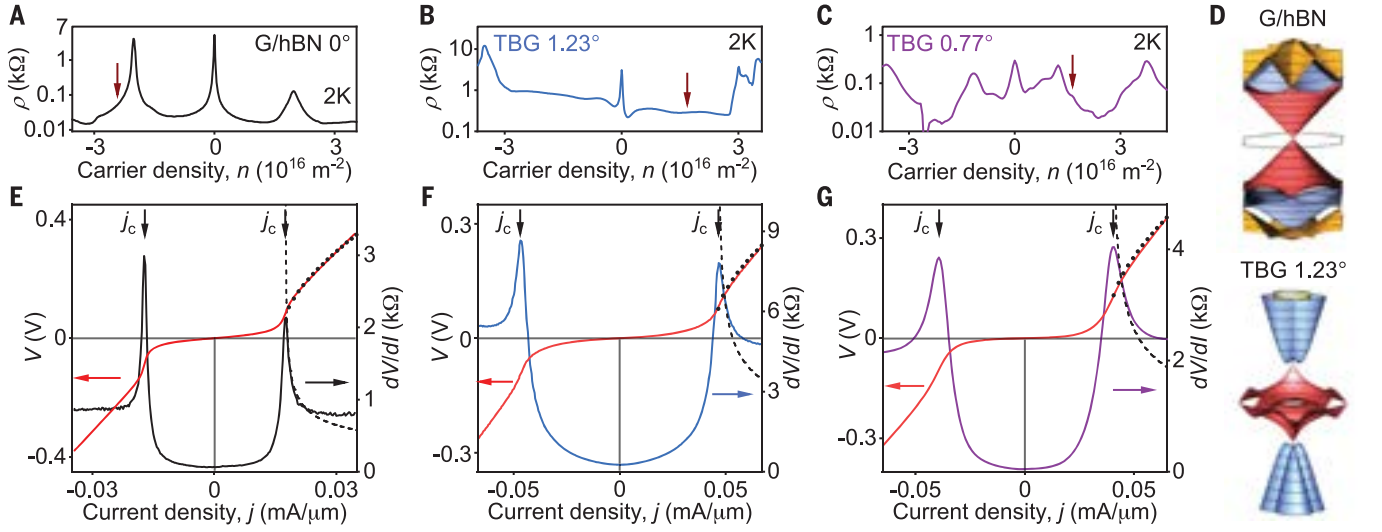

Fig. 1. Linear and nonlinear transport in graphene superlattices. (**A** to **C**) ρ(*n*) in the linear regime (*j* = 50 nA μm^{-1}) for (A) G/hBN with θ ≈ 0° and for TBG with (B) θ ≈ 1.23° and (C) θ ≈ 0.77°. Micrographs of the studied devices are provided in (*29*). (**D**) Band structures of G/hBN and TBG 1.23° superlattices (*29*). Colors indicate different energy bands. The bands are shown for the energy range of ±340 and ±80 meV for G/hBN and TBG 1.23°, respectively. (**E** to **G**) *I-V* characteristics for the devices in panels (A) to (C), respectively. The doping levels for the curves are indicated with the arrows in (A) to (C). The dependence $(j - j_c) \propto V^{3/2}$ expected above j_c is indicated by the dotted curves and the corresponding $dV/dI \propto (j - j_c)^{-1/3}$ is indicated by the dashed curves. All *V* and *dV/dI* are normalized according to devices' aspect ratios.

are clearly seen across different superlattice types. One feature shared by all the maps was the rapidly decreasing j_c as *n* approached NPs (Fig. 2, A to C, and figs. S2 and S6). The only exception was the main NP in G/hBN superlattices, where the resistivity in its vicinity increased monotonically for all accessible *j* (fig. S2).

To gain more insight, we studied the Hall effect in small (nonquantizing) magnetic fields *B*. An example of such measurements for G/hBN near the hole-side NP is shown in Fig. 2D. At small *j*, the Hall voltage V_{xy} increased linearly with *j*, and dV_{xy}/dI was positive, reflecting the hole doping. However, dV_{xy}/dI abruptly turned negative above j_c, revealing a change in the dominant-carrier type. dV_{xy}/dI maps for the G/hBN and TBG superlattices are shown in Fig. 2, E to G. There are clear correlations between the longitudinal and Hall maps so that the peaks in *dV/dI* and the Hall effect's reversal occurred at same j_c. The observed nonlinearities were robust against *T* up to ~50 K, above which the peaks in *dV/dI* became gradually smeared (fig. S4). This shows that Ohmic heating—which is generally expected at high *j* (*14*, *31*, *32*)—was not the reason for the critical-current behavior (*29*).

The rapid decrease in j_c near all secondary NPs prompts the question why such a critical-current behavior was not observed in graphene (*13*, *14*) or near the main NP of G/hBN (Fig. 2A) and whether it can be achieved at some higher *j*. With this in mind, we used a point contact geometry that funneled the current through a short constriction, whereas wide adjacent regions provided a thermal bath for electron cooling. This allowed us to reach *j* an order of magnitude greater than those achievable in the standard geometry. At these *j*, *I-V* characteristics near the main NP of G/hBN superlattices became similar to those near its secondary NPs (fig. S3), although they were more smeared because of Ohmic heating and, possibly, edge irregularities in the superlattice periodicity within narrow constrictions. To circumvent the latter problems and demonstrate the universality of the critical behavior at all NPs, we made constrictions from nonsuperlatticed graphene (monolayer graphene encapsulated in hBN but nonaligned). These devices also displayed a clear critical behavior, although peaks at j_c were notably broader because of heating (Fig. 3A).

To understand the criticalities, we first discuss the conceptually simplest case of the Dirac spectrum, such as in nonsuperlatticed graphene. We consistently observed that the transition between the low- and high-resistance states occurred at $j_c \approx nev_F$ (*e* is the electron charge)—that is, at $v_d \approx v_F$, independently of *n* (Fig. 3B). This condition means that the Fermi surface is shifted from equilibrium by the entire Fermi momentum, and all electrons in the conduction band move along *E* with a drift velocity of about v_F (Fig. 3C). If the spectrum were fully gapped, *j* could not increase any further because all available carriers already move at maximum speed. This should result in saturation of *j* as a function of *V*, which is in agreement with the observations at $j \lesssim j_c$. Simulations of this intraband-only transport corroborate our conclusions (Fig. 3A, dashed curves). To explain the supercritical behavior at $j > j_c$, for a gapless spectrum *E* can move electrons up in energy from the valence band into the conduction band, leaving empty states (holes) behind (Fig. 3C, bottom). The extra electrons and holes created by the interband transitions allow the current to exceed j_c. Accordingly, the apparent $v_d = j/ne$ seemingly exceeds the maximum possible group velocity, v_F (because *n* is fixed by gate voltage, but the actual concentration of carriers increases by Δ*n*). Quantitatively, the e-h production at $j > j_c$ can be described by the Schwinger (or Zener-Klein tunneling) mechanism. It can generate interband carriers at a rate $\propto E^{3/2}$ (*13*, *16*), but at small biases, the production is forbidden by the Pauli exclusion principle. Above j_c, the Fermi distribution is shifted sufficiently far from equilibrium so that *E* depletes the states near the NP, which eliminates the Pauli blocking and enables the e-h pair production (Fig. 3C). Accounting for e-h annihilation (recombination processes bring the electronic system back into the equilibrium), we found the stationary concentration of extra carriers Δ*n* to be $\propto E^{3/2} \propto V^{3/2}$, if $\Delta n \ll n$ (*29*). This translates into extra current $\Delta nev_F \propto V^{3/2}$ and $dV/dI \propto j^{-1/3}$. Because *dV/dI* decreases for $j > j_c$ but increases for $j < j_c$, a peak is expected at j_c, which is in agreement with Fig. 3A.

The above analysis can also be applied to graphene superlattices. Their narrow minibands display low v_F, and therefore, the onset of interband transitions is expected at small *j*. The switching transition in our superlattices occurred at v_d typically >10 times smaller than in nonsuperlatticed graphene (fig. S5). This yields a characteristic v_F of several 10^4 m s^{-1}, which translates into minibands' widths

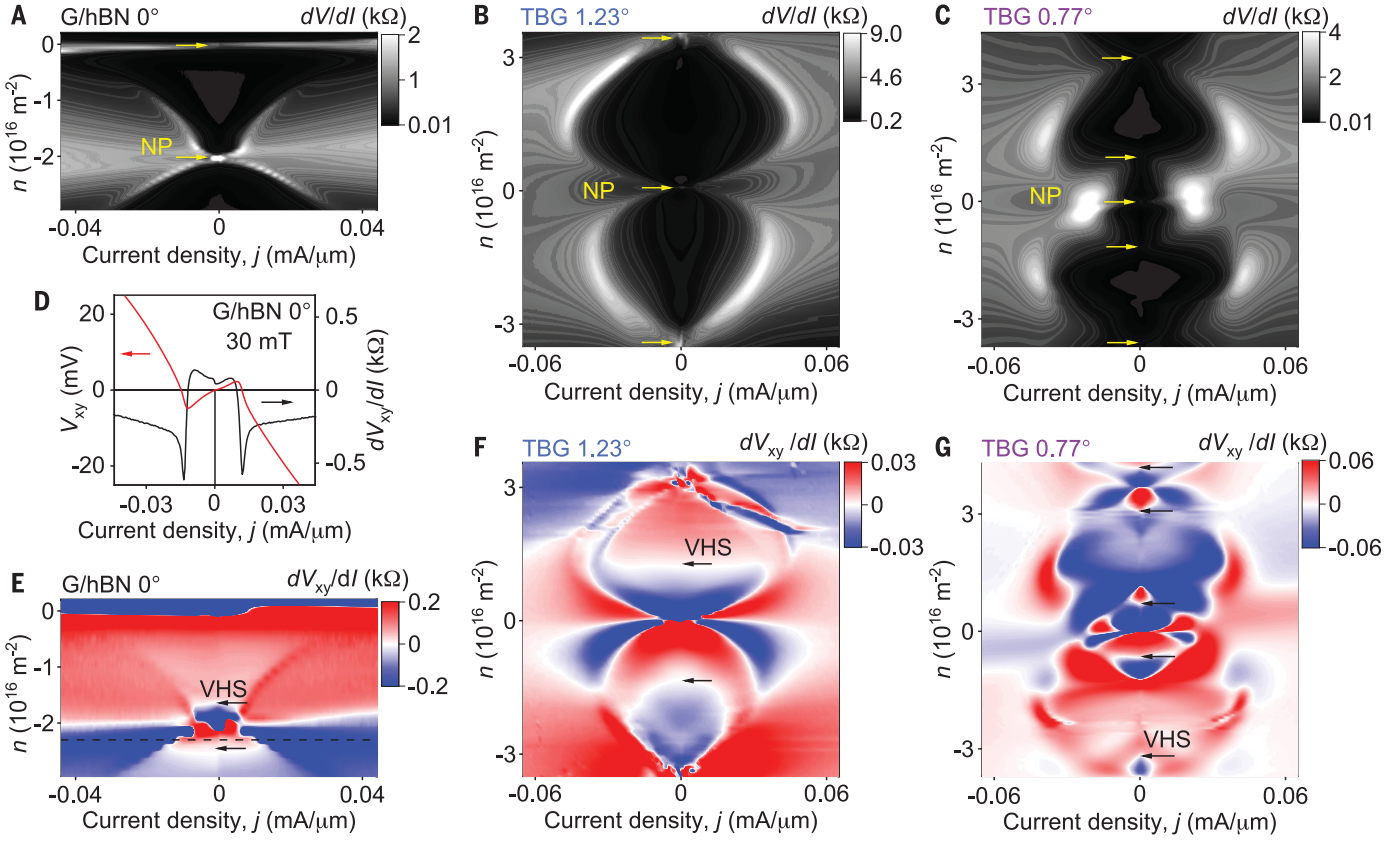

Fig. 2. Switching into the high-bias regime. (**A** to **C**) *dV/dI* as a function of *j* and *n* for the superlattices in Fig. 1, A, to C, respectively. Bright arcs appear at the critical current. Yellow arrows indicate NPs as found with low-bias measurements (*29*). (**D**) Hall voltage (red curve) and the corresponding differential resistivity (black curve) measured at *n* indicated by the dashed line in (E). (**E** to **G**) Maps of dV_{xy}/dI for the superlattices in (A) to (C), respectively. B = 30 mT; T = 2 K. The black arrows indicate positions of van Hove singularities.

of ~10 meV, as expected from band structure calculations (*19*). For the relatively small j_c, superlattices were much less affected by heating than graphene and, accordingly, exhibited sharper transitions (Figs. 2 and 3A). The experimental *I-V* curves are compared with the above predictions for Schwinger-like carrier generation in Fig. 1, E to G. Good agreement was found for $j \gtrsim j_c$. Notable deviations seen at highest j are expected because Δn is no longer small compared with n, the assumption used to derive the plotted dependences (*29*). Furthermore, j_c in graphene evolved $\propto n$ as expected for the Dirac spectrum (Fig. 3B). By contrast, superlattices exhibited clear deviations from the linear dependence (Figs. 2, A to C). This is attributed to the group velocity of charge carriers rapidly decreasing away from secondary NPs, dropping to zero at van Hove singularities (VHSs). If nonequilibrium carriers reside near VHSs, they move at low speed and contribute little to the current (fig. S5C), leading to the sublinear $j_c(n)$, as observed experimentally.

Extending the described physics onto the Hall effect, it is straightforward to understand the sign changes in Fig. 2, D to G. With reference to Fig. 3C, interband transitions result in extra holes near the NP plus extra electrons that effectively appear at higher energies in the out-of-equilibrium Fermi distribution (Fig. 3C). For superlattices, contributions of these e-h pairs into V_{xy} do not cancel each other because of the broken e-h symmetry, which results in different masses and mobilities of the extra carriers. The effect is particularly strong upon approaching a VHS. For example, if the dominant carriers are electrons, their distribution would be shifted by E upward toward a VHS (fig. S5C), and they should have heavy masses. By contrast, the reciprocal holes generated near the NP should be light (fig. S5C). These higher-mobility holes are expected to provide a dominant contribution into the Hall signal, and therefore, dV_{xy}/dI should change its sign from electron to hole near $j \approx j_c$, as observed experimentally. If the asymmetry is sufficiently strong, even V_{xy} can reverse its sign (Fig. 2D). The observed changes in the Hall effect can qualitatively be described by using the two-carrier model with different mobilities of out-of-equilibrium electrons and holes (fig. S7).

Last, we discuss the interband carrier generation at the main NP in graphene (Fig. 3), which closely mimics the Schwinger effect in quantum electrodynamics. Consequences of the Schwinger-like effect at the Dirac point are qualitatively different from those described by Zener-Klein tunneling at finite doping (*29*). In contrast to the latter case, there is no low-to-high resistance switching at n = 0, and *dV/dI* rapidly drops with increasing j, reaches a minimum, and then gradually increases (Fig. 3D). This behavior was highly reproducible for all graphene constrictions (fig. S8) but, because of self-gating and heating effects, could not be observed in the standard geometry, where *I-V* curves were similar to those in the literature (*6*). The initial drop is attributed to e-h puddles present at NPs, in which small E starts generating interband carriers along puddles' boundaries and enhances conductivity (*13*). Minima in *dV/dI* typically occurred at $j_m \approx 0.05$ mA μm^{-1} (Fig. 3D), which translates into $\Delta n = j_m/ev_F \approx 3 \times 10^{10}$ cm^{-2}, which is in agreement with the charge inhomogeneity δ found in our devices. In principle, the initial *dV/dI* drop could be fitted again by $\propto j^{-1/3}$, but such fits were inconclusive because of the involved inhomogeneity. For higher j so that $\Delta n \gg \delta$, the Schwinger production fills graphene with a plasma of electrons and holes in equal concentrations, $n_e \approx n_h = \Delta n$. Because

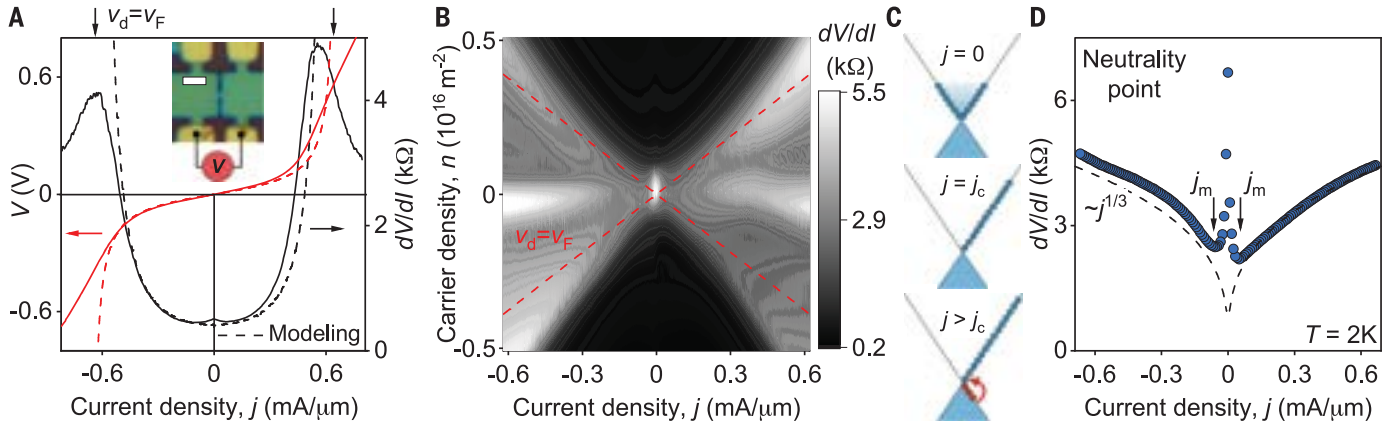

Fig. 3. Nonlinear transport in nonsuperlatticed graphene near the Dirac point. (**A**) Voltage and differential resistance (red and black curves, respectively) for a constriction of 0.4 μm in width; $n = 0.4 \times 10^{16}$ m^{-2}. (Inset) Optical micrograph of the graphene device and its measurement geometry. Scale bar, 2 μm. The small bump at zero bias is caused by electron-electron scattering (*34*). Dashed curves indicate *I-V* characteristics calculated for the Dirac spectrum at $j < j_c$ (*29*). The vertical arrows indicate j with $v_d = v_F = 1 \times 10^6$ m s^{-1}. (**B**) Example of *dV/dI* maps for graphene constrictions. Red lines indicate $j = nev_F$. (**C**) Schematic of graphene's spectrum and its occupancy in (top) equilibrium and in out-of-equilibrium for (middle) $j = j_c = nev_F$ and (bottom) $j > j_c$. Blue and red circles indicate electrons and holes, respectively. The red arrow illustrates e-h pair production. (**D**) *dV/dI* at the NP for a 0.6-μm-wide constriction. The arrows indicate minima.

the annihilation rate of e-h pairs scales with $n_e n_h = \Delta n^2$, theory predicts (*29*) that the Schwinger production rate ($\propto E^{3/2}$) leads to $\Delta n \propto E^{3/4}$, resulting in $dV/dI \propto j^{+1/3}$. This contrasts the reported Zener-Klein behavior at graphene's NP (*13*) but is in quantitative agreement with our experiment (Fig. 3D and fig. S8). For highest j, the hot e-h plasma inside graphene constrictions is expected to approach the quantum critical limit (*8*–*12*), in which e-h scattering is governed by the uncertainty principle and ρ is predicted to become rather universal, ~$1.3\alpha^2(h/e^2)$, where α is the interaction constant and h/e^2 is the resistance quantum (*8*, *9*). For encapsulated graphene, $\alpha \approx 0.3$, whereas the constriction geometry results in resistance of ~1.8ρ (*29*). Accordingly, the quantum-critical resistance for our constrictions is expected to be ~5 kilohms, which is in qualitative agreement with Fig. 3D and fig. S8, where the curves approach this value. We do not expect better agreement because E strongly disturbs the e-h plasma, making it anisotropic, which is rather different from the Dirac fluids in thermal equilibrium, which were discussed previously (*8*–*12*). This anisotropic regime requires further theoretical analysis and would be interesting to probe through other experimental techniques.

At high biases, Fermi liquids in graphene-based systems can be turned into Dirac-like fluids characterized by intense interband carrier generation. The transition between the weakly and strongly dissipative electronic states is marked by peculiar superconducting-like *dV/dI*. Such *I-V* characteristics, although of interest on their own right as a signature of out-of-equilibrium criticalities, also serve as a warning that they alone—without other essential attributes (such as zero resistance)—do not constitute a proof of "emerging/fragile" superconductivity. It is possible that the nonlinear response reported in some graphene-based flat-band systems [for example, (*33*)] was governed by the out-of-equilibrium physics rather than superconductivity. Other attributes of nonequilibrium behavior such as Bloch oscillations and associated terahertz radiation are likely to accompany the reported criticalities, which is an appealing opportunity for further investigation.

REFERENCES AND NOTES

1. C. Kittel, *Introduction to Solid State Physics* (Wiley, ed. 8, 2005).
2. C. Zener, *Proc. R. Soc. A Math. Phys. Eng. Sci.* **145**, 523–529 (1934).
3. W. Shockley, *Bell Syst. Tech. J.* **30**, 1035–1037 (1951).
4. E. J. Ryder, *Phys. Rev.* **90**, 766–769 (1953).
5. S. M. Sze, K. K. Ng, *Physics of Semiconductor Devices* (Wiley-Interscience, 2007).
6. I. Meric *et al.*, *Nat. Nanotechnol.* **3**, 654–659 (2008).
7. M. A. Yamoah, W. Yang, E. Pop, D. Goldhaber-Gordon, *ACS Nano* **11**, 9914–9919 (2017).
8. L. Fritz, J. Schmalian, M. Müller, S. Sachdev, *Phys. Rev. B Condens. Matter Mater. Phys.* **78**, 085416 (2008).
9. A. B. Kashuba, *Phys. Rev. B Condens. Matter Mater. Phys.* **78**, 085415 (2008).
10. J. Crossno *et al.*, *Science* **351**, 1058–1061 (2016).
11. P. Gallagher *et al.*, *Science* **364**, 158–162 (2019).
12. M. J. H. Ku *et al.*, *Nature* **583**, 537–541 (2020).
13. N. Vandecasteele, A. Barreiro, M. Lazzeri, A. Bachtold, F. Mauri, *Phys. Rev. B Condens. Matter Mater. Phys.* **82**, 045416 (2010).
14. W. Yang *et al.*, *Nat. Nanotechnol.* **13**, 47–52 (2018).
15. J. Schwinger, *Phys. Rev.* **82**, 664–679 (1951).
16. D. Allor, T. D. Cohen, D. A. McGady, *Phys. Rev. D Part. Fields Gravit. Cosmol.* **78**, 096009 (2008).
17. Y. Wu *et al.*, *ACS Nano* **6**, 2610–2616 (2012).
18. J. R. Wallbank, A. A. Patel, M. Mucha-Kruczynski, A. K. Geim, V. I. Fal'ko, *Phys. Rev. B Condens. Matter Mater. Phys.* **87**, 245408 (2013).
19. R. Bistritzer, A. H. MacDonald, *Proc. Natl. Acad. Sci. U.S.A.* **108**, 12233–12237 (2011).
20. L. A. Ponomarenko *et al.*, *Nature* **497**, 594–597 (2013).
21. C. R. Dean *et al.*, *Nature* **497**, 598–602 (2013).
22. B. Hunt *et al.*, *Science* **340**, 1427–1430 (2013).
23. M. Yankowitz, Q. Ma, P. Jarillo-Herrero, B. J. LeRoy, *Nat. Rev. Phys.* **1**, 112–125 (2019).
24. Y. Cao *et al.*, *Phys. Rev. Lett.* **117**, 116804 (2016).
25. K. Kim *et al.*, *Proc. Natl. Acad. Sci. U.S.A.* **114**, 3364–3369 (2017).
26. Y. Cao *et al.*, *Nature* **556**, 80–84 (2018).
27. L. Balents, C. R. Dean, D. K. Efetov, A. F. Young, *Nat. Phys.* **16**, 725–733 (2020).
28. E. Y. Andrei, A. H. MacDonald, *Nat. Mater.* **19**, 1265–1275 (2020).
29. Materials and methods are available in the supplementary materials.
30. R. Krishna Kumar *et al.*, *Science* **357**, 181–184 (2017).
31. D. A. Bandurin *et al.*, *Science* **351**, 1055–1058 (2016).
32. M. Freitag *et al.*, *Nano Lett.* **9**, 1883–1888 (2009).
33. S. Xu *et al.*, *Nat. Phys.* **17**, 619–626 (2021).
34. E. S. Tikhonov *et al.*, *Phys. Rev. B Condens. Matter Mater. Phys.* **90**, 161405 (2014).
35. A. I. Berdyugin *et al.*, Out-of-equilibrium criticalities in graphene superlattices. *Zenodo* (2021); doi:10.5281/zenodo.5639021.

ACKNOWLEDGMENTS

Funding: We acknowledge financial support from the European Research Agency (grants ARTIMATTER and VANDER), Lloyd's Register Foundation, Graphene Flagship Core3 Project, and the Royal Society. M.T.G acknowledges the support from EPSRC grant EP/V008110/1, and A.I.B. acknowledges the support from NOWNANO Doctoral Training Centre. R.K.K. acknowledges a ESPRC doctoral-prize fellowship award and the EU Horizon 2020 program under the Marie Skłodowska-Curie grants 754510 and 893030. V.I.F. was also supported by EU Quantum Flagship Project 2D-SIPC and EPSRC grants EP/V007033 and EP/S030719. L.L. acknowledges support from the Science and Technology Center for Integrated Quantum Materials, NSF grant DMR-1231319, and Army Research Office grant W911NF-18-1-0116. K.W. and T.T. acknowledge support from Elemental Strategy Initiative of Japan (grant JPMXP0112101001) and JSPS KAKENHI (19H05790, 20H00354, and 21H05233). L.S.L. acknowledges support by the Science and Technology Center for Integrated Quantum Materials, NSF grant DMR-1231319, and Army Research Office grant W911NF-18-1-0116. **Author contributions:** A.I.B., R.K.K., and A.K.G. conceived and led the project; N.X., P.K., S.X., M.H., and Y.C. made the studied devices; A.I.B., S.B., L.A.P., D.A.B., M.K., and R.K.K. carried out the measurements and analyzed their results, with help from N.X., S.S, P.K., K.S.N., I.V.G., L.S.L., V.I.F., and A.K.G.; H.G., S.S., Z.D., M.T.G., A.I.B., V.I.F., and L.S.L. provided theory; K.W. and T.T. supplied hBN crystals. A.I.B., R.K.K., and A.K.G. wrote the manuscript, with contributions from L.S.L., N.X., H.G., S.S., and I.V.G. All authors discussed the results and commented on the manuscript. **Competing interests:** The authors declare no competing interests. **Data and materials availability:** All data discussed in the main text and the supplementary materials are available at Zenodo (*35*).

SUPPLEMENTARY MATERIALS

science.org/doi/10.1126/science.abi8627
Supplementary Text
Figs. S1 to S8
References (*36*–*46*)

7 April 2021; accepted 16 December 2021
10.1126/science.abi8627

Science

Out-of-equilibrium criticalities in graphene superlattices

Alexey I. BerdyuginNa XinHaoyang GaoSergey SlizovskiyZhiyu DongShubhadeep BhattacharjeeP. KumaravadivelShuigang XuL. A. PonomarenkoMatthew HolwillD. A. BandurinMinsoo KimYang CaoM. T. GreenawayK. S. NovoselovI. V. GrigorievaK. WatanabeT. TaniguchiV. I. Fal'koL. S. LevitovRoshan Krishna KumarA. K. Geim

Science, 375 (6579), • DOI: 10.1126/science.abi8627

Displacing the Fermi surface

Electrons that contribute to electrical conduction in a metal typically occupy high energy levels near the Fermi level. To get electrons from lower bands to join the flow, extremely large electric fields would be needed. In graphene and its superlattices, Berdyugin *et al*. show that small, experimentally accessible fields are sufficient to achieve this regime. The researchers discerned the signatures of this highly nonequilibrium state in transport data. —JS

Science (ISSN) is published by the American Association for the Advancement of Science. 1200 New York Avenue NW, Washington, DC 20005. The title *Science* is a registered trademark of AAAS.

Complete absorption of topologically protected waves

Guido Baardink[1], Gino Cassella[1], Luke Neville[1], Paul A. Milewski[2], and Anton Souslov[1]

[1]Department of Physics/University of Bath, UK, [2]Department of Mathematical Sciences/University of Bath, UK

Chiral edge states can transmit energy along imperfect interfaces in a topologically robust and unidirectional manner when protected by bulk-boundary correspondence. However, in continuum systems, the number of states at an interface can depend on boundary conditions. Here we design interfaces that host a net flux of the number of modes into a region, trapping incoming energy. As a realization, we present a model system of two topological fluids composed of counter-spinning particles, which are separated by a boundary that transitions from a fluid-fluid interface into a no-slip wall. In these fluids, chiral edge states disappear, which implies non-Hermiticity and leads to an interplay between topology and energy dissipation. Solving the fluid equations of motion, we find explicit expressions for the disappearing modes. We then conclude that energy dissipation is sped up by mode trapping. Instead of making efficient waveguides, our paper shows how topology can be exploited for applications towards acoustic absorption, shielding, and soundproofing.

Quantum materials by design

Eva Benckiser

Max Planck Institute for Solid State Research, Stuttgart, Germany

Oxide heterostructures enable the targeted design of quantum materials with specific, functional properties such as magnetism and superconductivity for future information and energy technologies. Research in our group focuses on gaining a fundamental understanding of spin, orbital, charge, and lattice reconstructions in complex transition-metal oxide heterostructures, mainly using x-ray spectroscopy. Our goal is to identify the relevant interface reconstruction mechanisms that form the basis for a future rational design of these materials.

In recent years, we have focused on two prototypical correlated-electron compounds, namely RVO_3 and $RNiO_x$ with R = rare-earth ion or Y, and studied their ordered phases and electronic depth profiles with resonant x-ray scattering and reflectometry. Heterostructures are grown by either pulsed-laser deposition or ozone-assisted atomic layer-by-layer molecular beam epitaxy [1], and more recently, we extended the synthesis by soft-chemistry topotactical reactions to modify the anion sublattice [2]. In my talk, I will give an overview of studies dealing with the perspectives of orbital engineering [3], digital doping at interfaces of multilayer structures [4], facet-dependent modifications of a metal-insulator transition [5], the manipulation of complex spin orders [6], and a superlattice approach to the design of unconventional superconductors [2]. All of these studies were conducted in collaboration with many scientists who are co-authors of the publications listed below.

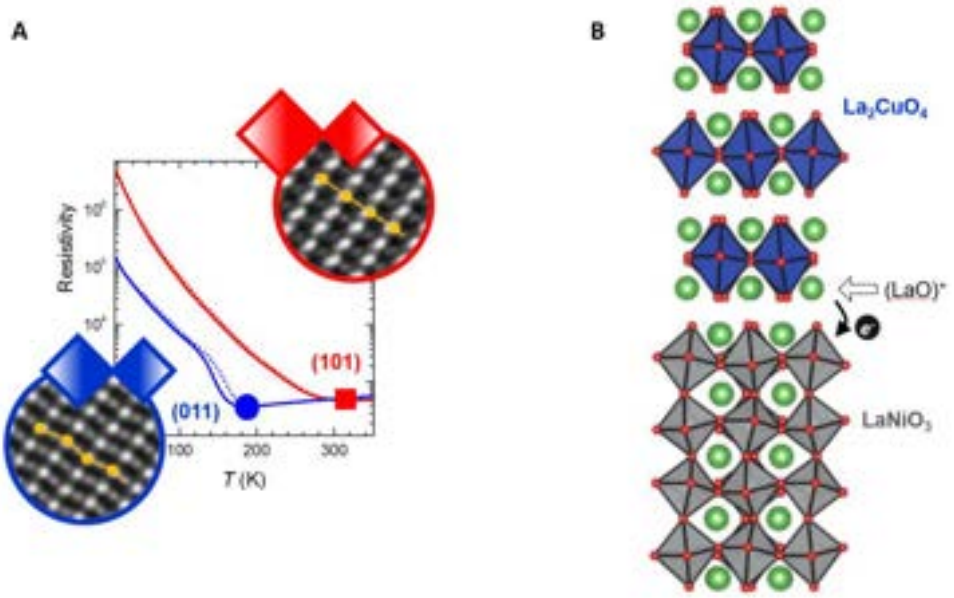

Fig. 1. (a) Facet dependence of the metal-insulator transition in $NdNiO_3$ thin films grown on two different facets of the same substrate material [5]; (b) Digital doping at the interfaces of a $(LaNiO_3)_n$ /LaO/ $(La_2CuO_4)_m$ multilayer structure grown by atomic layer-by-layer molecular beam epitaxy [4].

[1] F. Wrobel, *et al.*, Appl. Phys. Lett. 110, 4 (2017).
[2] R. A. Ortiz, *et al.*, Phys. Rev. B 104, 165137 (2021).
[3] P. Radhakrishnan, *et al.*, Phys. Rev. B 104, L121102 (2021).
[4] F. Wrobel, *et al.*, Phys. Rev. Materials 2, 035001 (2018).
[5] Y. E. Suyolcu, *et al.*, Phys. Rev. Materials 5, 045001 (2021).
[6] M. Hepting, *et al.*, Nature Physics 14, 1097–1102 (2018).

Long-lived photogenerated carriers in 2D TMDs nanosheets made by liquid-phase exfoliation (LPE)

Floriana Morabito[1,2], Kevin Synnatschke[3,4,5], Jonathan Coleman[3,5], Valeria Nicolosi[3,4], Giulio Cerullo[2], Christoph Gadermaier[1,2]

[1]Physics department, Politecnico di Milano, Italy

[2]Centre for Nano Science and Tecnology CNST @ Polimi – Istituto Italiano di Tecnologia (IIT), Italy

[3]CRANN & AMBER Research Centers, Trinity College Dublin, Dublin 2, Ireland

[4]Centre for Research on Adaptive Nanostructures and Nanodevices CRANN, School of Chemistry, Trinity College Dublin, Dublin 2, Ireland

[5]Sami Nasr Institute of Advanced Materials SNIAM, School of Physics, Trinity College Dublin, Dublin 2, Ireland

Two-dimensional (2D) transition metal dichalcogenides (TMDs) such as MoS_2 and WS_2 are excellent candidates for next generation energy storage and optoelectronics due to their strong light-matter interaction.

The preparation of monolayer TMDs by mechanical exfoliation is a labour-intensive process and lacks scalability. However, scalable alternatives reported and refined in the past years are based on liquid phase exfoliation (LPE). The nanomaterial fabrication and processing in liquid medium offers a versatile and scalable methodology which can produce reasonable qualities of nanosheets if the parameters are controlled carefully.

In this study, we investigate tiled thin films of LPE MoS_2, and WS_2, respectively, as well as a well-defined stack of nanosheets from both materials, forming a heterojunction (HJ). This work addresses the impact of different dielectric environments on the material optical response, using time-resolved optical spectroscopy. Transient states of these materials are dictated by the formation and recombination of bound states, such as excitons, trions, and biexcitons.

Using a specially designed pump-probe setup, we study the lifetime of such photoexcited states from the femto- (10^{-15} s) to microsecond range (10^{-6} s) and the impact of the material and the dielectric environment on their decay.

Measurements of transient absorption at long delays are performed for the first time on HJs made from liquid-phase exfoliated samples.

Pumping at 3.5 eV, we observe spectral features which exhibit dynamics up to hundreds of nanoseconds. This is an important result as an improved understanding of the origin of complex physical processes in this temporal range is crucial for applications which rely on charge extraction, i.e. long-lived states in view of employing TMDs in energy harvesting or optoelectronic applications.

Anomalous Split Peak Structures in Transverse Magnetic Focusing of GaAs Electrons

H. Smith[1], P. See[2], I. Farrer[3], D. Ritchie[4], M. Pepper[1], and S. Kumar[1]

[1]University College London, United Kingdom, [2]National Physical Laboratory, United Kingdom, [3]University of Sheffield, United Kingdom, [4]Cavendish Laboratory, United Kingdom

In condensed matter physics, physical phenomena occurring due to many-body interactions and scattering processes in semiconductors and their interfaces have been extensively investigated. One powerful method to create scattering processes is called Transverse Magnetic Focusing (TMF) which utilises the combination of a transverse magnetic field and electrical potential. Sharvin [1] was the first to propose the idea of TMF in metals, which was subsequently adopted for investigating scattering processes in the high-quality two-dimensional electron gas (2DEG) [2]. In high-quality 2DEGs, TMF resulted in the splitting of odd-numbered peaks from a classical single peak structure in the focusing spectrum [3]. Such splitting in peaks has been attributed to spin polarisation due to exchange interactions or spin-orbit interactions [4] and the formation of a 1D Wigner lattice [5]. Recently, TMF has been utilised for spin amplification and electronic hydrodynamic investigations [6].

In the present work, we shall present experimental results from TMF measurements of electrons in a two-dimensional electron gas (2DEG) utilising one-dimensional quantum wires (1DQW). The 2DEG is formed at the interface of GaAs/AlGaAs heterostructure, while linearly arranged 1DQWs, which make up the injector and detector for the TMF measurements, are formed via pairs of top gated, split gate devices defined on the surface of the heterostructure. The split gates allow for the confinement of electrons in the 2DEG down to one-dimension, while the top gate allows for manipulation of the carrier density in the channel. An additional global gate is placed over the 2DEG region between the injector and detector for the modulation of the charge carrier density of this 2DEG region.

In our results, we see anomalous sub-peaks occurring in addition to the previously reported two sub-peak structures. We will show the effects of applying potentials to the top gate over the injector channel and the global top gate over the 2DEG on these anomalous peaks. In such measurements, we find that the additional sub-peaks may be enhanced and suppressed as the charge carrier densities within the 1D and 2D systems are tuned. We also explore how varying the potentials on the split gates, and the subsequent change in confinement potential and allowed energy levels through the channel, affect the formation and relative peak heights of the TMF spectrum. We will discuss possible mechanisms based on spin polarisation and repulsion in these systems.

This work was funded by the United Kingdom Research and Innovation (UKRI) Future Leaders Fellowship, the Engineering and Physical Sciences Research Council (EPSRC) and the Royal Society.

[1] Y. V. Sharvin, JETP, **21** 655 (1965).
[2] H. van Houten, *et al.*, Europhys. Lett., **5**(8) 721-725 (1988).
[3] C. Yan, *et al.,* J. Phys.: Condens. Matter **30**(8), 08LT01 (2018).
[4] C. Yan, *et al.,* Appl. Phys. Lett. **111**(4), 042107 (2017).
[5] S. C. Ho, *et al.*, Phys. Rev. Lett. **121**(10), 106801 (2018).
[6] A. Gupta, *et al.*, Nat. Commun. **12**, 5048 (2021).

Displacive Raman Force and Coherent Shear Phonon in Layered Materials

Habib Rostami[1]

[1] Nordita, KTH Royal Institute of Technology and Stockholm University, Hannes Alfvéns väg 12, 10691 Stockholm, Sweden

Light-induced structural manipulation is a non-destructive method to control the electronic and optical properties of the system. Collective macroscopic oscillation of atoms in a solid, i.e., coherent phonons, facilitates reaching this aim. Coherent phonons can be excited by irradiating an ultrashort optical pulse and detected using transient optical transmission or reflection measurements using pump-probe spectroscopy.

Recently, there has been significant interest in photo-induced structural transition between crystalline layered MoTe2 using ultrafast pump-probe and time-resolved second-harmonic-generation spectroscopy. A displacive coherent excitation of Raman-active shear phonon in MoTe2 causes a first-order phase transition from inversion symmetric 1T' structure to non-centrosymmetric 1Td phase [1,2]. Similarly, it has been experimentally proven a switch from an ABA structural phase to ABC one by laser irradiation in trilayer graphene [3]. The other scenario is the laser-induced heating effect that can provide activation energy for the phase transition. However, it is unclear which of the two mechanisms are more relevant in different laser power and frequency and electron doping in the layered materials. In this work [4], I develop a systematic theory to investigate displacive excitation of coherent shear phonon in a bilayer system using a diagrammatic formalism. Using a Raman force mechanism, I predict a highly controllable relative lateral shift of layers (see Fig. 1) depending on the laser power and frequency in different electronic doping. My theoretical finding is consistent with available experiments and can be examined in other layered 2D materials.

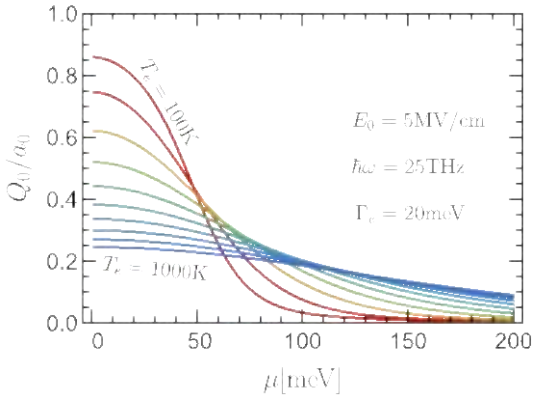

Fig. 1. Light-induced shear displacement in bilayer graphene versus chemical potential for realistic experimental values of frequency ω, electric field strength E_0, electron scattering rate Γ_e and electronic temperature T_e [4].

[1] M.Y.Zhang,Z.X.Wang,Y.N.Li,L.Y.Shi,D.Wu, T. Lin, S. J. Zhang, Y. Q. Liu, Q. M. Liu, J. Wang, T. Dong, and N. L. Wang, Phys. Rev. X 9, 021036 (2019).

[2] T. Fukuda, K. Makino, Y. Saito, P. Fons, A. V. Kolobov, K. Ueno, and M. Hase, Applied Physics Letters 116, 093103 (2020).

[3] J. Zhang, J. Han, G. Peng, X. Yang, X. Yuan, Y. Li, J. Chen, W. Xu, K. Liu, Z. Zhu, W. Cao, Z. Han, J. Dai, M. Zhu, S. Qin, and K. S. Novoselov, Light: Science & Applications 9, 174 (2020).

[4] H. Rostami, manuscript in preparation.

Investigation into Skyrmion Lattice Disorder using Resonant Elastic X-ray Scattering

Mr. Jack Bollard *Dr. Richard Brearton*
Prof Thorsten Hesjedal *Prof Gerrit van der Laan*

Resonant elastic x-ray scattering (REXS) is a powerful technique to provide surface-sensitive information on the state and structure of a magnetic lattice [1]. It can be used to study skyrmions, a special kind of topological magnetic vortex with a myriad of exciting properties. At the Diamond Light Source, we performed REXS measurements on the skyrmion lattice of Cu_2OSeO_3, in varying magnetic fields and temperatures within the skyrmion phase pocket. At the lower temperature (Figure 1a), the lattice is well ordered, as evidenced by a set of six sharp diffraction peaks, and hints of a domains can be seen as well (a weaker six-fold pattern). At a slightly higher temperature, the lattice is strongly disordered (Figure 1b). The analysis of this disordered state allowed us to identify several indicators of devolution: (i). an increase in variability of the scattering wavevector, (ii) a decrease in conical phase intensity, and (iii) the existence of multiple, lateral skyrmion domains. This highly disordered state can be understood as a result of a change in inter-skyrmion potentials, resulting from the presence of conical modulations. These factors cumulate to produce a devolution of the lattice structure.

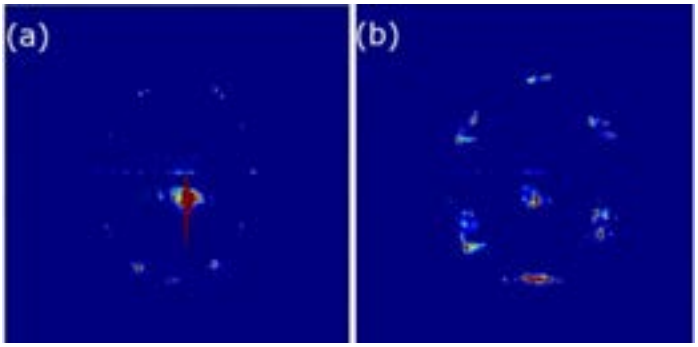

Figure 1: Skyrmion Diffraction patterns produced across a change in temperature of 0.25K

REXS on the Cu_2OSeO_3 crystal was conducted with right circularly polarized x-rays tuned to the Cu L_3-edge at ~930 eV. A complete mapping of both the B,T phase diagram, and the path taken through it were done using a clustering algorithm, which uses wavelet denoising techniques to prepare images, then prepares local statistics to determine statistically significant pixels and apply the DBSCAN algorithm to cluster statistically significant pixels.

Novel indicators of disorder were investigated in this experiment, with an important emphasis on the path taken through the phase diagram. This was studied using 'field-shakes', i.e., by drastically altering the applied magnetic field magnitude repeatedly in and out of a pocket skyrmions could exist in once created, in an attempt to reduce the skyrmion volume fraction. The parameters involved in this were mapped through the phase diagram. The observation of multiple scattering vectors within the same REXS scan implies the co-existence of domains with varying inter-skyrmion potentials. This was found to coincide with a decrease in conical intensity, which dictates that conical modulations within the sample can stabilise the skyrmion lattice by increasing the attractive potential.

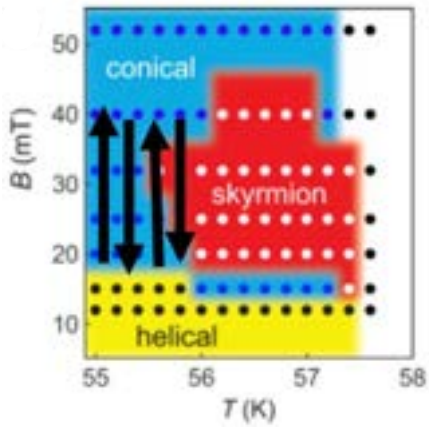

Figure 2: Field shakes (Black arrows defining the path through phase space) are a novel method to introduce disorder into a skyrmion lattice

The results from this experiment have introduced novel methods to manipulate skyrmion interactions using conical modulation, as well as several methods of indicating this disorde, rough quantifiable methods.

[1] S. L. Zhang *et al*., Phys. Rev. B **93**, 214420 (2016); Phys. Rev. Lett. **120**, 227202 (2018).

Quantum emitters and charge transfer in two-dimensional heterostructures: An *ab initio* study

Madhava Krishna Prasad [1,2], Oras A Al-Ani[1,3], Jonathan P Goss[1] and Jonathan D Mar[1,2]

[1]Newcastle University, United Kingdom, [2]Joint Quantum Centre Durham-Newcastle, United Kingdom,[3]Electrical Engineering Technical College, Iraq

An essential requirement for the physical implementation of quantum communication and a range of other quantum technologies is the realisation of bright and deterministic sources of single photons [1]. Such quantum emitters have been recently discovered in 2D hexagonal boron nitride (h-BN) and are the result of defect states located deep within the large bandgap of h-BN, allowing for single-photon emission up to room temperature [2]. Furthermore, there has been increasing interest in using such h-BN defects for optically addressable spin qubits [3].

2D h-BN films obtained in experiment typically host a large concentration and variety of defects introduced during growth and/or irradiation, with only a select few being suitable as single-photon sources for quantum technologies. Therefore, the controlled quenching of unwanted photoemission from particular defects will be key towards producing uniform arrays of single-photon-emitting devices in a scalable way. Recent experimental studies have shown that single-photon emitters in h-BN can be spectrally quenched when deposited on functionalised graphene and spatially quenched when deposited on patterned graphene, suggesting the existence of charge transfer processes occurring between the h-BN and graphene layers [4]. However, a rigorous theoretical study on the types of h-BN defect states involved in charge transfer and the modification of defect properties in such a heterostructure (e.g. defect energy levels and formation energies) is still lacking. Here, we present the results of an investigation on the propensity for charge transfer for different defects in h-BN deposited on graphene. Specifically, we perform simulations of intrinsic and extrinsic h-BN defects — nitrogen vacancies (V_N), boron vacancies (V_B), nitrogen antisite (N_B), boron antisite (B_N), nitrogen anitisite and nitrogen vacancy complex (N_BV_N), and substitutional carbon and nitrogen vacancy complex (C_BV_N) — and explore the possibility of charge transfer in such a 2D heterostructure.

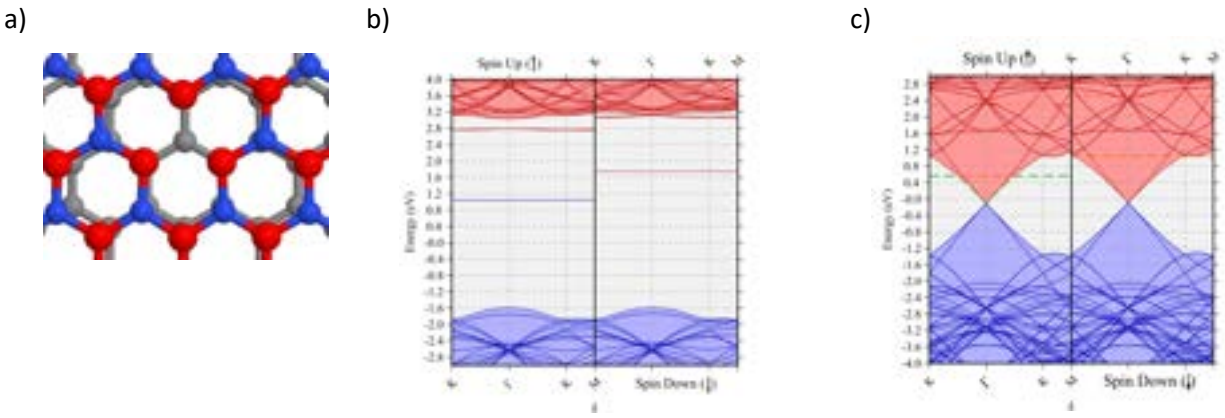

Fig. 1. (a) Geometry of a nitrogen vacancy (V_N) in the top h-BN layer with a bottom graphene layer; (b) band structure of an isolated layer of h-BN with V_N. The mid-gap states are localised states due to the vacancy; (c) The same layer of h-BN with V_N laid on the graphene layer. The change in the occupancies of the graphene bands as it crosses the empty defect states contributed by the h-BN layer indicates charge transfer. Here the unoccupied h-BN (graphene) levels are orange (red) and occupied levels are green (blue).

References:

[1] J. L. O'Brien, A. Furusawa, and J. Vučković , Nat. Photon. **3**, 687 (2009).
[2] T. T. Tran, *et.al.*, Nat. Nanotechnol. **11**, 37 (2015).
[3] T. T. Tran, *et.al.*, ACS Nano **10**, 7331 (2016).
[4] Z.-Q. Xu, *et. al.*, 2D Mater. **7**, 031001 (2020).

Robust antiferromagnetism in $NaOsO_3$ under pressure

Prasun Boyal and Priya Mahadevan
S N Bose National Centre for Basic Sciences
Email: prasun.boyal@gmail.com

Abstract

$NaOsO_3$ is known to be an insulator with a small band gap of 0.2 eV, favoring a G-type antiferromagnetic state below ??? K. It is believed to be an example of a Slater insulator [1], with spin-orbit interactions playing a significant role here in modifying the electronic structure[2]. The unusually high antiferromagnetic temperature has been explained as emerging from the half-filling of the t_{2g} state [3]. We have examined the pressure dependence of the electronic structure, as well its evolution under pressure both in the presence and absence of spin-orbit interactions within ab-initio electronic structure calculations. Mapping the Hamiltonian to a tight-binding model, we use pressure as a parameter to tune the interaction strengths and bring it to the point where magnetic order just sets in. This allows us to throw light on the mechanism of magnetism.

[1]. Slater insulator
[2]. Cesare's paper
[3]. My NaOsO3 paper with Srimanta

Analytic Theories for Magnetic Skrymions

E Lu[1], J C Davidson[2], A R Chalifour[2], C Quispe Flores[3], A R Stuart[3], P S Keatley[4], K S Buchanan[3] and K L Livesey[1]

[1]University of Newcastle, Australia, [2]University of Colorado at Colorado Springs, USA,
[3]Colorado State University, USA, [4]University of Exeter, United Kingdom

Magnetic skyrmions are tiny swirls in the direction of the local magnetization (see Figure 1). They are as small as a few nanometers wide and can be moved around inside a magnetic film or wire using very low energy currents, making them of interest for data storage and computing applications. For applications, it is important to be able to predict the size and type of isolated skyrmion that will form in a given thin film or multilayer stack, due to the interfacial Dzyaloshinskii-Moriya interaction. Moreover, an *analytic* prediction saves a great deal of time compared to running micromagnetic simulations, plus allows one to see the dependence of the skyrmion size on different magnetic parameters.

In this work, we have developed a semi-analytic theory to predict the size of a skyrmion in a magnetic thin film, with a given applied magnetic field. This is done by assuming a linear approximation for the magnetization variation as a function of the radial distance from the centre of the skyrmion, and by then minimizing the total energy. It also makes use of a Green's function approach to calculate the demagnetizing energy contribution. The Green's function approach is especially important for realistic film or stack thicknesses (several nm thick) where commonly-used approximations for the demagnetizing energy break down. Our results are compared to those from numerical integrations and micromagnetic simulations to ensure their accuracy.

Existing calculations to predict skyrmion size usually ignore the finite thickness of the magnetic film, in order to get closed-form results. [1] However, the demagnetizing energy does change markedly with the film thickness, having an effect on the skyrmion size. A notable exception is the theory by Buettner *et al* [2], which quotes lengthy equations for the skyrmion energy that are found by data fitting, rather than being derived. Our equations include finite-thickness effects, plus are easier to use and are derived using physical theories.

We extend our methods to analytically calculate the stray magnetic field produced above a skyrmion. This is important as skyrmions are imaged indirectly by measuring their stray field using Magnetic Force Microscopy or nitrogen-vacancy in diamond magnetometry.

It is hoped that our results will be useful to experimentalists working with magnetic skyrmions, to both make quick prediction of material properties, and to infer the skyrmion size and type from measurements.

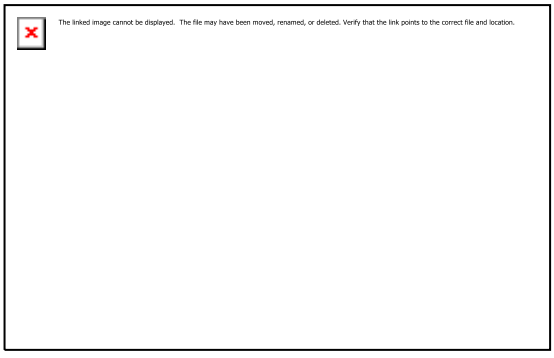

Fig. 1. Schematic of a magnetic skyrmion in a thin magnetic thin film. The coloured arrows indicate the local magnetization direction.

[1] X.S. Wang, H.Y. Yuan and X.R. Wang, Commun. Phys. **1**, 1 (2018).
[2] F. Buettner, I. Lamesh and G.S.D. Beach, Sci. Rep. **8**, 1 (2018).

Stark spectroscopy of high-lying interlayer excitons and trions in bilayer WSe_2

Kai-Qiang Lin[1], Sebastian Bange[1], and John M. Lupton[1]

[1]Department of Physics, University of Regensburg, Germany

Electronic correlations and topology, tunable by electrical gates, are remarkable thrusts in the research of stacked van der Waals quantum materials. Recent examples include metal–insulator quantum-phase transitions[1,2] as well as the topological phase transition from a Mott insulator to a quantum-anomalous Hall insulator[3] in transition-metal dichalcogenide (TMDC) bilayers. Independent control of the charge-carrier density and the out-of-plane electric field are key to exploring the rich phase diagrams of such systems. However, these two parameters are often not independent, and it remains challenging to quantify the interlayer electric field at different doping levels. Here, we demonstrate how to use narrow-linewidth transitions of high-lying interlayer excitons (Fig. 1) and trions in bilayer WSe_2 to disentangle these two parameters. This is based on our previous finding that narrow-band high-lying excitons exist in monolayer and bilayer WSe_2[4-6]. The Stark splitting of these trions quantifies the electric field as the charge density changes. Such excitonic complexes are sensitive to twist angle and offer new opportunities to explore emergent moiré physics under electrical control. Our discovery of high-lying interlayer excitonic complexes suggests many more interlayer excitonic species above the band edge that may be found for different applications.

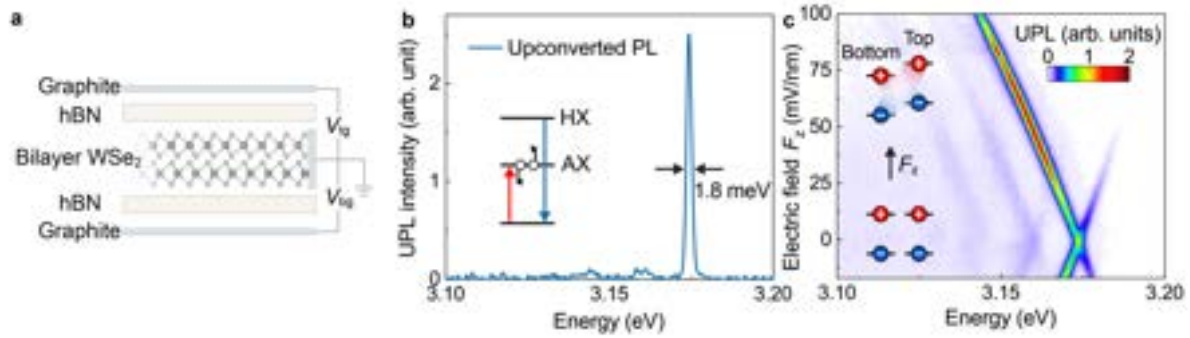

Fig. 1 Stark splitting of the interlayer high-lying exciton HX in a dual-gate bilayer WSe_2 device. (a) Schematic illustration of the device with a natural WSe_2 bilayer encapsulated by hBN. Thin graphite films (few-layer graphene) are used as the top and bottom gates and to contact the WSe_2; (b) Representative upconverted photoluminescence (UPL) spectrum of the HX at zero top and bottom gate voltages at 5 K. A continuous-wave laser (red arrow) resonantly excites the A-exciton (AX). The HX is populated by an Auger-like exciton-exciton annihilation process and gives rise to the UPL (blue arrow). (c) Dependence of the HX UPL on electric field F_z, showing Stark splitting of both the zero-phonon line and the phonon progression.

[1] Li, T. et al. Quantum anomalous Hall effect from intertwined moiré bands. Nature **600**, 641-646 (2021).
[2] Ghiotto, A. et al. Quantum criticality in twisted transition metal dichalcogenides. Nature **597**, 345-349 (2021).
[3] Li, T. et al. Continuous Mott transition in semiconductor moiré superlattices. Nature **597**, 350-354 (2021).
[4] Lin, K.-Q. et al. Narrow-band high-lying excitons with negative-mass electrons in monolayer WSe2. Nat. Commun. **12**, 5500 (2021).
[5] Lin, K.-Q. et al. Twist-angle engineering of excitonic quantum interference and optical nonlinearities in stacked 2D semiconductors. Nat. Commun. **12**, 1553 (2021).
[6] Lin, K.-Q. *et al.*, Quantum interference in second-harmonic generation from monolayer WSe2. Nat. Phys. **15**, 242 (2019).

Uniaxial strain-tuning of the surface electronic structure of Sr_2RuO_4

Edgar Abarca Morales[1,2], Gesa Siemann[2], Andela Zivanović[1,2], Igor Marković[1,2], Chris A. Hooley[2], Dmitry A. Sokolov[1], Naoki Kikugawa[3], Cephise Cacho[4], Matthew Watson[4], Clifford W. Hicks[1], Andrew P. Mackenzie[1,2] and Phil D. C. King[2]

[1]Max Planck Institute for Chemical Physics of Solids, Germany, [2]SUPA, School of Physics and Astronomy, University of St Andrews, UK, [3]National Institute for Materials Science, Japan, [4]Diamond Light Source, UK

Ruthenates are well known for their rich phase diagrams and distinct correlated electron states that are accessible via small changes in structure or composition [1]. Much of this richness can be attributed to the presence of van Hove singularities (vHS) in their electronic structure, which are located in close proximity to the Fermi level. In the unconventional superconductor Sr_2RuO_4 one such vHS is at sufficiently low energy that it can be driven through the Fermi level using uniaxial strain, which has been found to more than double the superconducting T_c and to stabilize a non-Fermi liquid state [2,3,4]. In the bilayer sister compound $Sr_3Ru_2O_7$, in-plane rotations of the RuO_6 octahedra and the corresponding doubling of the in-plane unit cell turn the vHS into higher (4^{th}) order [5]. Tuning this vHS to the Fermi level with large magnetic fields is thought to drive an exotic nematic state to emerge, which exhibits signatures of quantum criticality [6,7]. Interestingly, the octahedra rotations that characterize $Sr_3Ru_2O_7$ are also found for the surface layer of Sr_2RuO_4, potentially making such states accessible also at the surface of the single-layer compound [8]. Here, we report the evolution of the electronic structure at the surface layer of Sr_2RuO_4 under large in-plane uniaxial strains of $\varepsilon_{xx} - \varepsilon_{yy} = -0.8 \pm 0.1\%$. From angle-resolved photoemission, we show how the induced strain drives a sequence of Lifshitz transitions, fundamentally reshaping the low-energy electronic structure and the rich spectrum of van Hove singularities that the surface layer of Sr_2RuO_4 hosts. From comparison of tight-binding modelling to our measured dispersions, we show that, surprisingly, the uniaxial strain is accommodated predominantly by bond-length changes rather than modifications of the octahedral tilt and rotation angles. Our study thus sheds new light on the nature of structural distortions at oxide surfaces, and how targeted control of these can be used to tune density of states singularities to the Fermi level, in turn paving the way to the possible realization of quantum criticality.

[1] E. Dagotto, Science 309.5732 (2005): 257-262.
[2] V. Sunko, E. Abarca Morales, *et al*., npj Quantum Materials 4.1 (2019): 1-7.
[3] A. Steppke, *et al*., Science 355.6321 (2017): eaaf9398.
[4] M. E. Barber, *et al*., Physical review letters 120.7 (2018): 076602.
[5] D. V. Efremov, *et al*., Physical Review Letters 123.20 (2019): 207202.
[6] R. A. Borzi, *et al*., Science 315.5809 (2007): 214-217.
[7] S. A. Grigera, *et al*., Science 294.5541 (2001): 329-332.
[8] C. A. Marques, *et al*., Advanced Materials 33.32 (2021): 2100593.

Quantitative Measurements of Anisotropic Thermal Transport in Gamma Indium Selenide via Cross-Sectional Scanning Thermal Microscopy

Sergio Gonzalez-Munoz[1], Khushboo Agarwal[1], Eli G. Castanon[1,2], Zakhar R. Kudrynskyi[3], Zakhar D. Kovalyuk[4], Jean Spièce[5], Olga L. Kazakova[2], Amalia Patane[3] and Oleg V. Kolosov[1]

[1]Lancaster University, United Kingdom, [2]National Physical Laboratory, United Kingdom, [3]University of Nottingham, United Kingdom, [4]National Academy of Sciences of Ukraine, Ukraine, [5]Université Catholique de Louvain, Belgium

The versatility of van der Waals (vdW) materials and their heterostructures provide an extremely useful toolbox for addressing the control of thermal transport in diverse applications [1]. The challenge nevertheless lies in the difficulty of measuring and quantifying the thermal transport within atomically thin and highly anisotropic vdW materials and between these materials and substrates.

Here we report a novel powerful approach of cross-sectional scanning thermal microscopy (xSThM) for studying anisotropic heat transport in nanoscale layered vdW materials. We use beam exit cross-sectional polishing (BEXP) of vdW gamma indium selenide (γ-InSe) nanoflakes, shaping these into ultra-thin low angle wedges with atomic-scale surface flatness. InSe has high potential in thermoelectric (TE) applications due to its advantageous electrical and thermal properties [2]. By conducting an xSThM mapping in high vacuum (HV) conditions continuously varying sample thickness of the wedge, we eliminate artefacts of through-the-air heat transport and suppress a generally unknown SThM tip-surface interfacial thermal resistance. By comparing experimental results with the finite element analysis (FEA) simulation and analytical models, we can directly evaluate and quantify the anisotropy between the in-plane and cross-plane thermal conductivity of InSe ($k_{//}/k_{\perp}$), the local thermal resistance at the vdW material–substrate interface (r_{int}) and the SThM tip-material thermal resistance (R_c).

The xSThM technique allowed us to independently confirm the heat transport anisotropy and anomalous low thermal conductivity values of $k_{//}$ = 2.16 $Wm^{-1}K^{-1}$ and $k_{\perp}$ = 0.89 $Wm^{-1}K^{-1}$ for γ-InSe on Si, also extracting the interfacial thermal resistance between γ-InSe and Si (r_{int} = 9.60x10^{-11} Km^2W^{-1}). Our results support the potential of γ-InSe as a high TE efficiency material, where the low thermal conductivity values can be combined with a high power factor, ultimately enhancing the figure of merit (FoM).

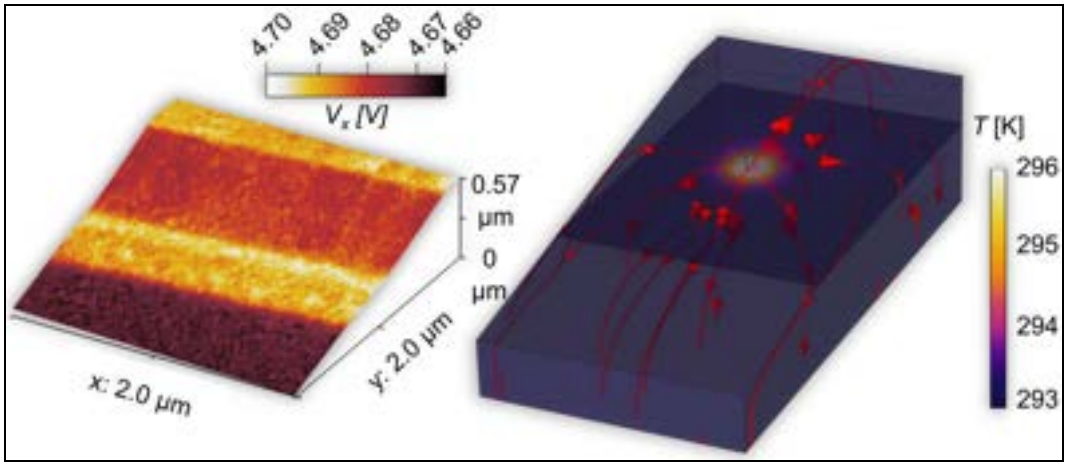

Fig. 1. (Left) 3D InSe wedge cut topographic angle with the thermal SThM signal; (Right) 3D InSe wedge cut FEA simulation of the temperature distribution and the heat flow lines.

[1] Kim, S. E. et al. Nature **597**, 660-665 (2021).
[2] Buckley, D. et al. Adv. Funct. Mater. **31**, 2008967 (2021).

Tuning the Van Hove singularity in $Sr_3Ru_2O_7$ via isovalent out-of-plane Ba doping

Caitlin O'Neil[1], Maximilian Pelly[1], Andreas W. Rost[1], and Alexandra S. Gibbs[2,3]

[1]School of Physics and Astronomy, University of St Andrews, UK
[2]School of Chemistry, University of St Andrews, UK
[3]ISIS Neutron and Muon Source, Rutherford Appleton Laboratory, UK

$Sr_3Ru_2O_7$ is a prime example of a strongly correlated oxide, displaying phenomena associated with a quantum critical end point and the formation of complex electronic phases [1,2]. The physics of this material is associated with an underlying Van Hove singularity in the band structure [3] and tuning its properties has been pursued through a number of strategies including magnetic field, pressure, uniaxial strain and doping.

Here we utilise isovalent Ba doping on the Sr sites as a chemical pathway to expand the lattice and increase the tolerance factor, driving the system closer to the aristotype structure. Being an out-of-plane dopant it is expected to minimally affect impurity scattering and thereby transport. We present synthesis and detailed characterisation by high resolution neutron diffraction, magnetisation and specific heat measurements of the series $(Sr_{1-x}Ba_x)_3Ru_2O_7$ for $x \leq 0.1$. Our data suggest a clear shift of the Van Hove singularity towards the Fermi energy, crossing it at approximately $x = 0.08$, with a subsequent sharp decrease in the density of states. These results indicate that the effect on the rotation angle of the RuO_6 octahedra is primarily to tune the Ru-O-Ru orbital overlap and move the material towards the undistorted limit, as realised in single layer relative Sr_2RuO_4.

We will discuss the details of this tuning of the band structure via structural distortions. In particular we will show how such tuning can provide a clear pathway to increasing the strength and impact of the Van Hove singularity on the physics of $Sr_3Ru_2O_7$, and by extension Ruddlesden-Popper ruthenates in general [4].

[1] A. P. Mackenzie *et al*., Physica C **481**, 207 (2012).
[2] C. Lester *et al*., Nature Communications **12**, 5798 (2021).
[3] A. Tamai *et al*., Physical Review Letters **101**, 026407 (2008)
[4] D.V. Efremov *et al*., Physical Review Letters **123**, 207202 (2019)

Imaging the field-induced changes in the electronic structure of metamagnetic $Sr_4Ru_3O_{10}$

Luke C. Rhodes[1], Izidor Benedičič[1], Masahiro Naritsuka[1], Carolina A. Marques[1], Weronika Osmolska[1] Christopher Trainer[1], Yoshinko Nanao[1], Aaron B Naden[2], Rosalba Fittipaldi[3], Veronica Granata[4], Mariateresa Lettieri[3], Antonio Vecchione[3] and Peter Wahl[1]

[1]School of Physics and Astronomy, University of St Andrews, St Andrews, UK,
[2]School of Chemistry, University of St Andrews, St Andrews, UK
[3]CNR-SPIN, UOS Salerno, Via Giovanni Paolo II 132, Fisciano, I-84084, Italy
[4]Dipartimento di Fisica "E. R. Caianiello", Università di Salerno, I-84084 Fisciano, Salerno, Italy

The ground state of metamagnetic materials can be precisely controlled by the application of magnetic field, making them exciting candidates for spintronic applications. However, in order to obtain a microscopic understanding and fully control these properties, it is important that we understand the interplay of magnetism, spin- orbit coupling and structural details on a materials electronic structure.
Here we report the study of the ferromagnetic trilayer ruthenate Sr4Ru3O10, which exhibits a metamagnetic transition around in-plane magnetic fields of 5T. Using low temperature scanning tunnelling microscopy and spectroscopy, we reveal the distinct changes to the electronic structure as a function of magnetic field. We find a strongly anisotropic response of the electronic structure under in-plane magnetic field, suggesting that the relatively small orthorhombic distortion has an unusually large effect on the metamagnetic electronic structure. For magnetic field applied out-of-plane, we find magnetic-field induced changes to the electronic structure, with significant variation of the effective g-factors describing the field-induced changes in the electronic structure. We discuss these field-induced changes in terms of spin-orbit coupling and the influence of electronic correlation effects.
Comparison of quasi-particle interference imaging with ab-initio simulations of the local density of states reveals how the interplay of ferromagnetism and spin orbit coupling enables us to constrain models of the microscopic electronic structure and demonstrates how a pronounced directional dependence of the electronic structure can result due to spin-orbit coupling, demonstrating a pathway to a realization of field-control of the electronic structure.

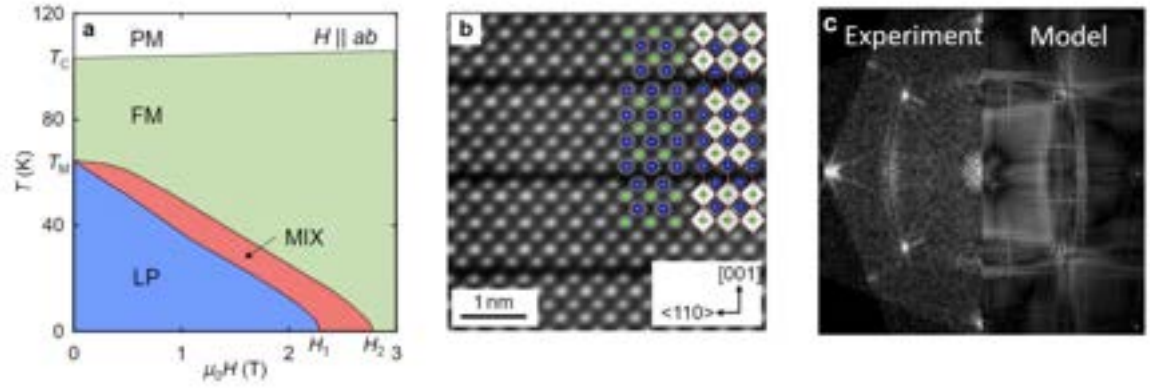

Fig. 1. (a) In-plane metamagnetic phase diagram of $Sr_4Ru_3O_{10}$; (b) Transmission electronic microscopy image and crystal structure of $Sr_4Ru_3O_{10}$, c) Fourier-transform scanning tunneling microscopy image of $Sr_4Ru_3O_{10}$ and comparison with theoretical simulations.

Memristive effects in graphene induced by two dimensional ferroelectric $CuInP_2S_6$

Anubhab Dey[1], Wenjing Yan[1], Nilanthy Balakrishan[2], James Kerfoot[3], Vladimir Korolkov[3], Shihong Xie[4], Zakhar R. Kudrynskyi[1], Oleg Makarovskiy[1], Faguang Yan[4], Kaiyou Wang[4], and Amalia Patanè[1]

[1]School of Physics and Astronomy, University of Nottingham, United Kingdom.
[2]School of Chemical and Physical Sciences, Keele University, United Kingdom.
[3]Park Systems UK Limited, MediCity Nottingham, Thane Road, Nottingham, United Kingdom.
[4]State Key Laboratory of Superlattices and Microstructures, Institute of Semiconductors, Chinese Academy of Sciences, China.

The miniaturization of ferroelectric devices offers prospects for non-volatile memories, low-power electrical switches and disruptive technologies beyond Si-based integrated circuit technology, such as neuromorphic computing and multi-functional sensing. Two-dimensional (2D) van der Waals (vdW) ferroelectrics and their combination with other 2D systems, such as graphene, open promising paths towards future advances in nano-ferroelectrics. Amongst 2D vdW crystals, the vdW ferroelectric $CuInP_2S_6$ (CIPS) has attracted much attention due to its robust ferroelectricity at room temperature and out-of-plane ferroelectricity[1, 2].

Here, we report on hybrid field effect transistors (FETs) based on CIPS and graphene[3]. In our hybrid FETs, the graphene channel is gated through ferroelectric CIPS (Figure a-b-c-d), acting as a sensitive probe of the polarization and charge transfer at the CIPS/graphene interface. The complex interplay between charge transfer at the CIPS/graphene interface and ferroelectric polarization phenomena is crucial to the operation of the FET. We present a comprehensive study of the hysteretic and memristive effects in these FETs by using electrical gating, temperature, high magnetic fields and light illumination, revealing different origins for the memristive behavior in the transport characteristics (Figure e-f-g-h). The understanding of these mechanisms is important for the development of 2D-ferroelectric devices and offer the potential for exploitation of new functionalities, including photodoping of graphene by a ferroelectric semiconductor. Thus, the ferroelectric/graphene heterostructure represents an emergent platform that could drive exciting advances in modern electronics.

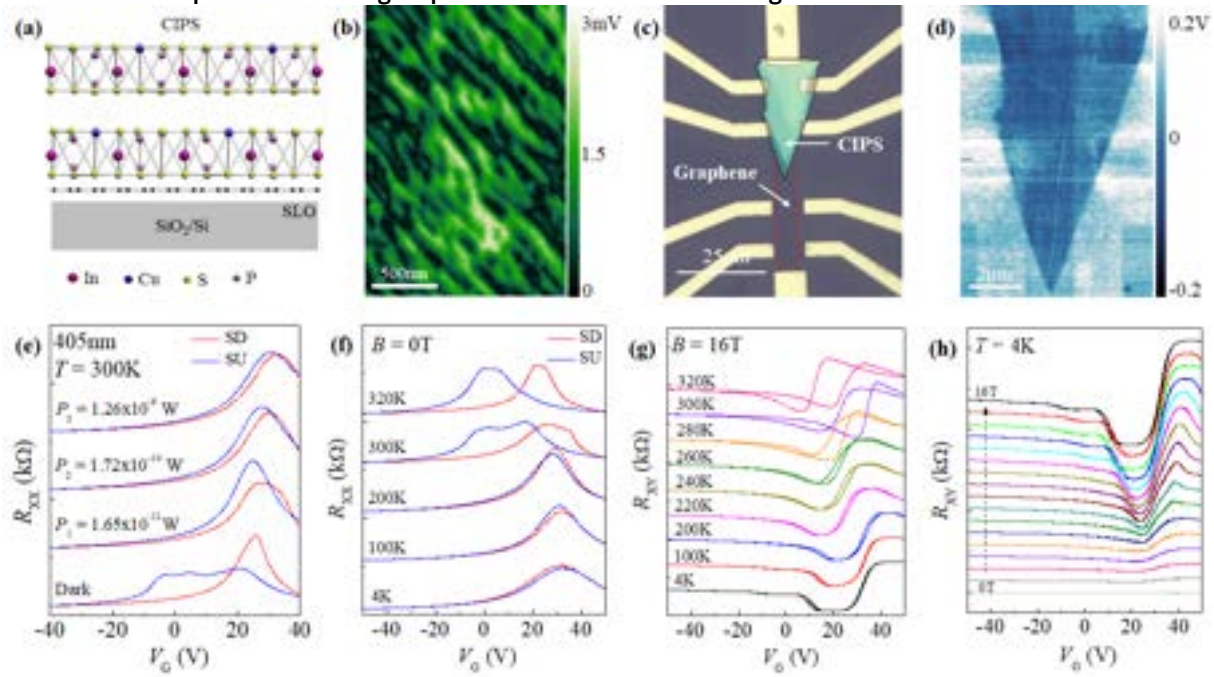

Fig. 1. (a) Schematic of a CIPS-graphene heterostructure (CG). (b) Ferroelectric domains in CIPS imaged by Piezoresponse Force Microscopy (PFM) (T = 300K). (c) Optical image of the CG FET. (d) Kelvin probe force microscopy (KPFM) image of the FET. (e) Dependence of the longitudinal resistance R_{XX} on the gate voltage, V_G, in the dark and under light (λ = 405nm, T = 300K). The sweep up/down (SU/SD) branches are shown in blue and red, respectively. (f) T-dependence of the $R_{XX}(V_G)$ curves at zero magnetic field, B = 0T. The SU/SD branches are shown in blue and red, respectively. (g) Hysteresis in the Hall resistance R_{XY} versus V_G at different T and B = 16T. (h) R_{XY} versus V_G at T = 4K and B from 0T to 16T.

[1] J. Brehm, *et al.*, Nat. Mater. **19**, 43 (2020).
[2] M. Si, *et al.*, Nat. Electron. **2**, 580 (2019).
[3] A. Dey *et al.* accepted in 2D Materials (2022).

Compass-like manipulation of nematicity in $Sr_3Ru_2O_7$

Izidor Benedičič[1], Masahiro Naritsuka[1], Luke C. Rhodes[1], Carolina A. Marques[1], Christopher Trainer[1], Zhiwei Li[2], Alexander C. Komarek[2], Andrew P. Mackenzie[2,1] and Peter Wahl[1]

[1]*SUPA, School of Physics and Astronomy, University of St Andrews, North Haugh, St Andrews, Fife, KY16 9SS, United Kingdom*
[2]*Max Planck Institute for Chemical Physics of Solids, Nöthnitzer Straße 40, 01178 Dresden, Germany*

Strong electron interactions in correlated materials give rise to a variety of emergent phases, including electronic nematic phases. Electronic nematicity has been found in a range of different materials, exhibiting strong symmetry-breaking reconstruction of electronic states without a significant lattice distortion. An enigmatic example of an electronic nematic state is found in $Sr_3Ru_2O_7$, where nematicity was shown to be stabilized by external magnetic field and manifests in anisotropic in-plane resistivity [1].

Recently, STM measurements have revealed a symmetry breaking electronic structure at the surface of $Sr_3Ru_2O_7$ which occurs even in zero magnetic field, providing new insights into the mechanism stabilizing the nematicity [2]. At the same time, it presents a valuable opportunity for spectroscopic study of nematic order in an external field.

Here, we use low-temperature scanning tunnelling microscopy to study the nematicity in $Sr_3Ru_2O_7$ in vector magnetic fields. We find the low-energy electronic structure is strongly affected by the in-plane direction of external field, and demonstrate control over the nematic axis even with modest magnetic fields. Quasiparticle interference measurements allow us to relate the observed angle dependence with the previously reported electronic structure of this material.

This result establishes compass-like control over the electronic structure in the surface layer of $Sr_3Ru_2O_7$ and emphasizes the importance of spin-orbit coupling in the formation of the field-controlled nematic state [3]. We also discuss possible implications for the field-induced nematicity found in the bulk.

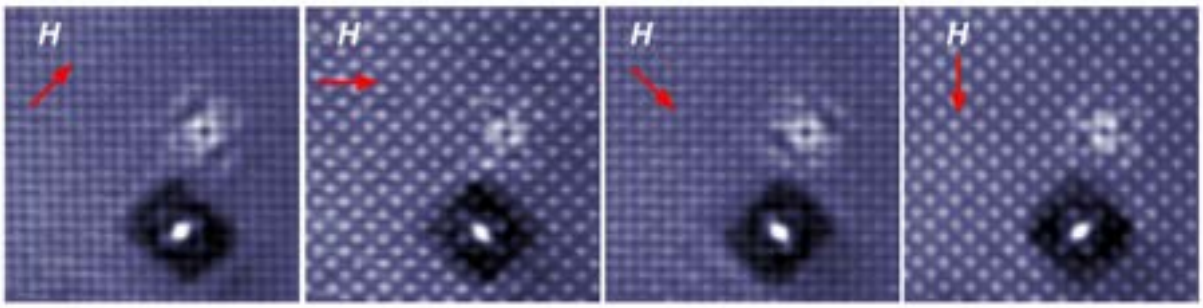

Fig. 1. Real-space quasiparticle interference pattern as function of magnetic field direction.

[1] R. A. Borzi *et al.*, Science **315,** 214 (2007).
[2] C. A. Marques *et al.*, arXiv*:2202.12351* (2022).
[3] S. Raghu *et al.*, Phys. Rev. B **79**, 214402 (2009)

Hilbert space fragmentation and weak thermalization in Bose-Hubbard diamond necklace models

Eulàlia Nicolau[1], Anselmo Marques[2], Ricardo G. Dias[2], Jordi Mompart[1] and Verònica Ahufinger[1]

[1] Departament de Física, Universitat Autònoma de Barcelona, Spain
[2] Departamento de Física & i3N, Universidade de Aveiro, Portugal

We study Bose-Hubbard models in a family of diamond necklace lattices with *n* horizontal couplings between each diamond. The single-particle spectrum of these models presents compact localized states (CLS) that occupy the up and down sites of each diamond. By performing an appropriate basis rotation, the fragmentation of the Hilbert space becomes apparent in the Hamiltonian graph, showing disconnected subsectors with a wide range of dimensions. The models present a conserved quantity related to the occupation of the single-particle CLS that uniquely identifies the different subsectors of the Hilbert space. Due to the fragmentation of the Hilbert space, the entanglement spectrum of the system is composed of multiple domes (see Fig. 1), which is reminiscent of the atypical entanglement spectrum found in some magnetically frustrated systems [1-3]. We find weak thermalization through subsector-restricted entanglement evolution and a wide range of entanglement entropy scalings from area-law to volume-law. Additionally, we observe how the distinguishability between the different domes increases with the number of horizontal couplings and we explain the mechanism behind it by analyzing the graph structure of the Hamiltonian. Although the structure of the entanglement spectrum becomes somewhat obscured for periodic boundary conditions, we show how this effect is a product of the degeneracy induced by translation symmetry, making the multi-dome entanglement structure observable both for open and periodic boundary conditions.

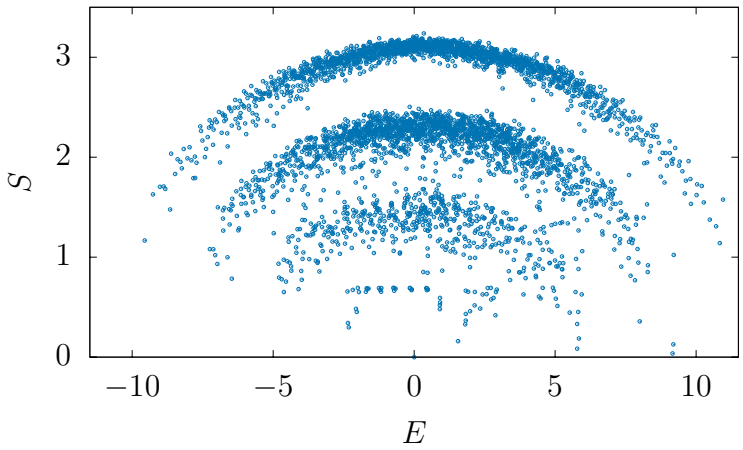

Fig. 1. Half chain entanglement entropy as a function of the energy for the diamond necklace with one horizontal coupling, four particles in four unit cells, and a tunneling to interaction ratio *J/U=1*.

[1] Lee, K., Melendrez, *et al.*, Phys. Rev. B, **101(24)**, 241111 (2020).
[2] McClarty, P. A., *et al.*, Phys. Rev. B, **102(22)**, 224303 (2020).
[3] Chertkov, E., *et al.*, Phys. Rev. B, **104(10)**, 104410 (2021).

CMQM 2022

20–22 June 2022

University of Bath, Bath, UK

IOP Institute of Physics